BRITISH ANTARCTIC SURVEY

SCIENTIFIC REPORTS

No. 111

THE GEOLOGY OF SOUTH GEORGIA:
VI. LARSEN HARBOUR FORMATION

By

B. F. MAIR, B.Sc., Ph.D.

Geology Division, British Antarctic Survey
and
Department of Geology, University of Aberdeen

CAMBRIDGE: PUBLISHED BY THE BRITISH ANTARCTIC SURVEY: 1987
NATURAL ENVIRONMENT RESEARCH COUNCIL

BRITISH ANTARCTIC SURVEY SCIENTIFIC REPORTS: No. 111

THE GEOLOGY OF SOUTH GEORGIA:
VI. LARSEN HARBOUR FORMATION

By

B. F. MAIR, B.Sc., Ph.D.

Geology Division, British Antarctic Survey
and
Department of Geology, University of Aberdeen

This report is based on a Ph.D. thesis by B. F. Mair submitted to the University of Aberdeen in August 1979, and entitled *The geology of the area between Drygalski Fjord and Annenkov Island, South Georgia, Antarctica.*

ABSTRACT

The field relations, petrography, geochemistry and mineralogy of the Larsen Harbour Formation, South Georgia, which represents the upper part of an autochthonous Jurassic–Cretaceous ophiolite, are described. The ophiolite crops out over 120 km^2 adjacent to an island arc assemblage and comprises a ~2 km thick sequence of mafic lavas and breccias, dacites, tuffs and basic dykes. A sheeted dyke layer was not recognized but the formation is intruded and in part structurally underlain by a plagiogranite pluton and minor gabbroic bodies. Both extrusive and plutonic rocks have suffered hydrothermal metamorphism during emplacement and the former were later subjected to burial metamorphism. Microprobe analyses of the main metamorphic mineral phases are given and a zonation of prehnite–pumpellyite, greenschist and amphibolite facies with increasing depth in the ophiolite is defined. 127 new geochemical analyses of the igneous rocks of the ophiolite and the adjacent island arc are presented and compared with those of equivalent tectonic situations. The similarity of the Larsen Harbour Formation to the Sarmiento marginal basin complex, southern Chile, on geochemical and lithological evidence re-affirms the correlation between the strato-tectonic units of the marginal basin system now exposed in South America and on South Georgia.

CONTENTS

I. INTRODUCTION

South Georgia lies 1 000 km east-south-east of the Falkland Islands of the North Scotia Ridge (lat. 54–55°S, long. 36–38°W; Fig. 1). The area surveyed for this report stretches over 75 km of coastline, from Undine South Harbour to Drygalski Fjord, and in total area covers about 120 km^2 (Figs 2 and 3). The coastline from Leon Head to Rogged Bay lies sub-parallel to the dominant structural trend of the island, and is less deeply indented than that from Rogged Bay to Drygalski Fjord. It is characterized by few well-formed bays, steep cliff sections and numerous raised foreshore rock platforms, exhibiting former cliff lines and relict sea stacks (cf. Diaz Cove and Ranvik). The coastal topography becomes more severe to the south and fjord-like inlets occur (e.g. Larsen Harbour and Esbensen Bay; Fig. 4).

Within the hinterland, mountain ranges lie parallel to the south-west-facing coast and within 2 km rise abruptly to an average height of 600 m, culminating in Mount Fraser (1 612 m) in the north and Mount Normann (1 238 m) in the south (Fig. 3). Large, active valley glaciers, namely Wheeler, Novosilski, Harmer, Graae, Philippi, and Jenkins glaciers, transect the mountain ridges and occupy over 60 % of the land surface.

A. Previous Work

South Georgia has been the focus of attention for a number of international expeditions (Roberts, 1958). As a member of the German South Polar Expedition, 1910–12, Heim (1912) discovered diabasic and melaphyric volcanic rocks (presumably the Larsen Harbour Formation) cropping out from Novosilski Glacier to Drygalski Fjord. Heim termed the volcanic rocks 'altvulcanischer', later interpreted by Wordie (1921) to mean 'pre-Tertiary igneous rocks'. Furthermore, he noted acid igneous rocks in 'Slosarczyk Bay' (now named Smaaland Cove), which can be correlated with the Smaaland Cove intrusion (Mair, 1983). His work supported that of Thurach (1890) in noting the link between South Georgia and the Patagonian Cordillera.

Ferguson visited the island in 1911 and 1912, and his collections formed the basis for later detailed work (Ferguson and others, 1914). Tyrrell (1915) classified the igneous rocks collected from the southern end of the island as ancient lavas and intrusions, felsites, quartz-trachytes and fresh ophitic dolerite dykes and sills. He later gave a more detailed account of the same collection (Tyrrell, 1916), mentioning quartz-felsites, 'lavaform tuffaceous rocks of doubtful affinities', varying forms of quartz–epidote rock or epidosite, and an augitic rock classified as a dark, fresh vesicular lava. All of the above types were correlated with the 'altvulcanischer' of Heim (1912). A further collection of samples from Larsen Harbour enabled Tyrrell (1918) to classify the extrusive rocks as spilites, found in association with a felsite–trachyte assemblage, decomposed greenstone and epidosite. This spilite assemblage was thought to be related to minor intrusions recorded previously within the greywacke-type sediments on South Georgia, and also to spilitic rocks reported from the South Orkney Islands.

The Larsen Harbour area was re-visited by Wordie during the early part of the British Imperial Trans-Antarctic Expedition, 1914–17, under Sir Ernest Shackleton but the samples collected were lost when the expedition's ship, *Endurance*, was later crushed by pack ice. Wordie (1921) specifically mentioned numerous vertical and inclined doleritic dykes forming two distinct sets.

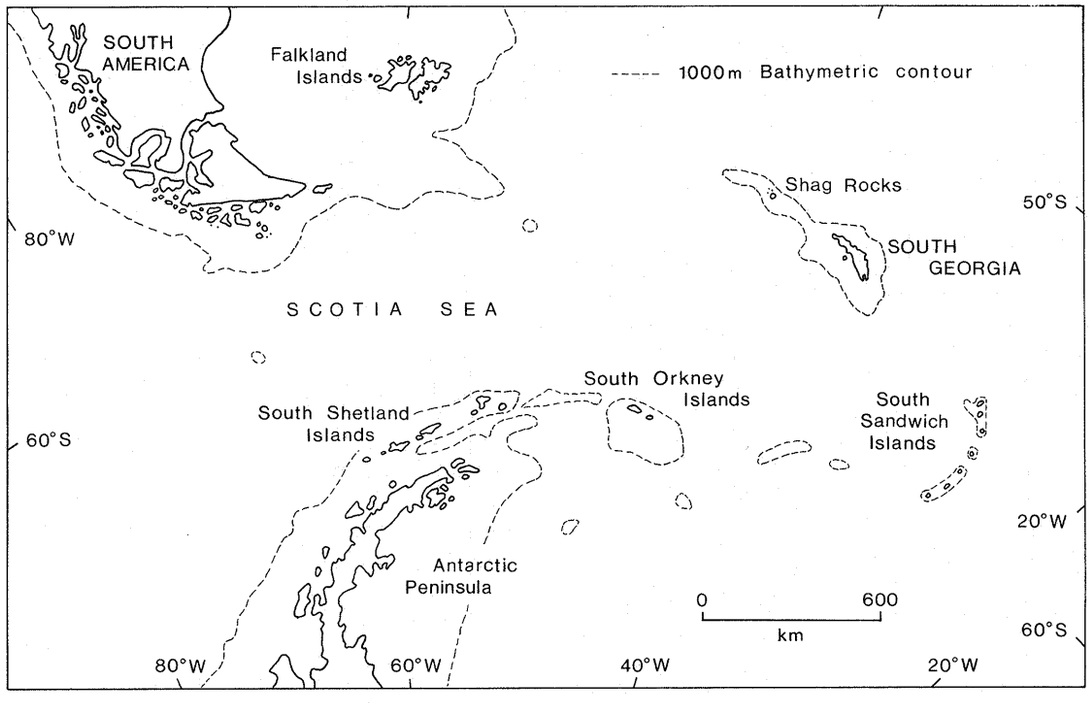

Fig. 1. Location map of South Georgia with respect to South America and the Antarctic Peninsula.

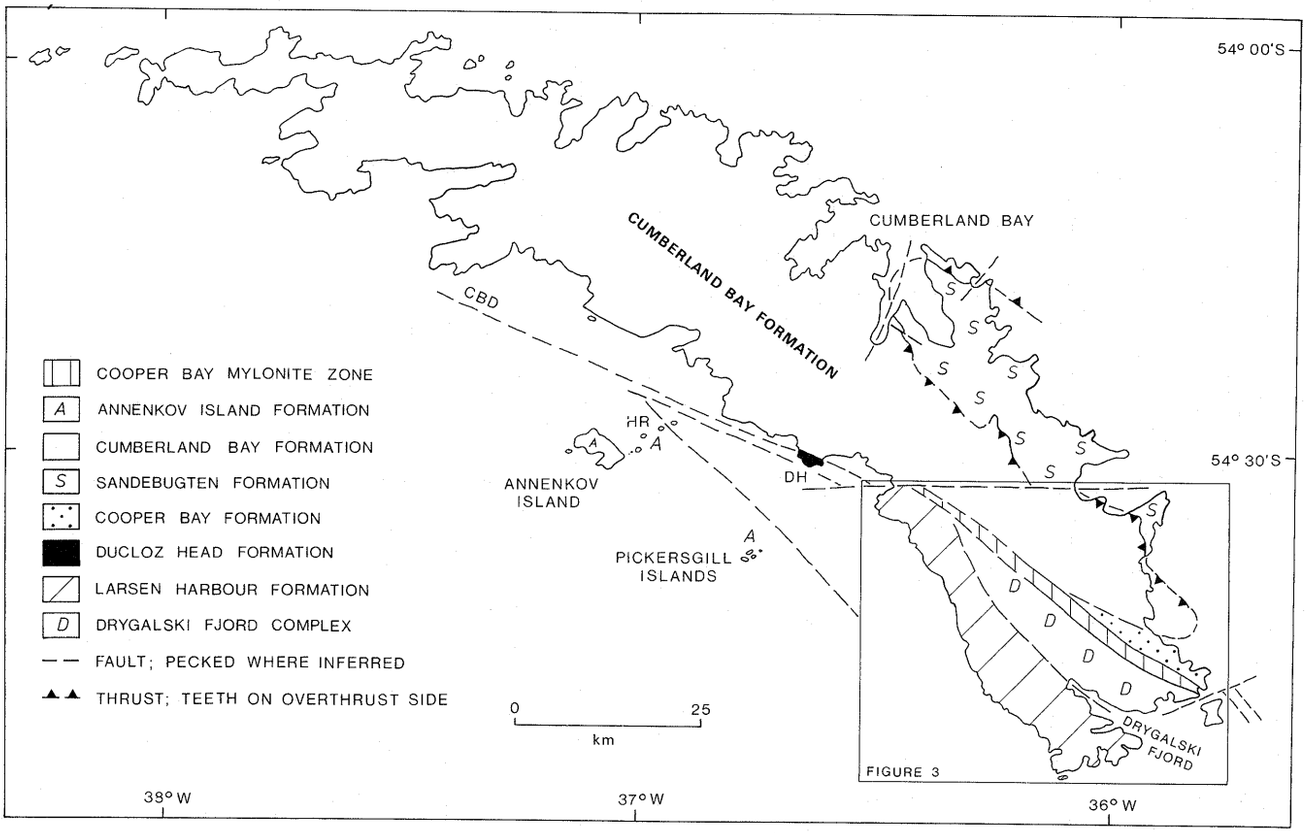

Fig. 2. Simplified geological map of South Georgia.

The earliest maps of Larsen Harbour and the southern coast of the island were compiled by Douglas (1930) during the Shackleton–Rowett Antarctic Expedition, 1921–22 (Figs 5 and 6). Douglas (1930) described an igneous series from Larsen Harbour as 'basement gabbro' overlain unconformably by lava flows of spilite and epidosite dipping to the north-east, and he also mentioned dykes of two ages with strikes varying from 016° to 163°, and dipping from 70°E to vertical. Tyrrell (1930) augmented the work by Douglas and described further rock types including gabbro, peridotite, quartz-diorite, vogesite and granite.

During the Norwegian Antarctic Expeditions, 1927–28, Holtedahl (1929) discovered lavas as far north as Undine South Harbour; he also noted the numerous dyke intrusions in Larsen Harbour. Barth and Holmsen (1939) made a petrological study of Holtedahl's collection and reported igneous breccias (cf. stratiform breccia of this report) containing lavaform fragments from Larsen Harbour and altered diabases from Undine South Harbour.

No further field work was carried out until that of Trendall (1953), who reported the sediment–lava boundary as lying north of Undine South Harbour. He also described well-formed pillow lavas dipping normally and evenly at 30° to the south-west near Undine South Harbour (Trendall, 1953, p. 21). Massive lavas, basalt and spilite were described by Trendall but there was no mention of the 'basement gabbro' or epidosite of Douglas (1930). He recorded lavas dipping at 80°SW in Larsen Harbour, 60°SW at Diaz Cove, and 30°SW near Brøgger Glacier (Trendall, 1959, p. 23), where he considered that they were probably interbedded with sediments of the Cumberland Bay Formation.

B. Present Work

A limited geological survey of this area was carried out in 1955 (Trendall, 1959). Reconnaissance sampling by Dr P. W. G. Tanner at Nattriss Head and Rogged Bay in 1973 led to the detailed survey of the area from Smaaland Cove to Brandt Cove during 10 weeks in 1974 by the author and colleagues (Bell and others, 1977; Storey and others, 1977; Mair, 1983). Additional work was carried out by B. C. Storey in 1975 at Diaz Cove, Wheeler Glacier and Leon Head, and the project was completed by the author in 1976.

The only accurate map of South Georgia (*Falkland Islands Dependencies, South Georgia, 1:200 000*, Tolworth, Directorate of Overseas Surveys, 1958) lacks sufficient detail to be used for field mapping. Vertical air photography, flown at a height of 2 000 m, of the coastline between Smaaland Cove and Drygalski Fjord was undertaken by the helicopter flight of HMS *Endurance* during 1973–74, and between Smaaland Cove and Leon Head in 1974–75. Oblique air photographs of the entire coast from Nattriss Head to Leon Head were taken at low altitudes in 1974–75, giving complete coverage of the coastal strip of the field area. Geological data were recorded on transparent overlays on photographs and later transferred to the base map. Plane-table surveys were made at 1:10 000 to supplement the photographic coverage, but extremes of relief did not allow extensive mapping to be carried out, and also

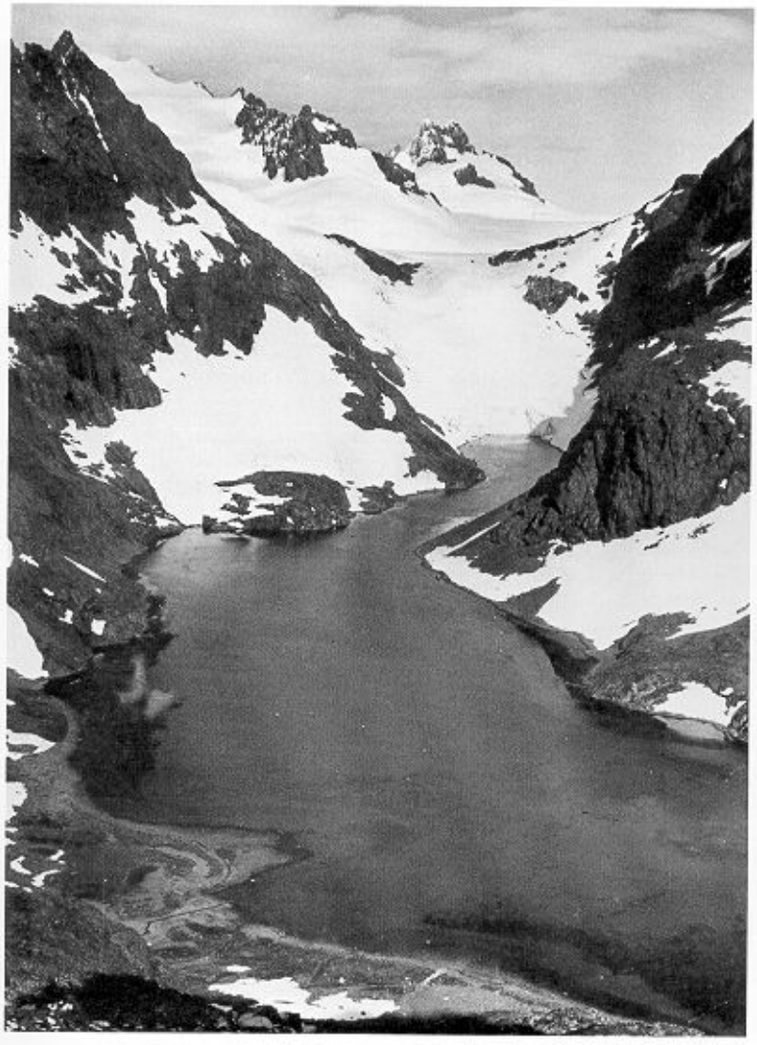

Fig. 4. Fjord-type topography, Larsen Harbour.

caused scale distortion in photographs of inland areas due to the low altitude at which the aerial survey had been flown. However, the scale of the coastal photographs was sufficiently accurate to allow a best-fit mosaic of the peninsula south-west of Drygalski Fjord to be constructed at a scale of 1:12 500. This was subsequently re-drawn at standard 1:10 000 and 1:25 000 scales. The coastal features were aligned, using the coordinates of peaks from the DOS 1:200 000 map, and compass bearings of specific features recorded in the field during the plane-table survey. The magnetic variation used throughout was 7°W and all bearings quoted in this report are given with respect to true north.

C. General Geology of South Georgia

The Larsen Harbour Formation is one of five major stratotectonic units which crop out on South Georgia (Fig. 2). They represent an Upper Jurassic–Lower Cretaceous island-arc–marginal basin system (Dalziel and others, 1975; Suárez and Pettigrew, 1976; Bell and others, 1977; Storey and others, 1977) similar to that from the southern Andes described initially by Katz (1972, 1973) and Dalziel and others (1974). Together with the Drygalski Fjord Complex, the mafic sequence floored the marginal basin which was infilled by the flysch of the Cumberland Bay, Sandebugten and Annenkov Island formations.

The Larsen Harbour Formation is the upper part of an ophiolite sequence which crops out in south-western South Georgia and comprises a tilted but undeformed sequence of mafic and silicic, volcanic and intrusive rocks which was affected by oceanic hydrothermal metamorphism. A sheeted dyke layer may not be present but a plagiogranite pluton and minor associated gabbroic rocks are exposed at the base of the formation.

Most of the island consists of the Cumberland Bay Formation, an ~8 km thick sequence (Trendall, 1959; Tanner, 1982) of polyphasally deformed volcaniclastic turbidites of essentially early Cretaceous but possibly also late Jurassic age (Thomson and others, 1982) thrust over the more quartzose Sandebugten Formation of Mesozoic age (Fig. 2). The sediments are of calc-alkaline parentage containing andesitic and dacitic clasts probably derived from an early island arc.

Regional metamorphism and deformation of the Cumberland Bay Formation increases from the south-west to

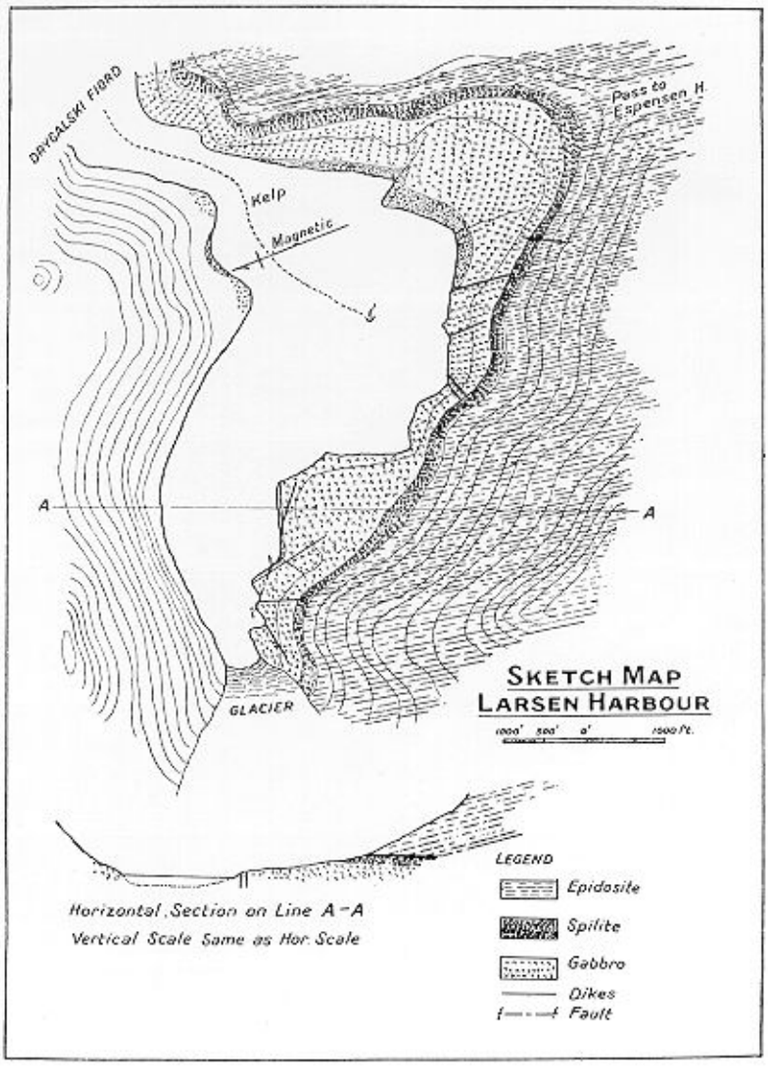

Fig. 5. Early geological sketch map of Larsen Harbour (Douglas, 1930).

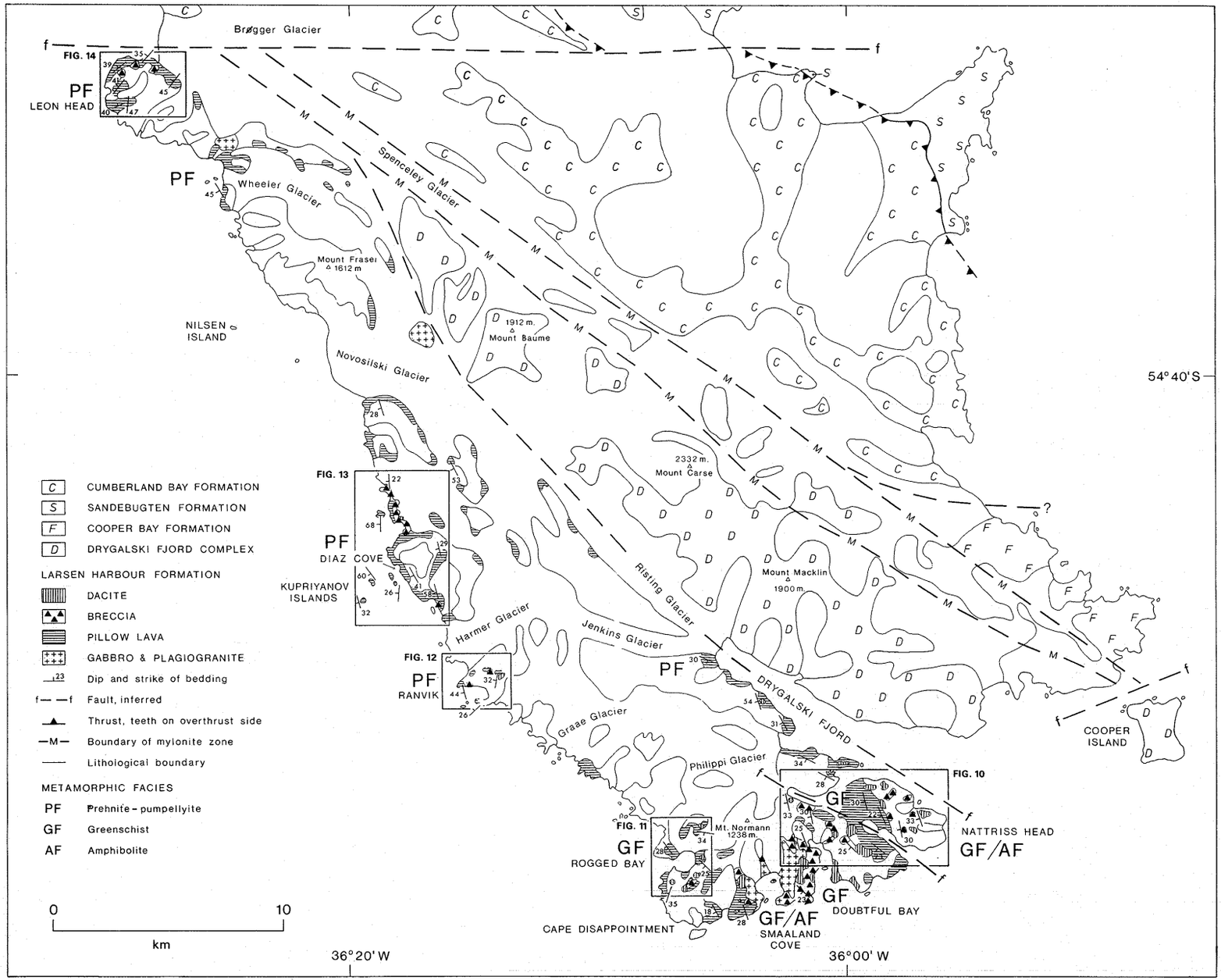

Fig. 3. Summary map of the Larsen Harbour Formation and adjacent units.

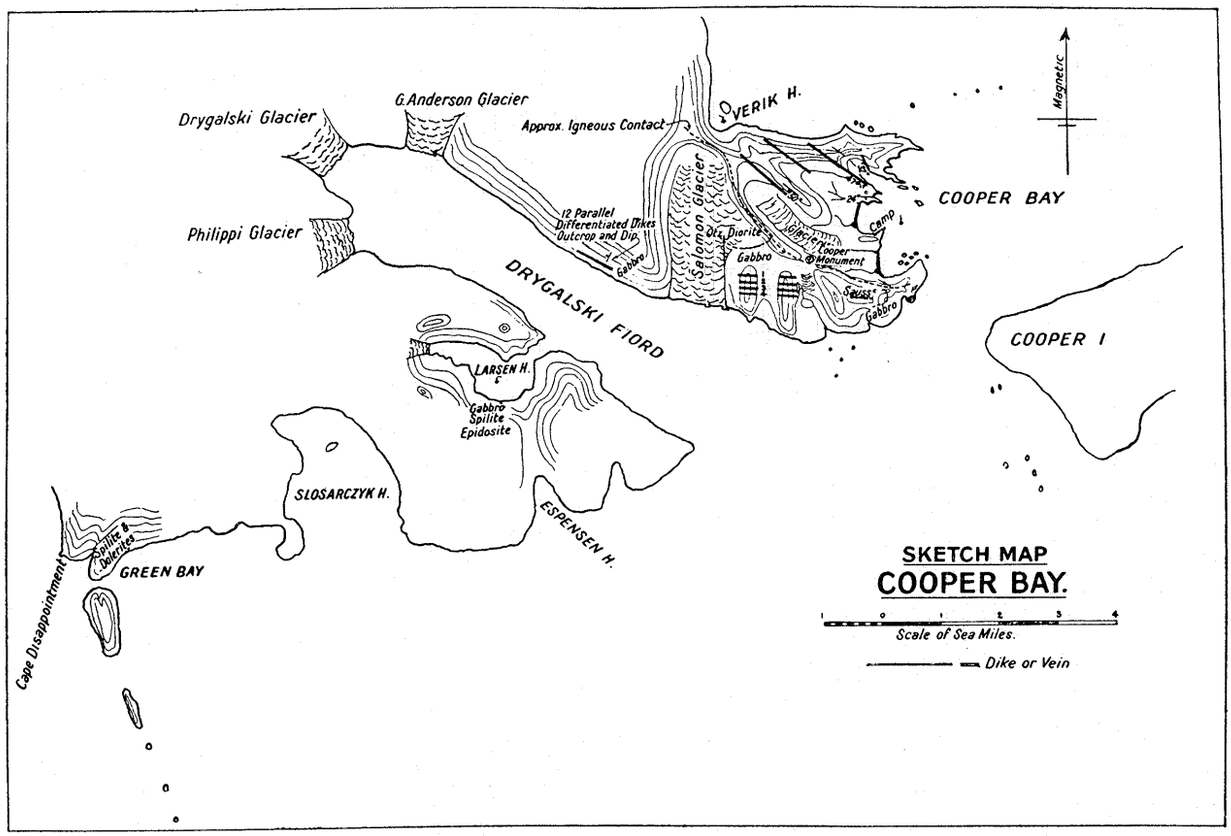

Fig. 6. Early geological sketch map of southern South Georgia (Douglas, 1930).

the north-east. This formation is thrust over the Sandebugten Formation, which comprises turbidite-facies rocks. They are more siliceous, less thickly bedded and more strongly deformed than those of the Cumberland Bay type. Both Sandebugten and Cumberland Bay formations are intruded by pre-tectonic gabbroic and diorite intrusions along the north-east coast of the island (Trendall, 1953; Stone, 1980, 1982; Mair, 1981) which are probably related to magmatism of the mafic volcanic sequence forming the floor of the marginal basin. The Ducloz Head Formation, which consists of massive silicic volcaniclastic sedimentary rocks and basaltic pillows, together with andesitic tuffs and mudstones, crops out north of Brøgger Glacier (Figs 2 and 3) and is correlated with the Sandebugten Formation (Storey, 1983*b*), as is the Cooper Bay Formation (Stone, 1982). A major break (Cooper Bay dislocation) separates the Larsen Harbour Formation, Drygalski Fjord Complex and Ducloz Head Formation from the two major flysch units on South Georgia (Figs 2 and 3) but the amount and direction of movement across it is unknown (Stone, 1980).

Cropping out to the west of the main island of South Georgia is the Annenkov Island Formation (Fig. 2), a gently tilted sequence of island-arc-derived pyroclastic rocks over 1 860 m thick and of intermediate composition (Suárez and Pettigrew, 1976). This sequence is subdivided into a Lower Tuff Member, consisting of finely laminated tuffaceous mudstones, and an Upper Breccia Member, which conformably overlies the former and includes coarse breccia units, volcaniclastic sandstones and subordinate mudstones. The sediments are intruded by irregular and sill-like andesite bodies and spilitic sills, and are metamorphosed to zeolite facies. Recent work by Tanner and others (1981) on Hauge Reef (Fig. 2) has shown that the total thickness of the Annenkov Island Formation is nearer 3 km. The geochemistry of the Annenkov Island Formation is discussed later in this report.

Immediately east of the mafic volcanic rocks comprising the Larsen Harbour Formation are the spatially separate intrusions of the Drygalski Fjord Complex (Figs 2 and 3), previously described by Trendall (1959), Bell and others (1977), and Storey and others (1977). The complex consists of polyphasally deformed siliceous metasediments and gneisses cut by a variety of dominantly gabbroic and minor granitic rocks, all of which are cross-cut by at least two basic dyke suites (Storey, 1983*a*). The dyke suites are possibly related to those of the Larsen Harbour Formation.

II. FIELD RELATIONSHIPS OF THE LARSEN HARBOUR FORMATION

The mafic volcanic and interbedded sedimentary rocks of the Larsen Harbour Formation comprise an autochthonous, composite unit, probably less than 2 km thick, which crops out in southern South Georgia (Figs 2 and 3). The lavas were metamorphosed to prehnite–pumpellyite and greenschist/lower amphibolite facies closely following their extrusion but

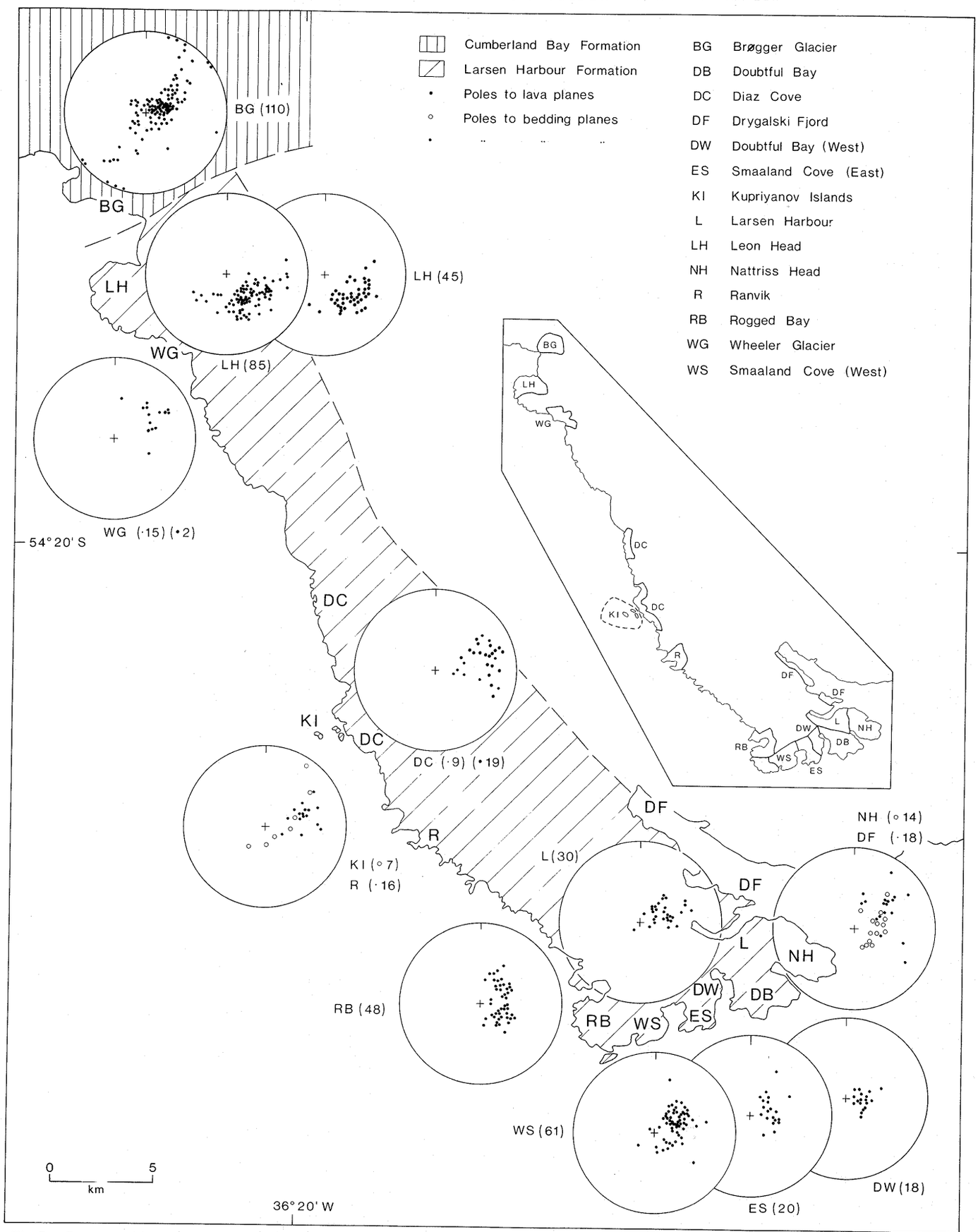

Fig. 7. Stereographic projections showing poles to bedding and pillow-lava planes of the Larsen Harbour Formation. The inset shows the division into sub-areas. Numbers of measurements made are shown in brackets.

are undeformed apart from post-depositional tilting and faulting. The dip of interbedded sedimentary rocks varies from 25° to the south-west in the south to 42° to the north-west in the north, generally increasing towards the west in the higher, younger lavas. Faulting may have caused displacement of adjacent blocks after deposition and consolidation. Where sedimentary units are indistinct, bedding data were recorded from the flat bases or tops of uniformly dipping pillow-lava sequences (Fig. 7). These dips are often steeper (>56°) than those measured from sedimentary bedding and may indicate extrusion on an inclined palaeosurface.

Cumberland Bay Formation sedimentary rocks crop out at Austin Head, and on the north side of Brøgger Glacier, 2 km from the nearest exposure of pillow lava on Leon Head. They have a predominant south-west dip but have been folded about north-west-trending axes, contrasting with the undeformed, north-westerly dipping lavas at Leon Head (Fig. 7). The south-westerly dip of the sediments parallels that of some lavas to the south and this, combined with the increase of sedimentary material associated with the more northerly volcanic rocks, may have led earlier workers to suggest that a conformable boundary exists between the two formations in the Novosilski Glacier area. Both areas have also been subjected to extensive quartz veining but these veins show dissimilar trends (Fig. 8).

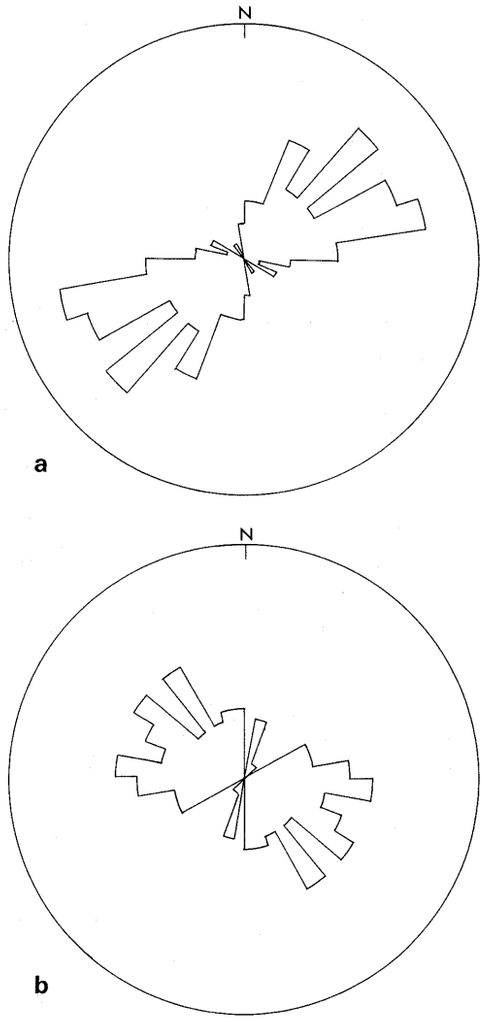

Fig. 8. Quartz vein trends in: a. Cumberland Bay Formation (74 veins); b. Larsen Harbour Formation, near Brøgger Glacier. Data are plotted as percentages and circle radii equal 20%.

A. Mafic Lavas

Geological stations and corresponding specimen localities (e.g. M.2397) referred to in the following text, figures, and tables of analyses, are shown in Fig. 9.

1. Pillow lavas

Pillow lavas form an estimated 60% of the extrusive rocks; they occur throughout the Larsen Harbour Formation but are less abundant on Nattriss Head in the south-east (Figs 3 and 10–14). Each pillow is a lensoid to sub-rounded individual unit moulded against its neighbour when seen in cross-section. In plan view they exhibit a more complex shape, having a bulbous, irregular, often bifurcating (Y-shape) form, as though solidified while in the process of splitting into smaller units (M.3771; Fig. 15). They resemble the tube-like bodies described by Vuagnat (1975). Jones (1969) stated that different pillow forms characterize their modes of formation, analogous to subaerial flows of pahoehoe lava which propagate by digital advance and successive protrusion of hot lava. This method has been discounted by Johnston (1969) but the idea of pillow lavas associated with connected tubes (Jones, 1969; Vuagnat, 1975) is strengthened by detailed observations of pillow lavas on the submarine Puna Ridge, Hawaii (Fornari and others, 1978). They stated that pillow forms accumulate vertically on the sea floor as 'pillow walls' fed internally by intrusive dykes. On the margins of the lava mounds, tubular forms of lava flow downslope and bifurcate into digital pillow units with ornamented skins (Fornari and others, 1978, p. 615, fig. 9). Other pillows are more regular in appearance, having a truly spherical shape.

Each pillow is enveloped in a skin generally 4 cm thick, usually darker and finer-grained than its interior; it may be unornamented, rippled or show intensive fracturing (Fig. 16). Pillow sizes vary but are more uniform in thicker flows. They average 75 cm long by 40 cm thick; in exceptional cases they may range from 1 m to 2.5 m in length, 35 cm to 45 cm in thickness and form lobate tongues that are almost unrecognizable as true pillows. The thickness and areal extent of separate flows are uncertain as successive flows are seldom separated by a breccia or sedimentary horizon. Overlapping lensoid slabs, emphasized by weathering along specific planes, may represent individual flow units up to 30 m thick at Leon Head (M.3774; Fig. 17). They are commonly interbedded with massive or amygdaloidal lavas, various breccias, tuffs or chert deposits, and represent submarine extrusion of basaltic magma.

2. Massive and amygdaloidal lavas

Massive and amygdaloidal basic lavas occur sporadically and form a minor part of the Larsen Harbour Formation. Massive lavas are locally abundant at Leon Head (M.3777) and beside Wheeler Glacier, whereas amygdaloidal lavas occur at Rogged Bay (M.3711) and Nattriss Head (M.3753; Figs 10–14). The textural similarity of the massive lavas to that of low-angle sills and dykes complicates their identification. The amygdaloidal types contain chlorite-, epidote- or quartz-infilled amygdales up to 4 cm in diameter. Outcrops of massive

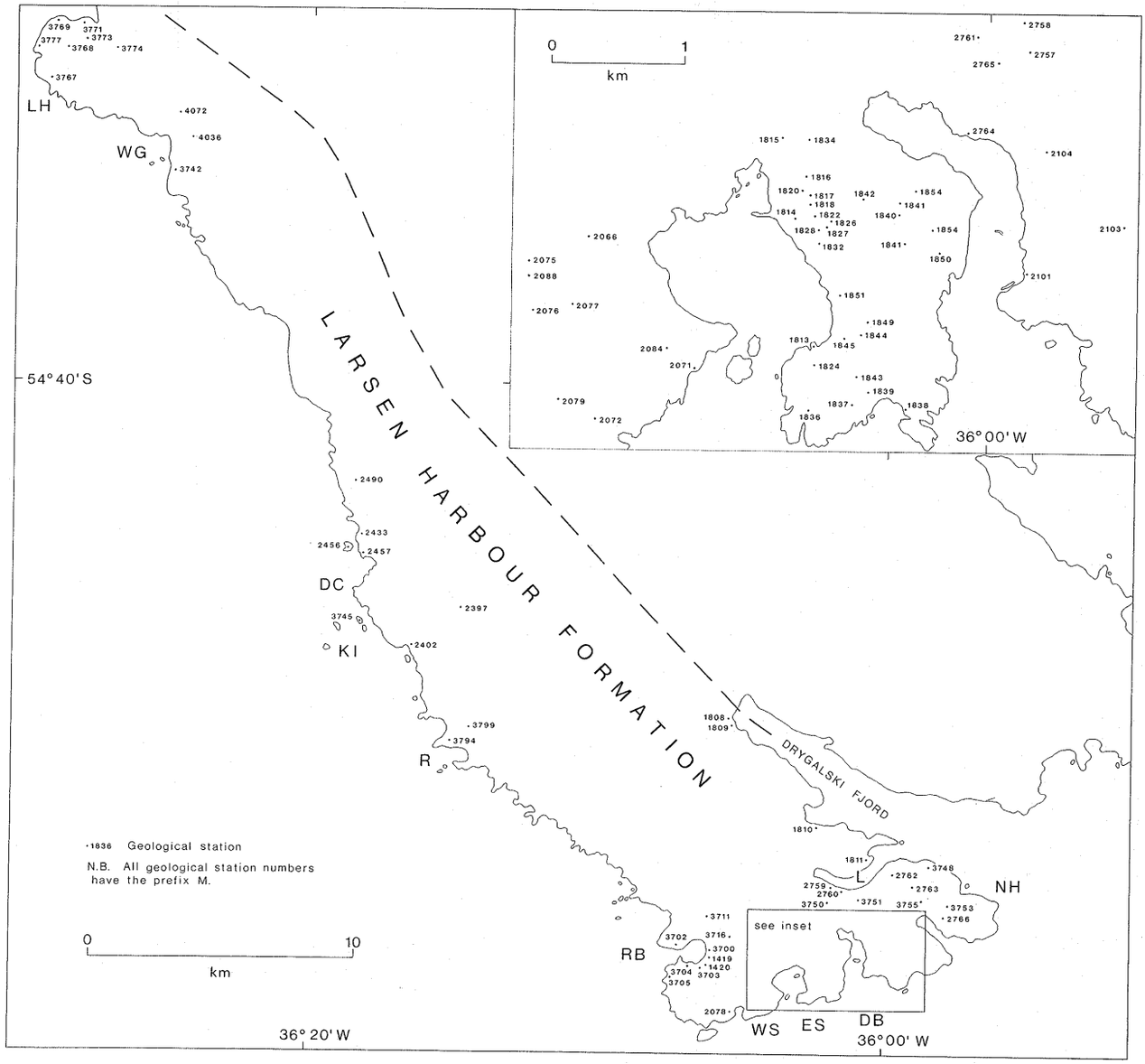

Fig. 9. Location of geological stations mentioned in the text and tables.

lava at Leon Head and Diaz Cove show crude columnar jointing and cooling cracks (personal communication from B. C. Storey; Fig. 18), and at Leon Head the tops of lava flows have a corrugated surface (M.3767; Fig. 19), not unlike pahoehoe flows. Amygdaloidal lava is thought to be the main source material of the xenoliths within the stratiform breccia (below).

B. Breccias

The mafic lavas of the Larsen Harbour Formation are commonly found associated with thick (~ 12 m) lensoid breccia units, caused by autobrecciation of the lavas or their post-consolidation fragmentation. Two main types have been recognized, namely a stratiform breccia (Mair, 1983) and a pillow breccia. These breccias may also contain fragments of re-worked dacites and tuffaceous sediments from within the extrusive sequence. Both occur together but are distinct in character and in origin. Breccia units may identify inter-lava flow boundaries, often being associated with minor tuff and chert bands, and pinch out along strike. Similar deposits infill a fissure developed within an earlier pillow-lava flow at Leon Head (M.3773), and on the Kupriyanov Islands a thick unsorted breccia unit cross-cuts an older dyke which in turn intrudes an underlying sequence of pillow lavas (M.3745; Fig. 20).

1. Stratiform breccia

This hyaloclastite breccia, limited to the lower levels of the formation and associated with tuffaceous sedimentary rocks, is composed of fresh, amygdaloidal, basaltic fragments set in an agglomeratic, epidote- and chlorite-rich matrix (Mair, 1983, figs 7 and 8; Fig. 21). It crops out over much of Nattriss Head (M.3749; Fig. 10) to the exclusion of pillow lavas, and also in Larsen Harbour, Doubtful Bay and Smaaland Cove (Mair, 1983, fig. 2). Locally it is derived by

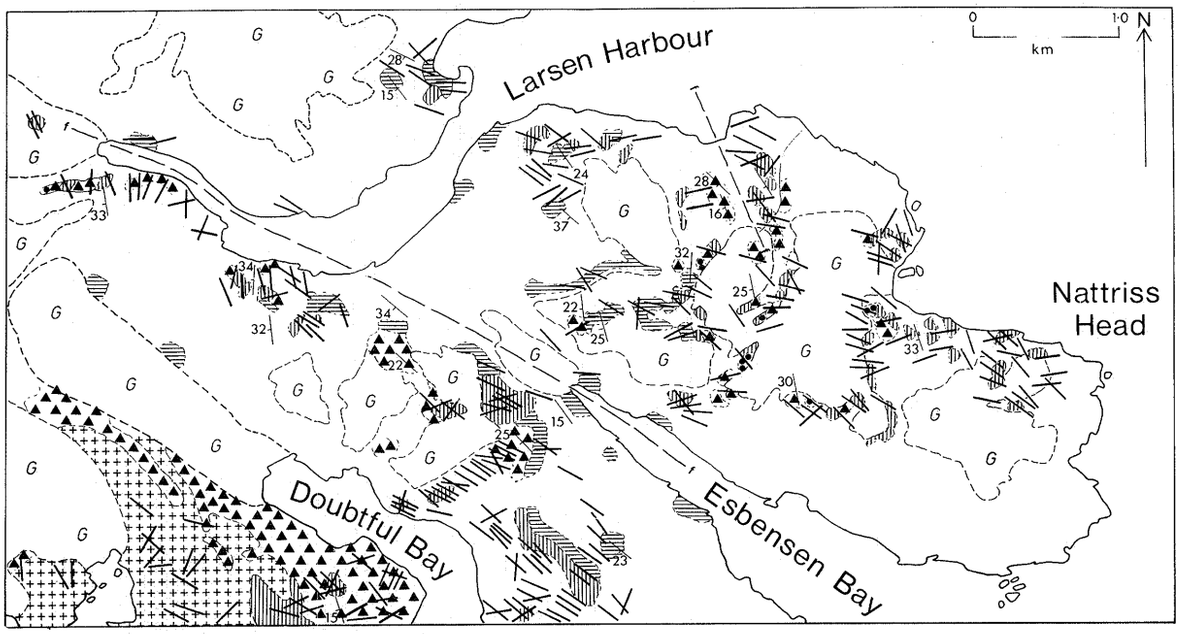

Fig. 10. Detailed geological map of Nattriss Head. The key is the same as in Fig. 11.

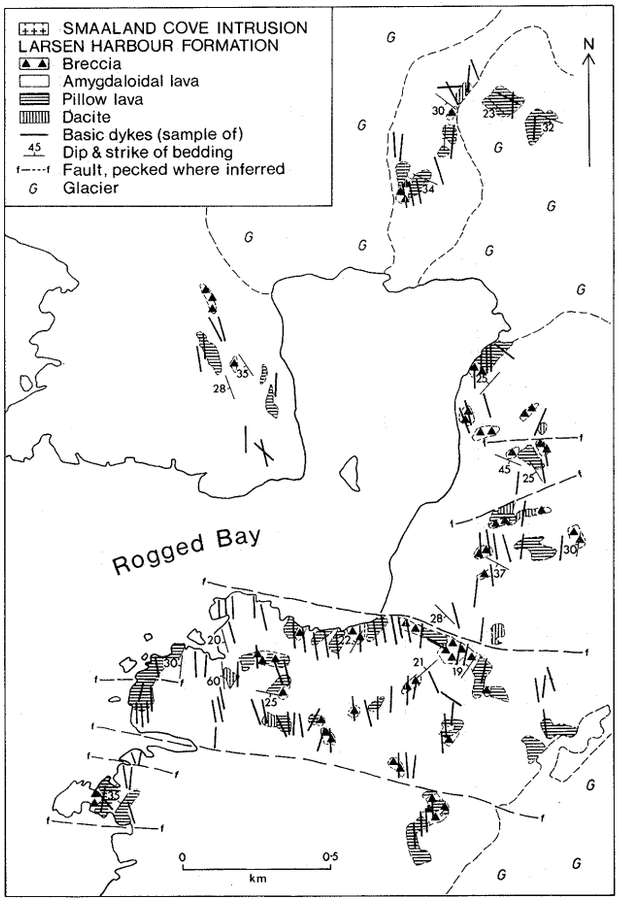

Fig. 11. Detailed geological map of Rogged Bay.

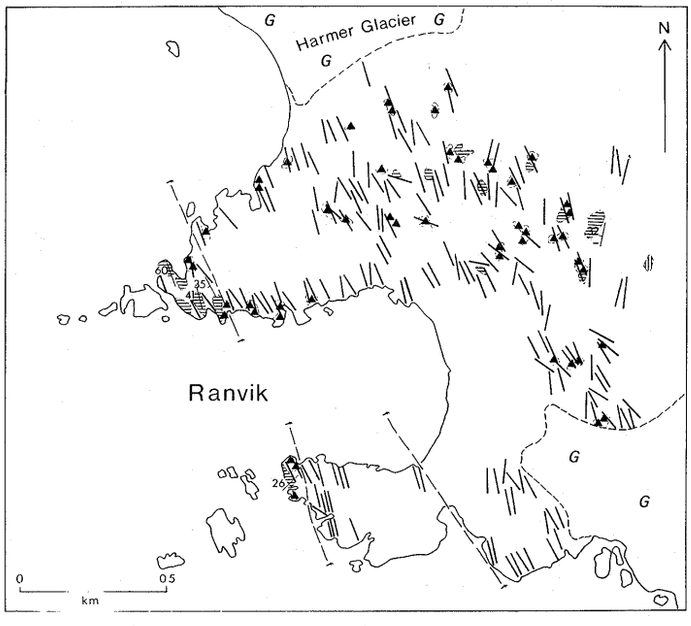

Fig. 12. Detailed geological map of Ranvik. The key is the same as in Fig. 11.

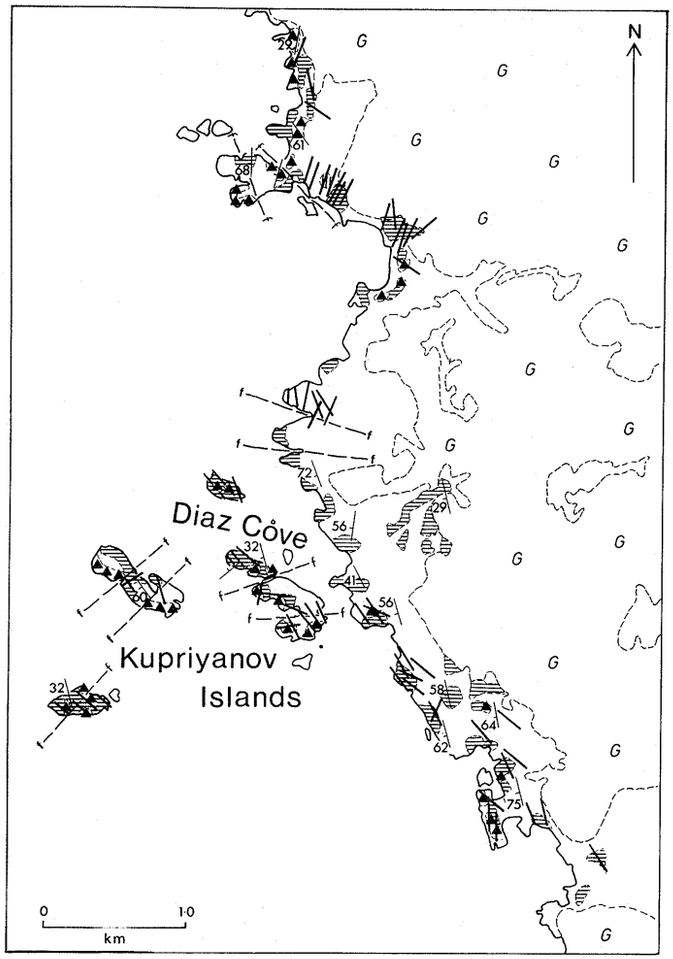

Fig. 13. Detailed geological map of Diaz Cove. The key is the same as in Fig. 11.

the autobrecciation of massive amygdaloidal and pillow lavas as a result of explosive interaction with sea-water. The stratiform breccia is generally matrix-supported, containing rounded, elongate basaltic fragments often orientated parallel to local bedding in a matrix of hyaloclastite debris. Alteration rims developed on the clasts suggest chemical interaction at high temperatures. The amount of matrix, roundness of clasts, percentage of amygdales and degree of alteration vary throughout. It resembles the hyaloclastite breccias described by Silvestri (1963). Similar breccias occur in the spilite–keratophyre suite of the Lahn–Dill region, Germany (Juteau and Rocci, 1974, p. 270, fig. 4), and in the Sarmiento ophiolite, South America (de Wit and Stern, 1978).

2. Pillow breccias

The pillow breccias lack the bedded and well-sorted character of the stratiform breccia (Fig. 22). The fragments are sharply truncated, retain their original textures and lack the pervasive alteration rim which encloses the xenoliths of the first breccia; this implies a 'cold', mechanical rather than 'hot', chemical method of brecciation. They form thick (> 3 m) units at Diaz Cove (M.2402), the Kupriyanov Islands (M.3745) and Leon Head (M.3767), in association with pillow lavas.

Both the 'isolated pillow breccia', and 'broken pillow breccia' of Carlisle (1963) have been observed, brecciation having taken place after initial consolidation of the pillow forms. The 'isolated pillow breccia' contains whole or fragmented detached pillow units within a tuffaceous matrix, usually overlying a homogeneous pillow-lava flow from which pillows have been eroded. Only limited transport of the pillowed material has

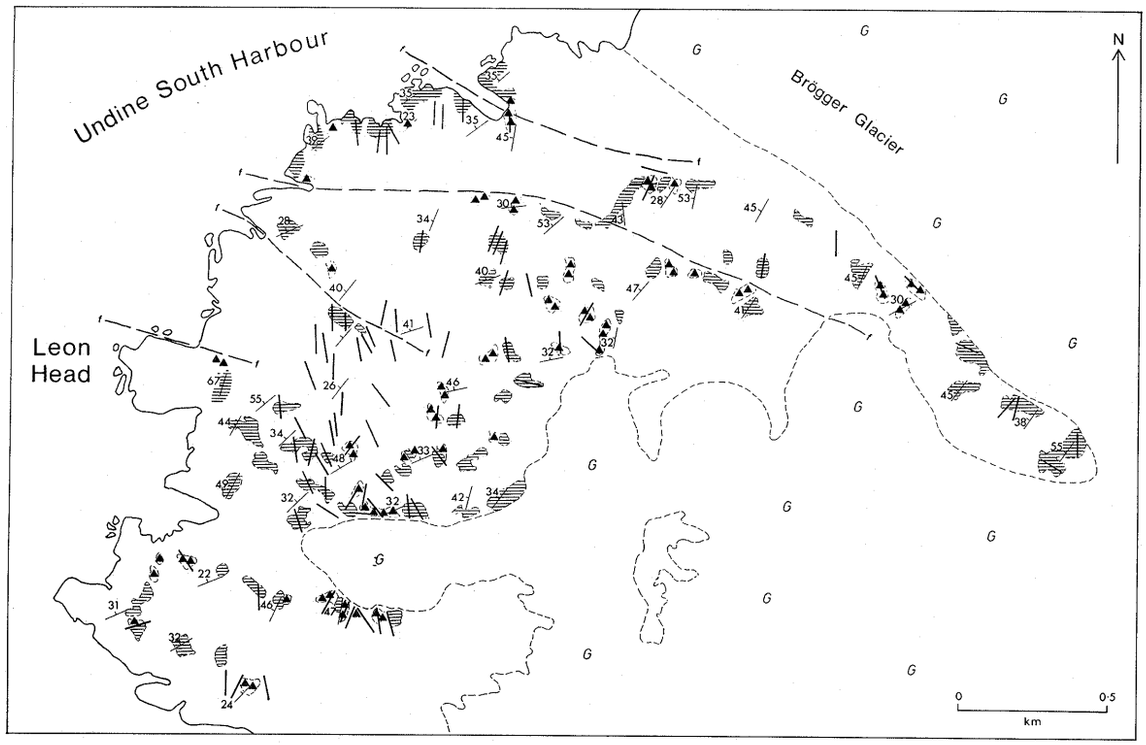

Fig. 14. Detailed geological map of Leon Head. The key is the same as in Fig. 11.

Fig. 15. Y-shaped pillow, bifurcating down-dip, Leon Head (M.3771). The hammer shaft is 60 cm long.

Fig. 16. Intensive fracturing in pillow lava, Diaz Cove (M.2390). The scale bar is 13 cm long.

Fig. 17. Gently dipping, overlapping 30 m thick pillow lava flows, Leon Head (M.3774). The cliff is approximately 130 m high.

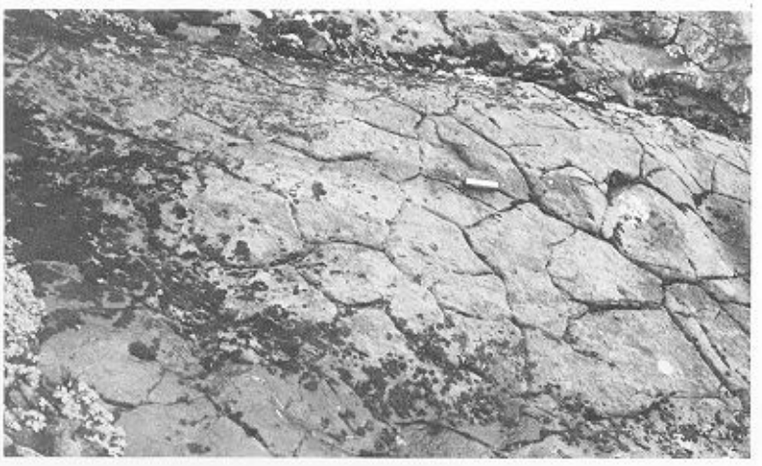

Fig. 18. Columnar jointing in basic lava, Leon Head (M.4044). The scale bar is 13 cm long.

Fig. 19. Pahoehoe-like ripples is basic lava, Leon Head (M.3767). The hammer shaft is 60 cm long.

occurred and complete pillows comprise only a minor part of the breccia, which is essentially matrix-supported. The 'broken pillow breccia' is found in association with the former type but represents a more advanced form. It contains less sedimentary material and is clast-supported, most of the pillows having been brecciated completely with only a few whole pillows remaining.

Fig. 20. Early basic dyke truncated by a later pillow breccia unit, Kupriyanov Islands (M.3745). The hammer shaft is 60 cm long.

Fig. 21. Stratiform breccia; lensoid lava fragments in hyaloclastite matrix, Nattriss Head (M.3749). The scale bar is 13 cm long.

Such breccias develop at the base of 'pillow walls' from which individual pillows or fragments have collected by gravity at ocean-ridge localities (Fornari and others, 1978). Both types occur in the Chilean ophiolites (de Wit and Stern, 1978).

C. Dacites

Silicic lavas and dykes crop out extensively in Doubtful Bay, Larsen Harbour and Smaaland Cove (Mair, 1983), at Nattriss Head and Rogged Bay, and isolated outcrops at Ranvik (M.3799) and Diaz Cove (M.2457; Figs 10–14). They are restricted to the lower levels of the mafic lava sequence. These rocks were described previously as rhyolites (Bell and others, 1977; Storey and others, 1977; Mair, 1983) but they are re-classified here as dacites.

Local deposits of silicic rocks, which crop out laterally over 100 m, are up to 50 m thick in west Smaaland Cove (M.2068) and Doubtful Bay (M.2757). On the eastern side of Nattriss Head a prominent boundary, traceable over 200 m and visible from seaward, separates a 250 m thick sequence of acidic rocks (Fig. 10) from bedded stratiform breccias without pillow lava (M.3748). These larger dacite bodies are probably unconformably overlain by and associated with mafic lava breccias (Mair, 1983, fig. 2). Dacite breccias containing infrequent mafic fragments are commonly developed as a result of autobrecciation of the acidic magma during its emplacement (M.2757; Fig. 23).

Fig. 22. Angular, unsorted pillow breccia fragments and dyke margins, Leon Head (M.3767).The hammer shaft is 60 cm long.

Fig. 23. Dacite breccia, Doubtful Bay (M.2757). The hammer shaft is 60 cm long.

The dacites were emplaced contemporaneously with the older pillow lavas and dykes at the base of the formation and pre-date the plagiogranite intrusion in Smaaland Cove. Silicic differentiates of basaltic magma are an important but minor constituent of ophiolite sequences (Coleman and Peterman, 1975) and mid-ocean ridges (Carmichael, 1964; Byerly and others, 1976).

The lava sequence is intruded by vertical silicic dykes in Doubtful Bay (M.2760) and Smaaland Cove (M.1854); these trend 130°. They occur as truncated screens within the abundant basic dyke sets and as distinct units associated with flow-banded and extrusive acid rocks. Unlike the basic dykes, the silicic dykes have more gradational and sinuous chilled margins against the country rock, and are generally less than 1 m thick. The dykes are light brown in colour, massive or porphyritic, often with feldspar phenocrysts displaying flow alignment in discrete bands. The larger intrusive bodies are less regular and often obscured by later basic dykes but, between Smaaland Cove and Rogged Bay, at least two 50 m high, upright, tapered units, 10 m across, cross-cut the pillow lavas (M.3716; Fig. 24) and have flow-banded margins and massive centres.

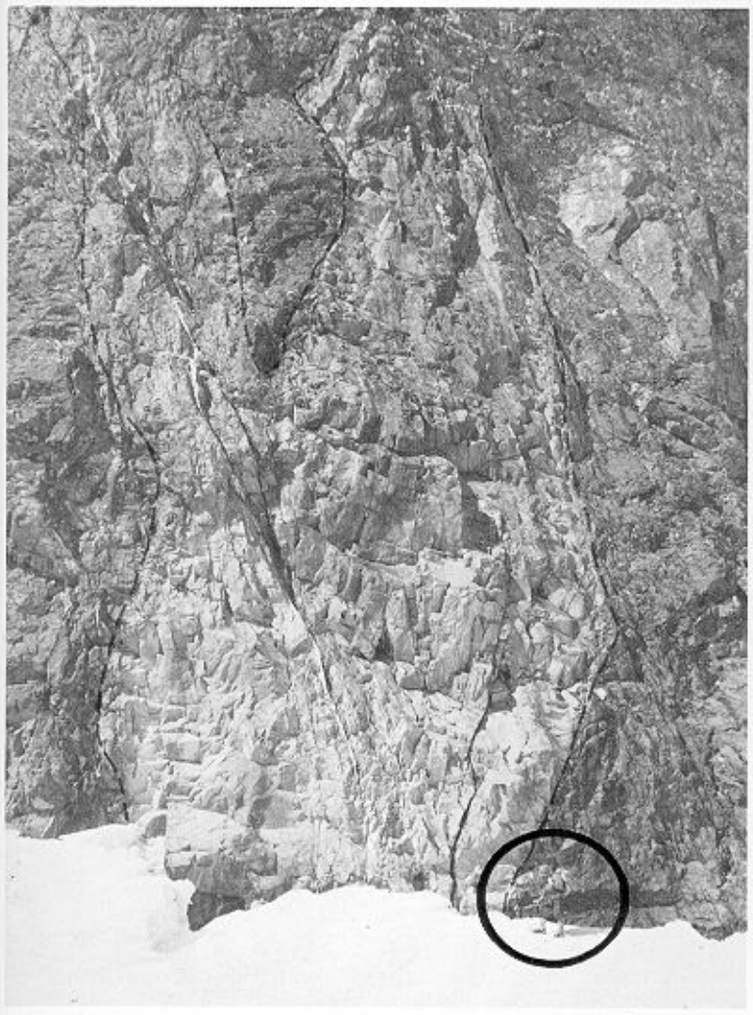

Fig. 24. Tapered dacite intrusion emplaced into pillow lava, near Rogged Bay (M.3716). Note the figure (ringed) for scale.

Extrusive silicic lavas, generally light-coloured, amygdaloidal and flow-banded, crop out concordantly with tuffaceous sediments in Larsen Harbour (M.3752), Doubtful Bay (M.2765) and Smaaland Cove (M.1842). The flow banding is seldom regular and locally may be steeply dipping due to flow folding (Mair, 1983, figs 9 and 11). Individual extrusive units are up to 5 m thick but more typically they are between 0.8 and 2.5 m thick and can be traced for up to 50 m. They are often amygdaloidal and/or porphyritic. Amygdales are up to 4 cm long, flow-orientated and filled with quartz, chlorite, calcite or epidote; feldspar phenocrysts and quartz spherules occur in the porphyritic type (Mair, 1983, fig. 10). The thicker silicic bodies grade upwards from a flow-banded base to a massive centre, with marginal breccias developed (M.2765).

D. Minor Intrusions

The dyke suites, following three main trends (070°, 130° and 175°), form an integral part of the mafic lava sequence and are a conspicuous feature of the Larsen Harbour Formation (Mair, 1983, fig. 3; Fig. 10). By contrast, low-angle sills are less abundant but occur throughout the area, often being indistinguishable from massive lava sequences. The number and thickness of basic dykes within the lavas varies from areas where country rock is totally excluded to those with 20% or less intrusive material. Limited screens of country rock (mafic lava), usually less than 10 m wide, occur within the complex dyke swarms in Doubtful Bay (M.2104) and near Wheeler Glacier (M.4036) where crustal extension has been calculated from measured sections as exceeding 53%. In contrast, at Leon Head (Fig. 14) screens of country rock are more abundant than dyke material.

1. Sills

A distinctive group of low-angle sills dipping at 30° or less crop out at Nattriss Head, Ranvik, the Kupriyanov Islands and Diaz Cove, but they show no preferred orientation (091°, Leon Head; 192°, Kupriyanov Islands; 137°, Nattriss Head). Well-defined sills are found in the breccias of the Kupriyanov Islands (M.3745) and at Nattriss Head (M.3753), where they exhibit upper and lower chilled margins and often show a regularly banded interior defined by feldspar laths (Fig. 25). The pattern of banding is not repeated across the centre of the sill, as in composite or multiple dykes and the resultant 'graded' feature is thought to be due to layering associated with its sub-horizontal intrusion. The sills are finer-grained than the dykes and are sometimes amygdaloidal.

2. Dykes

Texturally, the dykes vary from fine- to coarse-grained (depending on width), they show flow-banded margins defined by feldspar phenocrysts, and are porphyritic or homogeneous, and are dark-coloured. They form linear, straight-sided units with distinctive chilled margins, often repeated due to multiple and composite intrusions. Dyke widths range from 15 to 120 cm, with the majority being 30–55 cm or 75–90 cm across. Thicker dykes (> 5 m) with a consistent trend of 130° crop out at Larsen Harbour and Nattriss Head.

The Smaaland Cove intrusion post-dates the oldest dykes and lavas of the lower part of the formation but is itself cross-cut by younger dyke suites (e.g. at station M.1816). Fewer

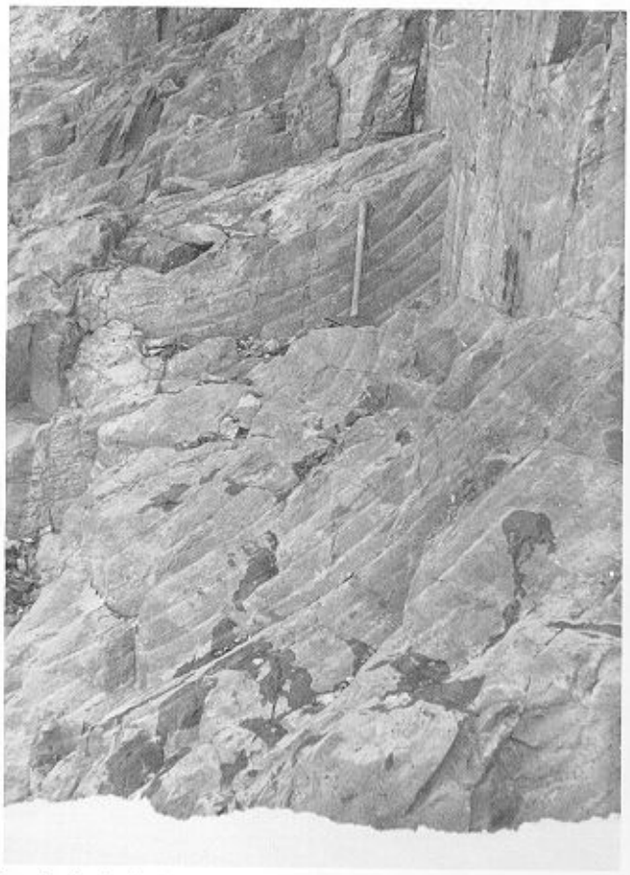

Fig. 25. Rythmically banded sil within stratiform breccia, Nattriss Head (M.3753). The hammer shaft is 60 cm long.

dykes therefore intrude the pluton than the surrounding country rock. Fractured or sheared dykes, which often pinch out and then re-appear in less than 1 m, or show lateral displacement, are common within the pluton (M.1831) but were not observed in the lavas. Similar features are present in the granites and gabbros of the Drygalski Fjord Complex. Quartz veins, up to 40 cm thick and composed of many thin irregular quartz bands, are commonly found along one margin of basic dykes which intrude the mafic lavas (M.3705; Fig. 26), especially at Rogged Bay, Ranvik and Leon Head. The veins are continuous over several metres and parallel systems are developed in the lavas; they may represent late shear zones which utilized the lines of weakness along the dyke margins. The parallelism of many quartz veins to the dykes in any one area is noticeable, although a second set strikes almost at right-angles to the main dyke trend.

1 644 dyke measurements were plotted stereographically and contoured (Fig. 27) for 13 areas within the Larsen Harbour Formation. Concentrations of the higher percentage values (> 10%) are thought to represent distinct dyke sets (Table I). Significant trends were then untilted (assuming that the sediments were horizontal during intrusion of the dykes). Tilted and untilted dyke trends show little change in strike, but most show a reversal of dip direction (Tables I and II). There are three main trends: 070° and 130° (which correspond to those of Trendall (1959)) and a previously unrecorded trend of 175° (Fig. 28).

The 130° trend is strongly developed within the southern part of the formation, especially towards the east and in the Drygalski Fjord Complex but may also be present at Ranvik, the Kupriyanov Islands, Diaz Cove and Wheeler Glacier (Fig. 28). This is the earliest dyke suite, being cross-cut almost without exception by the other two dyke sets. A second dyke suite (070°) is spatially restricted to the east of Doubtful Bay and the Drygalski Fjord Complex (Fig. 28). The 175° set is absent in Doubtful Bay, and only shows a vague correlation with those at Ranvik and the Kupriyanov Islands, which are assigned tentatively to the 130° suite. It occurs throughout the south-west coast, increasing in definition towards the north-west with weaker development to the east, and it is not found within the Drygalski Fjord Complex (Fig. 28). The time relationships of the 070° and 175° suites are ambiguous, possibly because of subsequent re-intrusion along previously established dyke planes, forming multiple or composite dykes, or alternatively both suites may have been intruded contemporaneously.

The structural level of individual areas is not apparent from field or petrological evidence, except that Leon Head represents the highest level and Nattriss Head the lowest and oldest level of the Larsen Harbour Formation. The dykes at Leon Head define a single trend, in contrast to the five trends interpreted from the contoured plots of the data from Nattriss Head. Thus further correlation is uncertain.

The dykes of different trends have a similar petrography suggesting a common parent magma and the changes in orientation may indicate that crustal rotation occurred between successive intrusive phases. Subsidence of the lavas must have taken place to accommodate the extrusion of new material by tilting, and by extensive faulting as in oceanic crust (Kidd, 1977), and these characteristics may explain the differing dips of the lavas. The steeply dipping youngest lavas at Leon Head suggest the close proximity of a former spreading centre and dip towards it.

3. Multiple and composite dykes

Upright multiple and composite dykes are exposed in the lower levels of the Larsen Harbour Formation (Mair, 1983) and occur in Larsen Harbour (M.3751), Brandt Cove (M.1810),

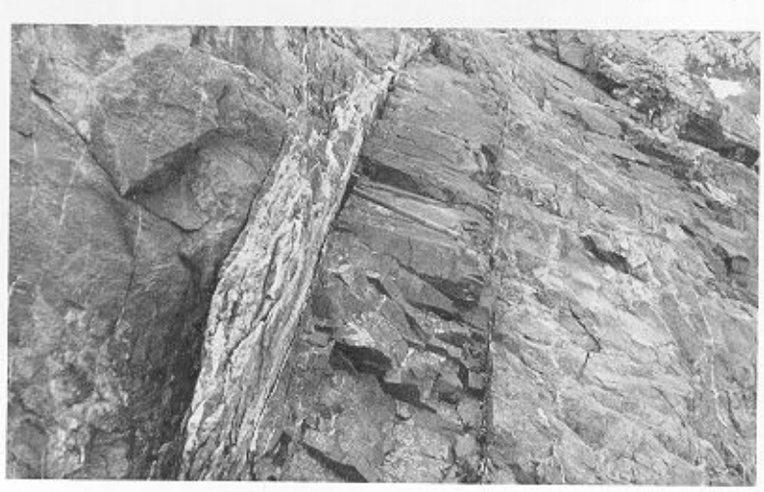

Fig. 26. Complex quartz-veining along one margin of a basic dyke, and thin sub-parallel veins in the adjacent country rock, Rogged Bay (M.3705). The hammer shaft is 60 cm long.

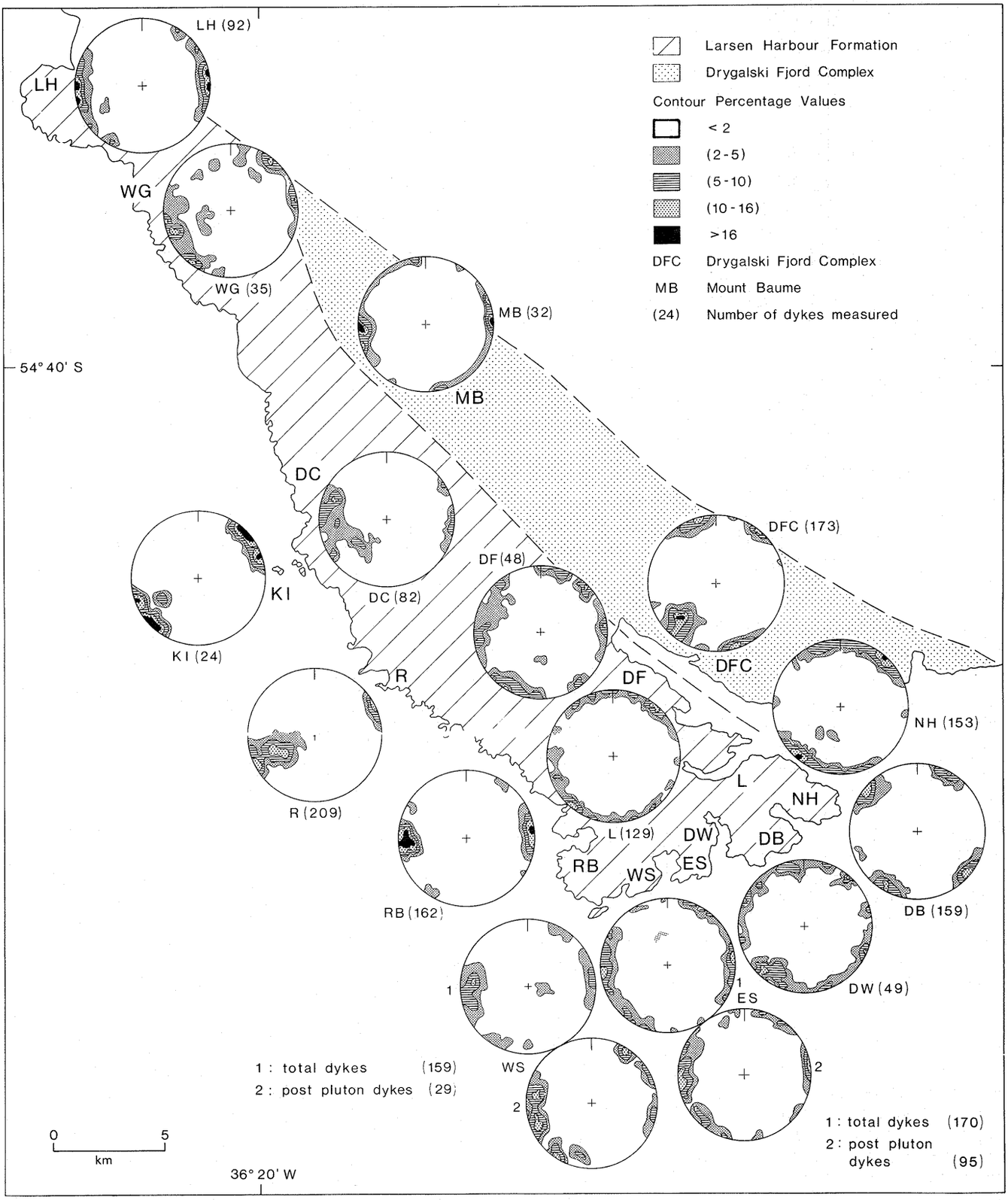

Fig. 27. Contoured, lower-hemisphere stereographic projections of poles to basic dykes. Sub-areas are as in Fig. 7.

Table I. Mean dyke trends for all areas (pre-untilting).

Locality	*ND*	*Attitude of lavas*[1]	*000°*	*030°*	*060°*	*090°*	*120°*	*150°*	*180°†*
Drygalski Fjord Complex*	173				071v			140.66°NE	
Nattriss Head	153	039.20°NW; 170.25°W[2]	006v		079v		107.37°N	129.42°NE 131.86°NE	
Drygalski Fjord	48	142.45°SW			051v	083.36°N	114.81°N	136v	173v
DL	177	162.27°W				072v		131v	
Larsen Harbour	129	148.20°SW; 176.32°W[2]				071v		134v	160.80°E
Doubtful Bay	159	148.20°SW; 176.32°W[2]		039v				123.80°NE	
West Doubtful Bay	49	026.18°W		023v		071.82°E		123.68°NE 133.82°NE	168v
DS	219	001.24°W						131.80°NE	174v
East Smaaland Cove[4]	170	007.25°W						132.82°NE	172v
East Smaaland Cove[3]	95	007.25°W					107v	132.82°NE	172v
West Smaaland Cove[3]	29	160.26°SW	007.77°E				102.72°N		156.79°E
West Smaaland Cove[4]	159	160.26°SW	006.73°E				122v 125v		
Rogged Bay	162	041.24°NW; 147.29°SW[2]					120v		175.80°E
Ranvik	209	160.44°W						152v	
Kupriyanov Islands	24	019.19°W						142v 147.55°E	
KD	106	163.61°W	006v	021.74°E				143v	
Diaz Cove	82	149.50°SW; 163.61°W[2]		020.76°E				144.50°E 148v	
Wheeler Glacier	35	150.58°SW; 165.40°W[2]						128v 160.80°E	172.32°E
WL	127	005.31°NW	002v					143v	178v
Leon Head	92	059.31°NW						153.58°NE 168v	

1, bedding planes, dykes shown thus: 039.20°NW (strike of plane, amount and direction of dip); 2, bimodal attitude of bedding, average value used for untilting in Table II; 3, post-pluton dykes; 4, total dykes; * 071v indicates trend outlined by 10% of dykes measured; † all bearings with respect to true north; DL, Drygalski Fjord and Larsen Harbour; DS, west Doubtful Bay and east Smaaland Cove; KD, Kupriyanov Islands and Diaz Cove; WL, Wheeler Glacier and Leon Head.

Smaaland Cove (M.1841) and Doubtful Bay (M.2764). Up to four chilled margins are repeated across the central zone of some dykes (Mair, 1983, fig. 20). Successive phases of the multiple type differ in texture but those of the composite dykes differ in composition, changing from basic to acid with time. Multiple dykes and repetitive chilled margins are indicative of crustal extension, possibly within a spreading centre (cf. Troodos ophiolite; Kidd, 1977).

E. Tuffaceous Sediments

Thin tuffaceous sequences occur throughout the lava pile, becoming more abundant in the upper levels at Leon Head (Fig. 14). Volcanogenic sediments which crop out in Larsen Harbour, Doubtful Bay and Smaaland Cove consist of thin-bedded, repetitive, graded units of altered lava and chert (Mair, 1983, figs 12–14). Similar sedimentary rocks occur elsewhere on the west coast (Fig. 29).

Jasper is an important constituent and forms units of brightly coloured green chert (M.3768) 30 cm thick at Leon Head. Tuffaceous and mudstone units, 2–3 m thick, more abundant than the cherts, are also present and exhibit graded bedding (M.3769; Fig. 30). They resemble rocks of the Lower Tuff Member of Annenkov Island in colour and texture. Similar tuffaceous material is present in the matrix of the stratiform breccia. Sedimentary breccias or agglomerates form minor bands within the tuff sequences but they are better described genetically as pillow breccias.

The tuffaceous material is thought to have been extruded and subsequently brecciated on the basin floor itself (cf. aquagene tuffs; Carlisle, 1963). Lithic and vitric shards in tuffs, although resembling subaerial types *sensu stricto*, are derived from the disintegration of amygdaloidal, submarine massive and pillowed lavas. Hyaloclastite debris may also have formed by granulation of massive lavas without pillow formation having taken place (Honnorez, 1963; Pichler, 1965).

Submarine volcanism produces pillowed lava forms by tranquil flow and ash-type deposits by explosive emanations (Menard, 1964), depending on the viscosity of the magma concerned (Bonatti, 1967). McBirney (1963) stated that explosive activity of basic magma does not take place below 500 m in water and that acidic magma is similarly restricted

Table II. Untilted mean dyke trends for all areas.

Locality	*000°*	*030°*	*060°*	*090°*	*120°*	*150°*	*180°†*
Nattriss Head*	005.70°W			080.82°N		132.84°SW 133.43°E 145.54°E	
Drygalski Fjord	004.54°W		052v		109.69°N	133.45°SW 121.56°SW	
DL				072v		132.66°SW	
Larsen Harbour				072.89°N		129.69°SW	160.75°W
Doubtful Bay			041.76°W			124.80°SW	
West Doubtful Bay		023.72°W		071.85°W		131.70°NE 136.88°NE	167.76°N
DS						131.84°SW	173.67°W
East Smaaland Cove[1]						134.83°SW	172.65°W
West Smaaland Cove[1]	006.85°W				121.69°SW		
Rogged Bay					119.79°S		176.79°W
Ranvik						149.46°SW 160.80°W	
Kupriyanov Islands						142.80°SW 156.68°NE	
KD		025.36°W 027.58°W			126.35°SW		
Diaz Cove		026.64°W				142.36°SW 147.75°SW	
Wheeler Glacier					117.48°S		161.75°W 167.75°W
WL						144.88°NE	173.74°W
Leon Head							165.80°W 170.65°E 177.74°W

1, total dykes used; remainder of key as for Table I.

unless the magma is water-saturated, whereby the limit is increased to 2 000 m. By contrast, Bonatti (1965) reported that explosive activity is substantial at depth and, similarly, Moore (1965) mentioned that at abyssal depths pulverized glass (hyaloclastite) is the dominant volcanic ash constituent. The action of sea-water within saturated sediment on hot pillowed or massive magma causing disintegration at depth is thought to be an important process in producing tuffaceous debris within the Larsen Harbour Formation. The xenoliths of fresh non-pillowed lava in stratiform breccia are the remnants of initial magma extrusion which formed tuffaceous debris immediately on extrusion. De Wit and Stern (1978) have recently given a similar review of the formation of tuffs within the extrusive units of the Chilean ophiolites.

F. Smaaland Cove Intrusion

The Smaaland Cove intrusion is a multi-phase pluton of dioritic to granitic composition emplaced in the lower part of the lava pile (Figs 3 and 31). It has been dated at 127 ± 4 Ma (Tanner and Rex, 1979) which may be its time of intrusion or subsequent metamorphism. Heim (1912) recorded acid igneous rocks from the southern coast of South Georgia but not *in situ* and the body was first described by the author and colleagues (Bell and others, 1977; Storey and others, 1977; Mair, 1983, figs 2 and 16–18). The roof contact of the 6 km^2 intrusion is 250 m high in the east and 70 m high in the west from where it dips gently south-eastward. Its eastern contact is not seen but is probably bounded by a fault in Doubtful Bay. The pluton was intruded after initial extrusion of the mafic lavas and is thought to be an oceanic plagiogranite (Coleman and Peterman, 1975). It resembles leucocratic rocks described from other ophiolites (Aldiss, 1978), although this implies that it should lie beneath the sheeted dyke zone (Christensen, 1977).

The body intrudes and brecciates the overlying volcanic rocks and xenolith screens are well developed towards the east (e.g. station M.1813; Fig. 31); elsewhere the contact is sharply defined with limited diffusion or interaction of material across it. Xenoliths, where fresh, are distinct and angular, and are often only slightly displaced from their original position. Elsewhere they may be more completely assimilated and occur several metres from the contact. The rocks of the intrusion are of leucocratic to melanocratic aspect, of granular texture and have been shown by modal analysis to comprise quartz-diorite and quartz-gabbro, quartz-monzodiorite, granodiorite, granite and granitoid rocks with minor tonalite and quartzolite. These rock types were not mapped in the field because individual contacts between them are vaguely defined. However, field relationships indicate that the more abundant leucocratic phases are younger than the layered diorites and gabbros which

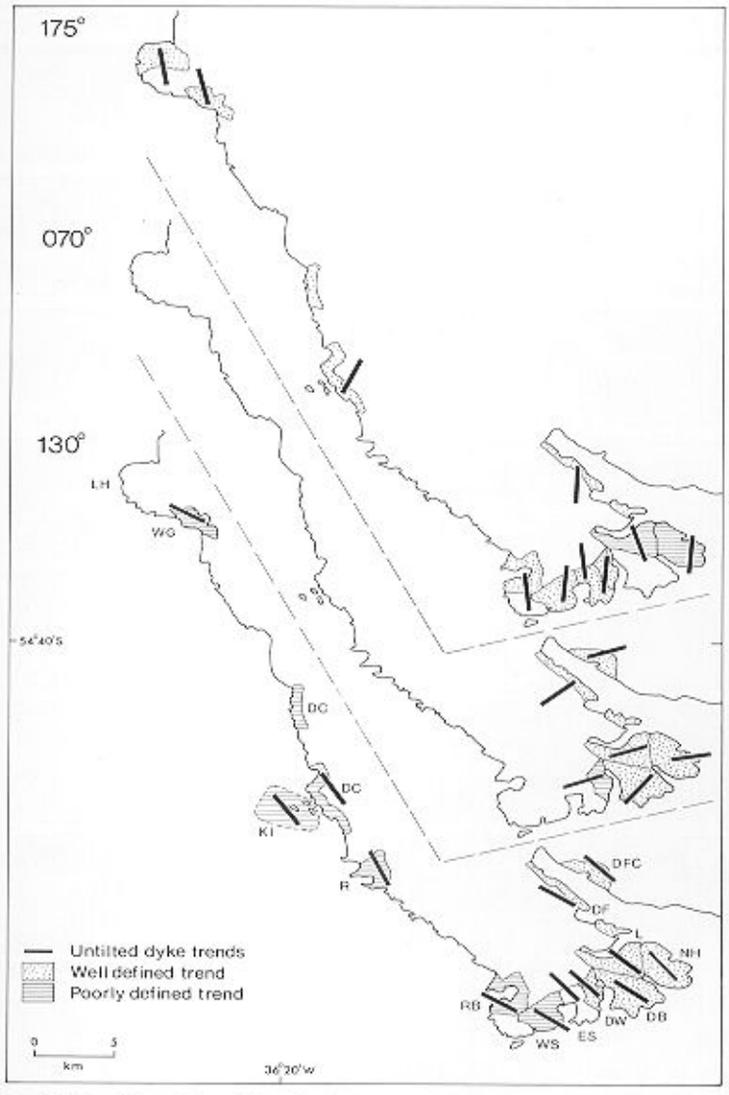

Fig. 28. Spatial relationships of three mean dyke sets, extrapolated from Fig. 27.

crop out at sea-level. These mafic rocks (M.1852 and 1853) may represent part of the stratiform sequence of the ophiolite below the lavas and sheeted dyke layer. No metamorphic aureole is developed around the intrusion, apart from local loss of texture in the overlying lavas and has itself been altered by subsequent oceanic hydrothermal metamorphism.

G. Wheeler Glacier Gabbro

The Wheeler Glacier gabbro is a coarse-grained leucocratic gabbroic body less than 1 km^2 in area which intrudes the lava sequence north of Wheeler Glacier (M.4072; Fig. 3). Much of its contact zone with the pillow lavas is obscured by snow but where visible it is seen to have caused recrystallization and an aureole may be developed. Large irregular patches of epidote and apophyses of coarse mafic minerals are common in the recrystallization zone. It is cross-cut by younger basic dykes. Another isolated gabbro intrusion, which may be equivalent to the Wheeler Glacier gabbro, is exposed at the head of Novosilski Glacier (Fig. 3).

H. Thickness of the Mafic Volcanic Rocks

Preliminary analysis of data (Bell and others, 1977; Storey and others, 1977) suggested that the Larsen Harbour Formation possibly comprises up to 5 km of oceanic crust,

Fig. 29. Finely laminated graded tuffs within stratiform breccia, Nattriss Head (M.3755). The hammer shaft is 60 cm long.

Fig. 30. Thick bedded sequence of tuffaceous mudstones within pillow lavas, Leon Head (M.3769). The scale bar is 13 cm long.

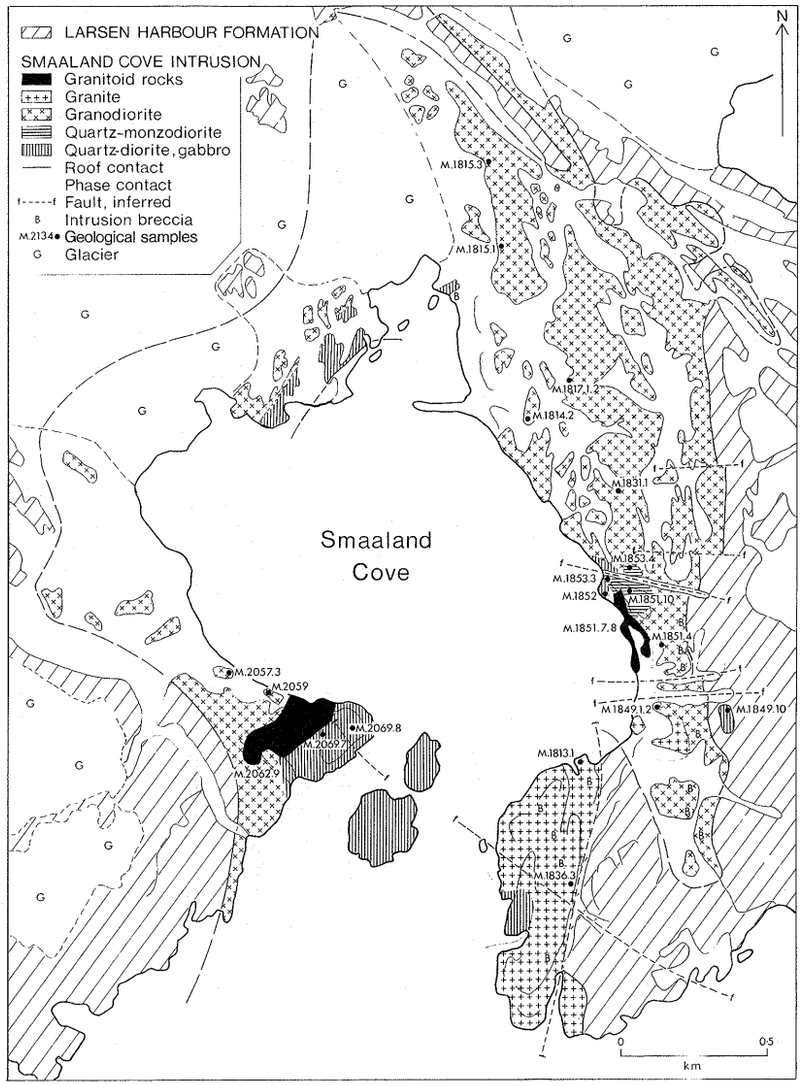

Fig. 31. Geological map of the Smaaland Cove intrusion.

forming the upper part of an ophiolite complex. This original estimate must now be modified in the light of further work by the author and extrapolation of earlier data. Four horizontal sections, 35–270 m long, were measured across the dominant local dyke trends of the formation in three areas: Doubtful Bay (M.2757 and 2764), Larsen Harbour (M.2762) and Wheeler Glacier (M.4036), in order to establish the actual amount of intrusive material. At certain localities, the country rock cannot be identified between adjacent dykes and up to 90% intrusive material has been estimated to crop out in parts of Doubtful Bay. The transition between zones of differing extension by dyke intrusion takes place rapidly over short distances.

The measured sections and relative proportions of dykes, pillow lavas and silicic rocks are given in Table III. The extension factor (*I*) is calculated assuming that the silicic rocks represent country rock, and is equivalent to the 'stretch value' determined for dykes in Iceland by Walker (1960). This extension factor varies from 25% to 54%. A minimum value of 7.2 km and a maximum value of 10.2 km for the present width of outcrop of the lavas was measured from the Directorate of Overseas Surveys 1:200 000 map of South Georgia. By applying the extension factor and dip correction, minimum (1.36–2.54 km) and maximum (1.92–3.54 km) thicknesses were derived. A second extension factor (*II*) assumes that the silicic rocks assisted spreading; extension values are increased and eventual thicknesses decreased. As not all silicic rocks are truly intrusive, this second extension value is thought to be exaggerated. No account was taken of major faults which are inferred to displace the lava sequence and therefore the thicknesses given are probably those of a repeated sequence.

The well-documented ophiolites, such as those of Betts Cove, Bay of Islands and Troodos, have zones of 60% dyke extension at depths of 1000, 700 and 1000 m, respectively, and the increase from 20% to 70% dykes occurs vertically within 25–50 m (Kidd, 1977). This rapid change in extension value explains the differences calculated in Doubtful Bay and the extension value itself suggests that the dyke zone at Wheeler Glacier and Doubtful Bay are equivalent and occur at depths

Table III. Thickness of the Larsen Harbour Formation.

Selection location	*DB1*	*DB2*	*L*	*WG*
Pillow laval thickness (m)	74.55	15.68	26.30	32.35
Dacite thickness (DA) (m)	108.30	38.11	–	–
Dyke thickness (DY) (m)	87.71	61.92	8.87	36.74
Total length of section (T) (m)	270.56	115.71	35.17	69.09
I. *Dacites do not assist extension*				
Extension factor (*I*) = DY/T (%)	32	54	25	53
Minimum apparent thickness (dykes removed)* (km)	4.9	3.3	5.4	3.4
Maximum apparent thickness (dykes removed)† (km)	6.9	4.7	7.7	4.8
Dip correction	24°	24°	24°	49°
Minimum corrected thickness (dykes removed)* (km)	2.0	1.4	2.2	2.5
Maximum corrected thickness (dykes removed)† (km)	2.9	1.9	2.5	3.6
II. *Dacites assist extension*				
Extension factor (*II*) = (DA + DY)/T (%)	72	86	–	–
Minimum apparent thickness (dykes removed)* (km)	1.3	1.0	–	–
Maximum apparent thickness (dykes removed)† (km)	1.8	1.4	–	–
Minimum corrected thickness (dykes removed)* (km)	0.5	0.4	–	–
Maximum corrected thickness (dykes removed)† (km)	0.8	0.6	–	–

DB1 and DB2, first and second measured sections, Doubtful Bay; L and WG, measured sections in Larsen Harbour and Wheeler Glacier, respectively.
*, † Calculated using minimum (7.2 km) and maximum (10.2 km) apparent thicknesses of the Larsen Harbour Formation.

between just less than 700 or 1 000 m when compared with other ophiolites. Thus the mafic extrusive sequence of the Larsen Harbour Formation may be little over 1 000 m thick if extension factor *II* is used.

I. Summary and Discussion

The stratigraphy of a typical ophiolite sequence is well documented (Coleman, 1977) and comprises, from base to top, the following units:

i. Metamorphic peridotite.
ii. Cumulative peridotite grading into layered gabbro containing plagiogranite differentiates at the top.
iii. Sheeted dyke swarms usually consisting of 100% dykes without country rock screens, varying in composition from basalt to keratophyre.
iv. Pillow lavas interlayered at the top with pelagic sediments.

The Larsen Harbour Formation and associated Smaaland Cove intrusion represent the upper part of a similar ophiolite sequence and a schematic representation (not to scale) is given in Fig. 32.

The Larsen Harbour Formation ophiolite is autochthonous, comprising nearly 2 km of basic, massive and pillow lavas, dacites, breccias, tuffs and basic dykes. It is underlain structurally and intruded by a multi-phase pluton of plagiogranite and minor banded gabbros. A sheeted dyke layer (ii) has not been positively identified but at low levels country rock occurs only as limited screens or is excluded, and multiple and composite dykes are present. Dykes are less common at high levels. Pillow lavas are more widely developed higher in the sequence; massive lavas occur throughout and amygdaloidal lavas are more prominent at low levels. Dacites, as dykes and lavas, maintain complex relationships with the mafic rocks (cf. composite dykes) near the base of the extrusive sequence. Stratiform and broken pillow breccias are almost mutually exclusive, being developed at lower and higher levels, respectively. Tuffs and cherts are present throughout, especially in association with stratiform breccias; those from the higher levels are lithologically similar to the tuffs of the Annenkov Island Formation rather than the mafic volcanic rocks of the Larsen Harbour Formation.

The internal stratigraphy of the Larsen Harbour Formation (Fig. 32) can be compared with that of the Chilean ophiolites described in detail by de Wit and Stern (1978). The Sarmiento and Tortuga complexes were formed at different stages in the development of a marginal basin (de Wit and Stern, 1978) and represent ophiolites from 'youthful island-arc or embryonic marginal basin' and 'more mature marginal basin or mid-ocean ridge' situations, respectively. The mafic extrusive sequences in the former comprise: 'intrusive [into tuff] pillow lava, primary [explosive] tuffs and pillow breccias, extrusive [water-lain] pillow and massive lavas, and secondary [sedimentary] pillow breccias'. Silicic differentiates are not developed in the latter sequence.

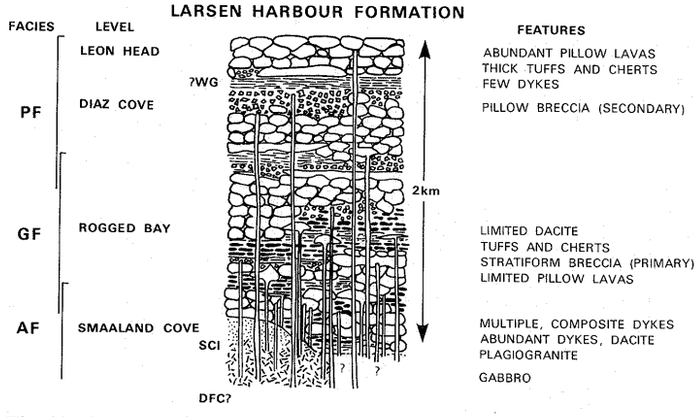

Fig. 32. Composite diagrammatic cross-section of the Larsen Harbour Formation (WG, Wheeler Glacier gabbro; SCI, Smaaland Cove intrusion; DFC, Drygalski Fjord Complex).

The significant features of the mafic extrusive unit of the Larsen Harbour Formation are:

Lower level	*Upper level*
1. Subordinate pillow lava	Abundant pillow lava
2. Silicic differentiates	No silicic differentiates
3. Extensive (primary) breccias	Extensive (secondary) breccias

The primary co-magmatic mode of formation of the stratiform breccia corresponds to that outlined for the intrusive pillow lavas and explosive tuffs of the Sarmiento ophiolite (de Wit and Stern, 1978). The presence of silicic rocks and the paucity of pillow lavas at low levels in both ophiolites adds further emphasis to the similarities between them. The secondary pillow breccias of the Larsen Harbour Formation may represent the more mature stage of development of the marginal basin corresponding to that typified by the Tortuga Complex (de Wit and Stern, 1978).

III. PETROGRAPHY

A. Pillow, Massive and Amygdaloidal Lavas

All three lava types are petrographically equivalent and contain similar relict primary and secondary phases. They are dark grey or green in the lower parts of the sequence (e.g. Doubtful Bay and Smaaland Cove) and reddish brown at higher levels (Leon Head). The sac-form of the pillows distinguishes them from the continuous massive or amygdaloidal types, individual pillows showing wide textural variation. The massive lavas are the most homogeneous group, without amygdales. All are fine-grained, melanocratic and may be porphyritic.

A variolitic texture, comprising radiating aggregates of small (0.5 mm) forked albite laths with zoned interior and square cross-section (M.1810.1A and 2088.1A), is widely developed in the pillow lavas (Fig. 33a) but is less common in the non-pillow types. The crystals are set in an altered formerly glassy matrix which is often nearly isotropic due to abundant opaque minerals. Where a variolitic texture is not present, in the cores of pillows and in the non-pillow lavas, plagioclase laths are larger (0.3–0.8 mm) and define a doleritic texture. These laths are randomly orientated in the pillow cores but can be fluidally aligned in the non-pillow lavas. Most lavas are porphyritic with anhedral andesine or albite phenocrysts (>0.4 mm) occurring in the finer-grained matrix. Relict calcic plagioclase is more common in the massive and amygdaloidal lavas, especially at a low metamorphic grade. Similarly, anhedral augite (<0.2 mm) survives only in low-grade lavas (M.3742 and 3774.2C) as interstitial crystals between plagioclase laths. Lensoid or spherical amygdales, up to 1.2 cm long but usually ~5 mm in diameter, are infilled by secondary minerals and rimmed by granular opaque minerals. Amygdales are distributed throughout the amygdaloidal lavas and occur as single tubular forms or in discrete concentric bands within the pillow lava.

Secondary phases developed are related to the local metamorphic grade. Augite is replaced completely by amphibole (actinolite in M.3700.7; hornblende in M2072.2), chlorite and epidote at higher grades. Most primary calcic plagioclase has been albitized completely at all levels; remaining phenocrysts are clouded, containing epidote and occasionally prehnite. The matrix is a felted aggregate of amphibole, chlorite, epidote and sphene in the high-grade lavas in which only albite laths and amygdales retain any form. At a lower grade, the doleritic texture may survive, with epidote, chlorite, prehnite and pumpellyite occurring in interstitial patches. Amygdales contain various combinations of epidote, chlorite, quartz and calcite or interlocking mosaics of amphibole (M.1837.1). Sphene is common in the matrix and as euhedral forms in amygdales; haematite staining is found at lower grades.

B. Breccias

Two types of mafic lava breccia have been identified: a stratiform breccia (Mair, 1983) and a pillow breccia of variable character. The former is found only in the lower levels of the formation but the other occurs throughout, although more abundantly at higher levels.

1. Stratiform breccia

This is a two-part unit consisting of fresh, glassy, amygdaloidal lava fragments set in an altered, tuffaceous, hyaloclastite, flow-aligned matrix (M.1845.2 and 2104.6; Mair, 1983, fig. 8). The dark lava fragments of rounded lensoid shape, 2–15 cm long, are nearly isotropic and have a glassy matrix, within which only albite microlites and amygdales are commonly visible (Fig. 33b). The isotropic character of the clasts is generally lost towards their margins, which tend to be translucent or dusty brown in colour and sometimes appear to grade into the surrounding hyaloclastite matrix (M.1847.2). Internally, the clasts resemble true glassy basalts. Amygdales (up to 1 cm) are infilled by quartz alone in the fresh cores of the clasts but epidote, chlorite and actinolite are found in increasing amounts in amygdales towards the edges of the clasts (Fig. 33b). Irregular, single or composite sphene crystals are common in the amygdales (M.1848).

The lava clasts are matrix-supported. The dark green hyaloclastite matrix has a dusty agglomeratic character, containing partly or completely disaggregated lava fragments replaced by epidote, chlorite and actinolite. Albite crystals of the original lava occur in isolation with sphene, leucoxene and opaque minerals. The amygdaloidal clasts lose their form when incorporated in the hyaloclastite matrix, which is seen to physically intrude and brecciate the former (Fig. 33b). The pervasive alteration rim on the clasts, and their gradual assimilation into the surrounding matrix, suggests that the hyaloclastite was formed as a result of brecciation of hot magma during its extrusion. It can be regarded as a primary breccia.

2. Pillow breccias

Pillow breccia crops out in isolation from stratiform breccia as thick irregular units in Rogged Bay (M.1420 and 3703.13A)

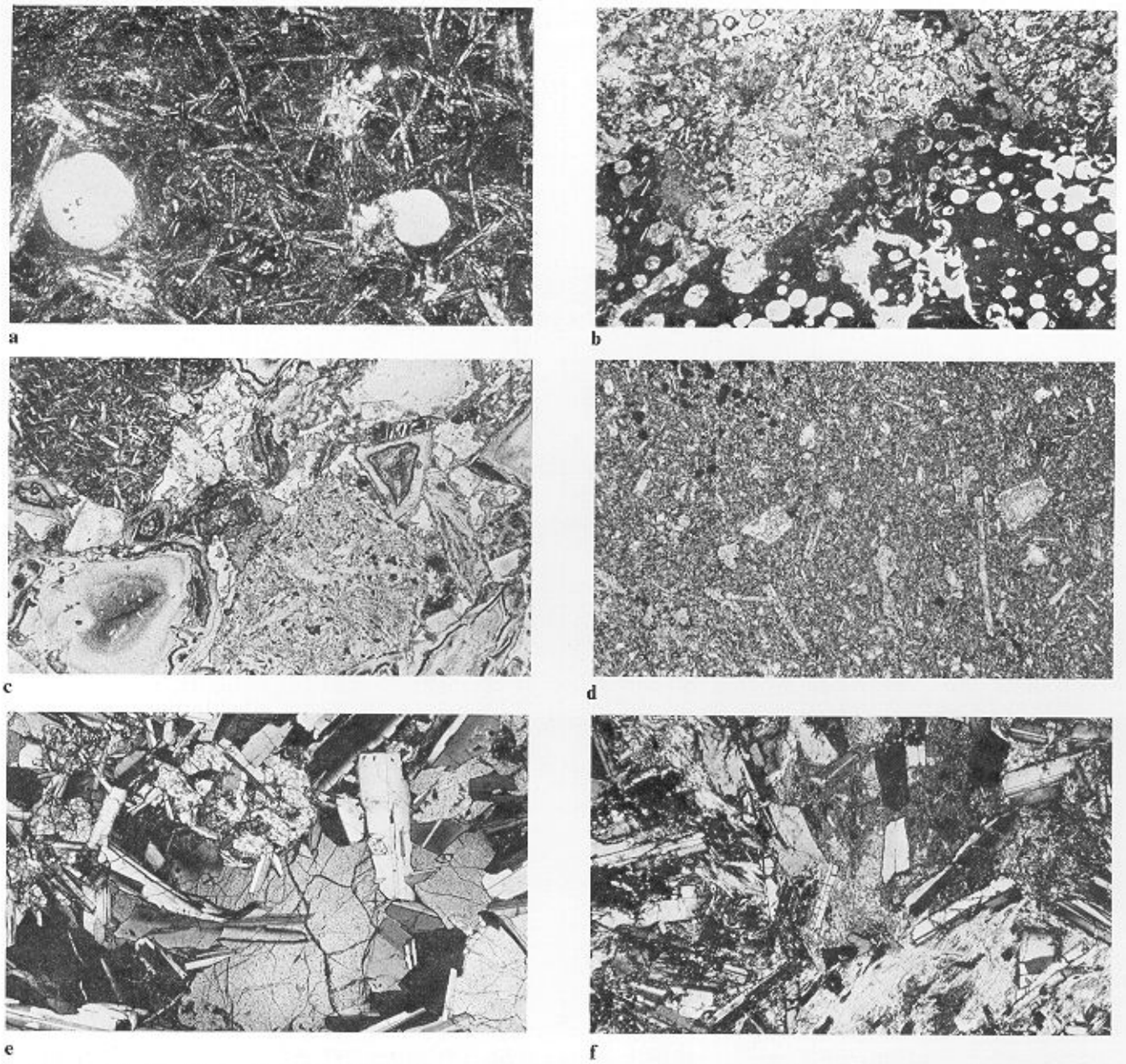

Fig. 33. a. Variolitic zone of a pillow lava; albite laths with hollow square cross-section and chlorite- and epidote-rich amygdales in an altered glassy matrix; Ranvik. (M.3796.10H; plane polarized light; × 25.) b. Zone of alteration between dark glassy lava clast and lighter hyaloclastite matrix in stratiform breccia; Smaaland Cove. (M.2104.6; plane polarized light; × 25.) c. Angular basaltic lava and altered glass fragments in a 'broken pillow breccia'; pale green chlorite replaces the former glass and epidote occurs interstitially; Diaz Cove. (M.2433.7; plane polarized light; × 25.) d. Epidote replacing subhedral and lath-like albite crystals in a fine-grained basic sill; Nattriss Head. (M.3753.3; plane polarized light; × 25.) e. Augite crystals with alteration on fractures, enclosing fresh labradorite in ophitic texture within a basic dyke; chlorite and epidote alteration occurs in interstitial areas; Leon Head. (M.3777.7B; X-nicols; × 25.) f. Fibrous mats of actinolite and chlorite replacing augite with plagioclase retaining its form in an altered basic dyke; Rogged Bay. (M.1421; X-nicols; × 25.)

and at Diaz Cove (M.2433.7 and 2490.1) but it is associated with the stratiform type at Doubtful Bay (M.2761).

This lithological unit resembles both the 'isolated pillow breccia' and the 'broken pillow breccia' of Carlisle (1963), depending on the relative proportions of lava fragments or tuffaceous matrix present (Mair, 1983). Both lack the uniformity of the stratiform breccia, and the absence of an alteration rim on the lava clasts suggests the lavas were brecciated after cooling and crystallization by a secondary mechanism.

They consist of unsorted, angular pillow fragments of varying sizes (1–8 cm) and texture, and clasts of other rock types of the Larsen Harbour Formation. The original textures and mineralogy of each fragment are retained without the alteration typical of the stratiform breccia (Fig. 33c). The matrix is similar to that of the stratiform breccia, containing irregular, former glass fragments replaced by chlorite, prehnite, calcite and quartz.

C. Dacites

Silicic lavas and minor acidic intrusions within the lower mafic lavas of the formation, previously termed rhyolite (Mair, 1983), are now classified generally as dacites. A variety of textural types occurs within both extrusive and intrusive silicic types but all are petrographically similar. The dacites can be flow-banded (M.2075.6), porphyritic (M.1854.1), amygdaloidal (M.2757.2), agglomeratic (M.1850.1) or massive (M.2101.12). All are essentially fine-grained, microcrystalline leucocratic rocks containing quartz and plagioclase phenocrysts (up to 3 mm) and amygdales (>2 mm) in an altered quartz–feldspar matrix. Flow banding, where developed, is defined by thin laminae of epidote and intervening quartz and feldspar bands (Mair, 1983, fig. 11). Agglomeratic types contain a variety of rock fragments, including clasts of dacite and basic lava. The dacites are petrographically similar to keratophyres described from spilitic environments elsewhere (Hughes, 1973).

Quartz and feldspar are the dominant primary phases, all former mafic minerals having been replaced (below). Quartz occurs throughout the matrix as microcrystalline aggregates, as subhedral phenocrysts and infilling amygdales. It may also form delicate micrographic intergrowths with albite, oligoclase and andesine throughout the rock (M.2066.4). Coarser graphic textures are found in the porphyritic dacites. The subhedral quartz phenocrysts (up to 2 mm) show recrystallized (M.1836.6) or embayed margins (M.1854.1) as though corroded but this may indicate the amoeboid growth of the crystal (Moorhouse, 1959, p. 207). Plagioclase feldspar is dominant in part as fluidally arranged microlites and in part as albite (M.2764.2) and andesine (An_{33}; M.1854.1) phenocrysts. Alkali feldspar is present in the graphic intergrowths and in the matrix of a rhyodacite (M.3750.2B). Euhedral apatite and zircon are accessory phases, and granular magnetite and pyrite are disseminated throughout. Amygdales and flow banding are retained and emphasized by concentrations of secondary minerals.

Epidote and chlorite are widely developed in the matrix, the former as individual crystals and complex mosaics and the latter as interstitial pools, replacing former glass or mafic minerals. Both minerals also occur with quartz and calcite in amygdales. Plagioclase is clouded by saussuritization and is patchily or completely altered to epidote. Allanite, intergrown with epidote (M.1843.2), occurs rarely and interstitial pumpellyite is present in an epidosite (M.1419) from Rogged Bay. Sphene, after original opaque minerals, is common. The absence of amphibole in the dacites, in contrast to adjacent mafic lavas of equivalent metamorphic grade, implies compositional restriction on the formation of this phase.

D. Minor Intrusions

1. Basic sills

Low-angle sills crop out at all stratigraphical levels and are petrographically similar to the mafic lavas. They have a massive, even-grained aphanitic texture, finer-grained than the equivalent gabbroic and doleritic dykes. Elongated laths (>2 mm) and subhedral crystals of albite occur as phenocrysts (Fig. 33d) in an altered, sub-variolitic basaltic matrix consisting of albite micro-laths (<1.5 mm), relict augite and granular magnetite (M.3745.3). The original feldspar was albitized during alteration and subsequently saussuritized (Fig. 33d), and augite survives only in rocks at low metamorphic grade. Epidote, chlorite, actinolite, prehnite and calcite are developed in the matrix and infill the few amygdales present. Magnetite, ilmenite and sphene are concentrated on amygdale rims or are randomly scattered throughout the rock.

2. Basic dykes

All of the basic dykes have a similar mineralogy and are classified as dolerites but they show variation in grain-size, texture and plagioclase composition. They are medium- to coarse-grained, dark grey melanocratic rocks with ophitic, intersertal or basaltic textures involving augite and plagioclase. Porphyritic varieties are common.

In thin section almost colourless augite crystals (up to 4 mm), exhibit core-to-rim zoning in the larger crystals, and ophitically enclose plagioclase laths in many of the doleritic and gabbroic dykes (Fig. 33e). In other rocks, small augite crystals are interstitial to plagioclase and form a doleritic texture. Augite phenocrysts are rare. Olivine, reported by Trendall (1959), was not identified. Primary labradorite (M.3704.C), bytownite (M.3777.7B) and rare andesine (M.3745.2) form 0.5–1.5 mm euhedral laths with calcic cores and sodic rims. Andesine is rimmed by albite (An_{29-9}, core to rim) but the more calcic feldspars have less sodic margins (An_{75-48}, core to rim). Zoning is usually complex and non-gradational. Feldspar phenocrysts (up to 7 mm) of similar composition occur in the porphyritic dykes. Minor interstitial quartz, subhedral magnetite and skeletal ilmenite are scattered throughout.

Igneous textures survive at all metamorphic grades, except in the most heavily altered examples, and plagioclase laths remain when all adjacent augite has been replaced by amphibole (Fig. 33f). Albite rims on andesine may be a primary feature but more commonly secondary albite has replaced former calcic feldspar either partly or completely (M.1822 and 1844.1). Augite is rimmed or pseudomorphed completely by fibrous mats of actinolite (M.1421) or green-brown hornblende (M.1818 and 3753.8) in association with chlorite and epidote in the more altered dykes (Fig. 33f). In the less altered dykes, secondary phases are restricted to minor interstitial areas (Fig. 34a) where combinations of chlorite, epidote, prehnite (M.3745.2) and rare pumpellyite (M.1823) occur at different levels in the sequence. Plagioclase is often altered to epidote, sericite and prehnite in patches or along transverse fractures. Sphene and leucoxene replace primary magnetite in the altered dykes.

3. Multiple and composite dykes

The successive units of the multiple dykes differ mainly in grain-size and texture, whereas a change with time from basic to acidic composition of intrusions is typical of the composite dykes (Mair, 1983).

The coarser units of the multiple dykes contain plagioclase laths (An_{58}) and relict augite or its replacement products in a crude, altered ophitic texture (M.1810.8A). Subsequent phases are finer-grained and aphanitic, containing few phenocrysts of altered plagioclase and abundant albite micro-laths in a dark, possibly originally glassy, matrix (Fig. 34a). The groundmass of all units is invariably altered; former pyroxene or glass is replaced by epidote, chlorite and actinolite aggregates, and feldspar by epidote. Magnetite, replaced by ilmenite and leucoxene, and sphene are concentrated along the chilled

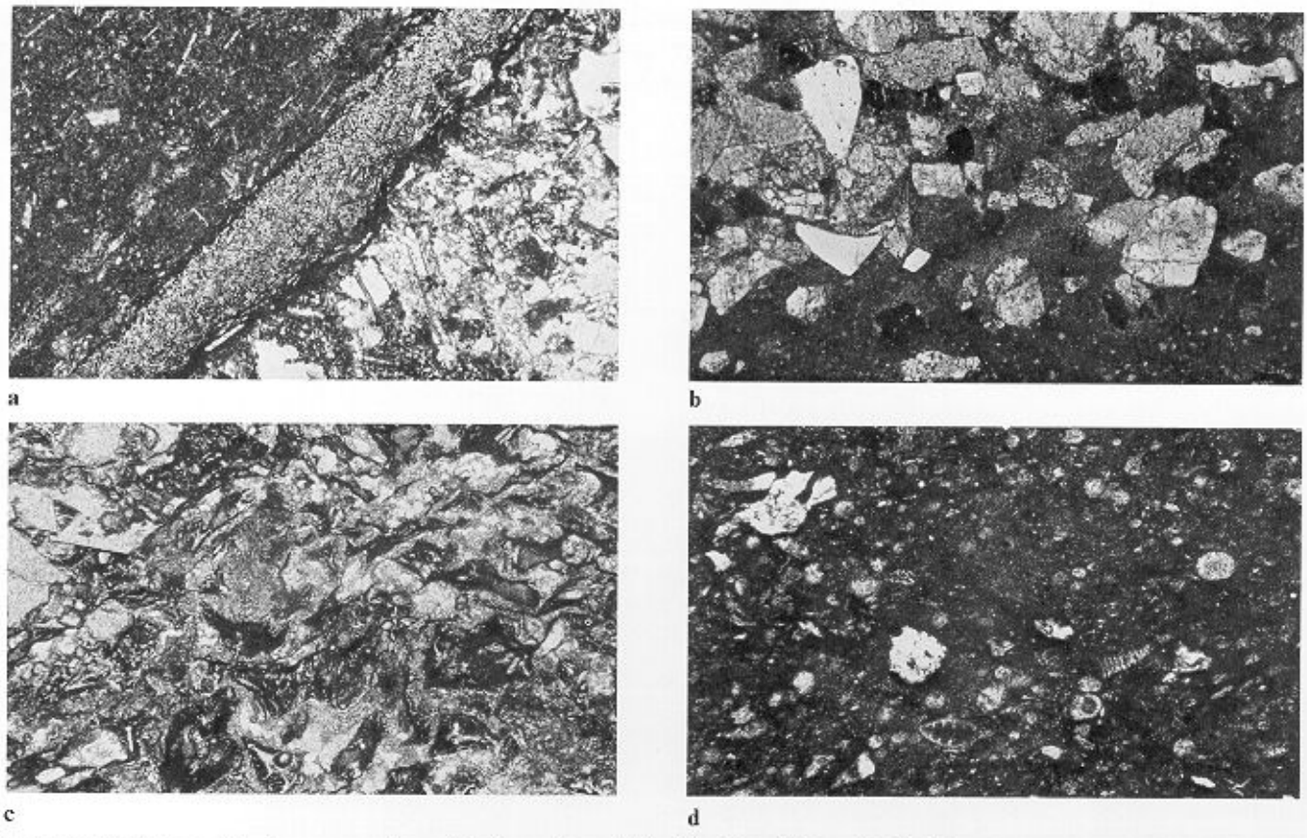

Fig. 34. a. Opaque-rich chilled margin between successive mafic phases of a multiple dyke; Brandt Cove. (M.1810.8A; plane polarized light; × 25.) b. Angular clouded plagioclase, clear quartz and dark opaque mineral fragments in a partly matrix-supported crystal tuff; Smaaland Cove. (M.2078.8; X-nicols; × 25.) c. Cuspate shard-like fragments in an epidote- and chlorite-rich matrix of a vitric tuff; Nattriss Head. (M.3755.9A; plane polarized light; × 25.) d. Silicified Radiolaria and minor altered crystal fragments in a radiolarian tuff; Larsen Harbour. (M.2759.2B; plane polarized light; × 25.)

margins between phases (Fig. 34a) and occur in the matrix. Secondary minerals infill the few amygdales present.

A composite dyke from Smaaland Cove (M.1840.1) contains early phases equivalent to altered basic dykes and a later phase resembling the intrusive dacites.

E. Tuffaceous Sediments

Individual sedimentary units vary in thickness from 1 to 7 cm and in texture; they include green, white and red cherts, green and brown tuffs, and coarser agglomeratic units. Minor load structures, and graded- and current-bedding are developed in the thinner finer-grained bands of massive tuff (Mair, 1983, fig. 12). The thicker agglomeratic, lithic tuff units are commonly associated with the pillow and stratiform breccias. Tuffs from Leon Head are petrographically similar to those rocks comprising the Lower Tuff Member of the adjacent Annenkov Island Formation and to those described from Hauge Reef (Tanner and others, 1981). The tuffs from the base of the Larsen Harbour Formation are chemically and petrologically distinct from the tuffs of the Annenkov Island Formation, although they display similar textures. The tuffs comprise crystal, lithic, vitric and Radiolaria-bearing types, usually occurring together within a composite sedimentary unit. Thin brightly coloured (jasper) radiolarian cherts are found in association with the tuffs and as separate inter-pillow deposits.

The microcrystalline quartz-rich matrix in all tuffs has a brown sub-isotropic character and may originally have contained volcanic glass. Crystal fragments (up to 1.5 mm) of plagioclase, opaque minerals and quartz are common in the crystal tuffs (M.1809.1 and 2078.8; Fig. 34b). Fresh augite crystal are retained only in the crystal tuffs from Leon Head (M.3769.5). The feldspar is often cloudy and heavily altered, but twinning survives and relict andesine (An_{34}), and more commonly, secondary albite are found. Clear, unaltered quartz fragments (< 0.7 mm) and sub-rounded, smaller magnetite granules are less abundant than the feldspar (Fig. 34b). Alteration of the matrix and the mafic and felsic crystal fragments to epidote, prehnite, chlorite and actinolite is widespread.

Basic lava, dacite and re-worked tuff clasts (4–6 mm) are found in the lithic tuffs (M.2759.2B and 3702.7C), which may grade locally into units of pillow or stratiform breccia, and are usually interbedded with other tuff types. They display similar alteration to the parent rock of the clasts and to the crystal tuffs. Material for the vitric tuffs (M.2759.2A and 3755.9A) is derived from the break-up of larger amygdaloidal lithic fragments or directly from the disintegration of amygdaloidal lava (cf. stratiform breccia), the fragments having a cuspate shard-like form (Fig. 34c). The glass fragments are extensively altered but retain their morphology (Mair, 1983). Radiolaria are present in the matrix of the crystal and lithic tuffs and are locally abundant within massive tuffs (M.1841.1B and 2759.2B; Fig. 34d).

F. Smaaland Cove Intrusion

This intrusion was originally described as a single body of quartz-diorite (Bell and others, 1977) and later as a tonalite (Storey and others, 1977). A more detailed study of the pluton (Mair, 1983) has established its heterogeneous character.

The different phases of the intrusion have been classified in Fig. 35 according to the scheme of Streckeisen (1973). The pluton comprises two main units: older melanocratic rocks (quartz-diorite, quartz-gabbro and quartz-monzodiorite) and younger leucocratic rocks (granodiorite, granite and granitoid rocks). All have undergone a similar hydrothermal metamorphism but to different degrees. The leucocratic rocks form the bulk of the intrusion and they intrude and structurally overlie the subordinate mafic rocks which crop out at sea-level (Fig. 31).

1. Quartz-diorite and quartz-gabbro

Both rock types have a similar texture but are distinguished by differences in plagioclase composition. No primary clinopyroxene or pseudomorphs after pyroxene were noted, and hornblende is the dominant primary mafic phase. The term gabbro is therefore not strictly applicable, although Moorhouse (1959, p. 291) referred to such rocks as hornblende-gabbro. An alternative classification is quartz-labradorite-diorite.

These rocks are medium-grained (up to 4 mm) and contain approximately 6% quartz, 49% plagioclase and 43% mafic minerals in a doleritic and ophitic relationship. Andesine (An_{45}) in the quartz-diorite and andesine/labradorite (An_{47}/An_{70}) in the quartz-gabbro, occur as euhedral and subhedral laths showing limited compositional zoning. Primary igneous hornblende (α = yellowish green, β = brown, γ = dark green) is found as subhedral, twinned ragged prisms interstitial to or poikilitically enclosing plagioclase laths (quartz-diorite, M.1852.6; quartz-gabbro, M.1852.5). Minor quartz infills interstitial areas and forms rare graphic intergrowths with potash feldspar in the quartz-gabbro. Skeletal ilmenite and magnetite are present as are euhedral apatite, sphene and rare zircon.

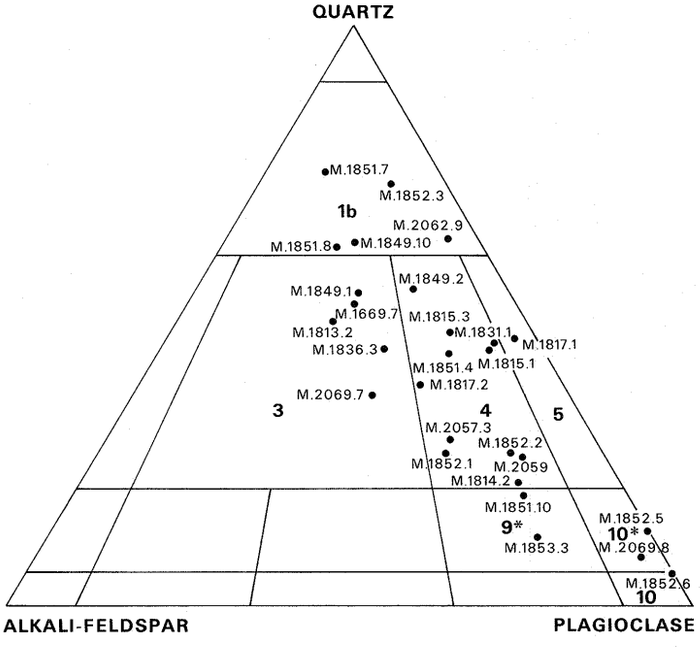

Fig. 35. Classification of the Smaaland Cove intrusion after Streckeisen (1973). Groups are as follows: 1b, quartz-rich granitoids; 3, granite; 4, granodiorite; 5, tonalite; 9*, quartz-monzodiorite and quartz monzogabbro; 10*, quartz-diorite, quartz-gabbro and quartz-anorthosite; 10, gabbro, diorite and anorthosite.

Alteration is variable and can be extensive (M.2069.8). The plagioclase is clouded by saussuritization and contains patches of colourless epidote and sericite. Secondary albite was not identified. Hornblende may be partly or completely replaced by pale-coloured actinolite (α = colourless, β = green, γ = greenish blue), especially on crystal rims. A metamorphic hornblende, isolated subsequently by microprobe analysis, is optically contiguous with the primary amphibole, occurring as minor patches and rims, and is closely associated with actinolite (see p. 40). Chlorite is found in association with amphibole and in interstitial areas within iron-poor epidote. Amorphous sphene mantles magnetite and leucoxene intergrowths.

2. Quartz-monzodiorite

The textures and mineralogy of this medium-grained group of rocks are gradational between those of the previous group and the mafic granodiorites. Large-scale segregations (up to 5 cm) of coarse, mafic and felsic minerals are commonly developed, and define a vague banding in the rocks (M.1853.3) that resembles the 'synneusis' texture of gabbroic rocks as described by Moorhouse (1959, p. 241).

Andesine (An_{33}) with sodic rims, hornblende, minor green biotite (α = brown-green, $\beta = \gamma$ = dark green), quartz and opaque minerals form a subophitic to granular texture (M.1851.10). Graphic and micrographic intergrowths, more typical of the granodiorite group, may be well developed (M.1853.3; Fig. 36a). Sphene, apatite and zircon are common accessories.

The alteration of the quartz-monzodiorites corresponds to that of the previous groups and includes albitization of the rims of primary plagioclase, and chlorite forming after biotite as well as amphibole. Sphene occurs in association with magnetite and ilmenite.

3. Granodiorite

The granodiorites comprise nearly 60% of the Smaaland Cove intrusion (Fig. 31) and are a heterogeneous group containing subsidiary melanocratic types (approximately 10–18% quartz, 16–25% mafic minerals) and predominantly leucocratic granodiorites (approximately 21–37% quartz, 1–25% mafic minerals). One specimen, classified as tonalite (M.1817.1; Fig. 35), is included in the granodiorite group. The melanocratic types resemble the quartz-monzodiorites and are transitional between them and the leucocratic granodiorites.

Both melanocratic and leucocratic rock types are medium-grained (up to 4 mm), containing plagioclase and amphibole in a subophitic or granular texture, respectively, in association with quartz, graphic intergrowth and minor biotite. Andesine (An_{50-41}, core to rim) occurs in the mafic-rich types (M.1814.2). Unzoned andesine (An_{32}) and andesine with sodic rims (An_{36-18}, core to rim) are both present in a leucocratic granodiorite (M.1831.1). Extensive perthitic margins of potash feldspar are developed on many of the plagioclase crystals

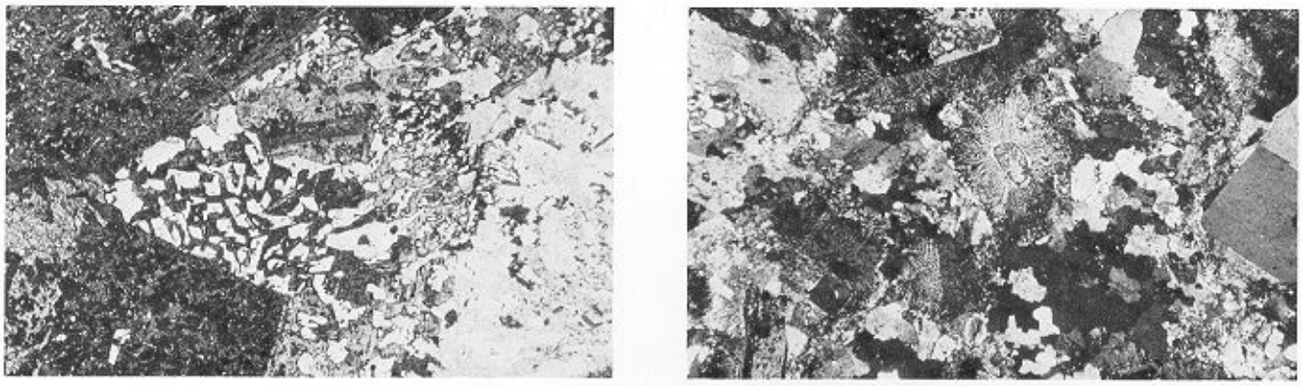

a b

Fig. 36. a. Coarse graphic intergrowth bordering heavily altered plagioclase laths in a quartz-monzodiorite; Smaaland Cove. (M.1853.3; X-nicols; ×25.
b. Micrographic intergrowths around plagioclase laths in a quartz-rich granitoid rock; epidote replaces the central lath of the intergrowth and albit phenocrysts remain unaltered; Smaaland Cove. (M.1849.10; X-nicols; ×25.)

(M.1817.2). Euhedral green hornblende, often with ragged margins due to alteration, and green biotite occur in interstitial areas and are less common in the leucocratic granodiorites. Quartz is present as anhedral interstitial crystals in the mafic rocks and as larger subhedral grains, equivalent in size to the plagioclase crystals in the more leucocratic varieties. This mineral is also associated with the extensive micrographic intergrowths which may form up to 20% of the rocks (M.1815.3 and 1831.1). Magnetite and ilmenite are present in the matrix; apatite and zircon are abundant accessory phases.

Alteration in the granodiorites is equivalent to that in the other rock types and includes allanite (α = light brown, β = brown, γ = dark brown) intergrown with epidote. Albite occurs as thin rims on calcic plagioclase and within the perthitic intergrowths. Sphene is found as coarse mantles on magnetite.

4. Granite and granitoid rocks

These younger phases of the intrusion are predominantly leucocratic, containing more quartz and less mafic minerals than the granodiorites. Calcic plagioclase is less common, and albite and potash feldspar (detected by staining) are present. Both granite and granitoid rocks have a fine- to medium-grained (1–4 mm) granular texture and may be porphyritic; they differ essentially in quartz content.

The granites and granitoid rocks contain approximately 36–46% and 49% quartz, respectively. Alkali and plagioclase feldspar are present in equivalent amounts, the former as separate perthitic crystals and also in graphic intergrowths. Euhedral green hornblende and green biotite are minor phases constituting less than 10% of the rocks. Quartz occurs as anhedral crystals in irregular mosaics, and in graphic and micrographic intergrowths (Fig. 36b) forming up to 40% of the matrix of the granitoid rocks (M.1849.10) but less in the granites (M.1836.3). Zoned crystals of oligoclase-albite (An_{19-9}, An_{26-3}, core to rim; M.1813.2) are mantled by potassium feldspar perthites or by graphic intergrowths, but they also occur as single fresh phenocrysts (Fig. 36b). Opaqu minerals are rare and accessory minerals are identical to thos in previous groups.

Epidote and chlorite are conspicuous alteration phases in th granites and granitoid rocks and occur with actinolite hornblende, allanite and sphene, as described for other roc groups. The albite rims on oligoclase may be a primary feature

G. Wheeler Glacier Gabbro

The Wheeler Glacier gabbro intrudes the Larsen Harbou Formation at a high level and is spatially and petrologicall distinct from the Smaaland Cove intrusion. It contains a lowe grade metamorphic assemblage than the gabbroic rocks of th latter intrusion. The gabbro is a coarse-grained mesocratic roc containing fresh anhedral clinopyroxene, elongated plagioclas laths (<6 mm) and minor opaque minerals with an ophitic o sometimes doleritic texture.

Augite crystals (up to 4 mm) comprise 50% of the rock showing little compositional variation from core to rim (M.4072.8 and 11), and may be interstitial to or poikilitically enclosing plagioclase laths. The feldspar, labradorite (An_{66}) retains its form in spite of alteration and has thin sodic rim (An_{30}) without a gradational change from core to rim (M.4072.8). Anhedral magnetite granules (3.0 mm) with altered rims form the remainder of the primary assemblage; accessory phases include sphene, zircon and apatite.

The texture is unaffected by alteration except in rocks from the margins of the intrusion where epidotization is severe. Even in the fresher rocks, plagioclase is heavily saussuritized and altered to epidote and sericite. The less-altered gabbros contain secondary phases in discrete interstitial patches (<2 mm comprising combinations of prehnite, pumpellyite, chlorite and epidote. Sphene occurs as amorphous patches with leucoxene replacing magnetite.

IV. WHOLE ROCK GEOCHEMISTRY

A. Introduction

A total of 127 specimens of the Annenkov Island and Larsen Harbour formations have been analysed for 10 major oxides and 10 trace elements. The specimens of the Annenkov Island Formation comprise 13 andesites and 18 basic sills, collected by T. H. Pettigrew in 1973, and those of the Larsen Harbour Formation include 28 pillow and massive lavas, 24 basic dykes, 17 dacites, 10 gabbros and diorites, and 11 plagiogranites, collected by the author and colleagues in 1974. Six gabbro specimens from the adjacent Drygalski Fjord Complex, collected by B. C. Storey in 1974, are also included for comparison with the Larsen Harbour Formation.

Chemical analyses of all rocks described in this report were carried out by X-ray fluorescence methods at the University of Birmingham, using techniques described by Leake and others (1969). Total iron oxide is given in the tables as Fe_2O_3 since no gravimetric determinations were undertaken.

Average analyses for each rock type are given in Table IV. Copies of the full data set may be obtained on request from the Chief Geologist, British Antarctic Survey, High Cross, Madingley Road, Cambridge CB3 0ET, U.K. The symbols for the different rock types that appear in the text-figures are given below.

Key to Symbols and Abbreviations used in Figs 37–66

(The abbreviations in brackets are used in all figure captions; exceptions to the above key are indicated where appropriate.)

Larsen Harbour Formation (LHF)
- ● Pillow lava
- ○ Massive lava
- ◒ Sill
- ⊙ Dacite
- ▲ Dyke

Smaaland Cove intrusion (SCI)
- ▧ Plagiogranite
- ■ Diorite

Wheeler Glacier (WG)
- ◪ Gabbro

Drygalski Fjord Complex (DFC)
- \+ Gabbro

Annenkov Island Formation (AIF)
- □ Andesite
- ▽ Sill

Table IV. Mean analyses of Larsen Harbour Formation ophiolite and Annenkov Island Formation island-arc rocks.

	1	*2*	*3*	*4*	*5*	*6*	*7*	*8*	*9*	*10*
Oxides (%)										
SiO_2	52.68	52.32	47.34	51.35	49.36	48.33	73.51	70.45	59.16	47.11
TiO_2	1.27	1.33	1.26	1.57	0.92	0.62	0.37	0.57	0.53	0.95
Al_2O_3	11.06	12.83	14.96	12.77	15.66	15.27	11.76	12.80	18.08	15.18
Fe_2O_3	11.63	12.51	11.65	12.11	8.87	10.58	4.73	4.99	6.49	9.96
MnO	0.20	0.20	na	0.32	na	0.18	0.10	na	na	na
MgO	7.97	7.31	8.36	6.47	7.54	10.62	0.97	0.77	3.30	8.70
CaO	9.43	8.25	11.15	9.01	13.10	11.24	2.99	3.08	4.65	9.34
Na_2O	3.32	2.77	1.88	2.97	3.11	1.93	4.29	5.34	4.73	2.63
K_2O	0.09	0.39	0.31	0.34	0.37	0.31	1.12	0.85	3.08	1.46
P_2O_5	0.17	0.18	0.12	0.20	0.05	0.11	0.05	0.13	0.24	0.27
Trace elements (ppm)										
Cr	191	113	236	143	200	290	2	4	19	226
Ni	105	69	134	94	52	217	10	11	15	135
Rb	3	8	8	6	5	8	14	17	59	34
Sr	144	162	102	139	154	212	164	105	905	444
Y	27	31	33	64	22	15	66	99	18	19
Zr	93	89	84	192	43	59	357	415	187	105
Nb	4	4	4	5	3	4	11	11	7	6
Ba	53	102	123	122	49	78	480	358	997	679
La	14	16	12	21	6	11	26	32	28	22
Ce	18	20	12	32	7	14	55	66	51	35
Fe*/Mg	1.70	1.99	1.62	2.18	1.37	1.16	5.71	7.59	2.29	1.34
K/Rb	249	405	322	470	614	322	664	415	433	356
Rb/Sr	0.02	0.05	0.08	0.04	0.03	0.04	0.09	0.16	0.07	0.08
$\frac{K_2O.100}{(Na_2O + K_2O)}$	–	–	–	–	–	–	20.7	13.7	39.4	–

1, 2 and 3, pillow lavas (12 samples), massive lavas (16 samples), dykes (24 samples), respectively, Larsen Harbour Formation; 4, diorites (7 samples), Smaaland Cove intrusion; 5, Wheeler Glacier gabbros (3 samples); 6, gabbros (6 samples), Drygalski Fjord Complex; 7, dacites (17 samples), Larsen Harbour Formation; 8, plagiogranites (11 samples), Smaaland Cove intrusion; 9 and 10, andesites (13 samples) and basic sills (18 samples), respectively, Annenkov Island Formation. Fe_2O_3, total iron as Fe_2O_3; Fe*, total iron as Fe^{2+}; na, not analysed.

Aspects of previous work

The alteration of ocean-floor or island-arc rocks by metamorphic or metasomatic processes leads to element mobility (e.g. Coish, 1977; Garcia, 1978) and this places constraints on their effective use as discriminants. Element mobility in rocks of the Betts Cove ophiolite, Newfoundland, has been discussed by Coish (1977), who deduced that Fe_2O_3, MgO and Na_2O contents increase, CaO and Cu contents decrease, and SiO_2, total Fe, K_2O, Ba and Rb contents may be depleted or enhanced by metamorphism and metasomatism with respect to fresh rocks.

In spite of the known mobility of the major elements during alteration and metamorphism, Pearce and others (1977) have used MgO–Al_2O_3–FeO (total) relationships to determine the tectonic environment of intermediate volcanic rocks (51–56% SiO_2). FeO and Al_2O_3 are regarded as relatively immobile, and although MgO content varies during submarine alteration, the scheme has been applied successfully to analyses of Archaean greenstones. Miyashiro (1973) stated that there is limited change in the FeO/MgO ratio during metamorphism; he also used SiO_2 and alkali contents as a means of ophiolite classification but problems inherent in the scheme were later outlined by Church and Coish (1976). The possible mobility of the components of an AFM diagram due to alteration is an accepted problem and therefore the relationships of the less mobile trace and minor elements may be more diagnostic.

A limited number of minor and trace elements appear to be immobile and have been used to distinguish rocks from different tectonic environments. Early work that identified the immobility of Zr, Nb, Y and Ti (Cann, 1970; Pearce and Cann, 1971) was later expanded to incorporate partly mobile Sr (Pearce and Cann, 1973) to define the tectonic setting of basic volcanic rocks. The Y/Nb ratio was used by these workers to discriminate between alkalic and tholeiitic magma and was subsequently used with TiO_2, P_2O_5 and Zr by Floyd and Winchester (1975) for a similar purpose. Although K_2O may show enrichment or depletion during metamorphism or metasomatism, its relationship with TiO_2 and P_2O_5 allows separation of oceanic and non-oceanic rocks (Pearce and others, 1975). The behaviour of minor and trace elements of the Annenkov Island and Larsen Harbour Formations forms the greater part of the present investigation.

B. Larsen Harbour Formation

The geochemical data from other ophiolites are extensive and have been reviewed by Coleman (1977). The geochemistry of the Sarmiento Complex, Chile, has recently been described by Saunders and others (1979), and this work provides the basis for the present investigation. It allows a direct comparison to be made between the Chilean and the suspected South Georgia ophiolites, both of which probably formed within the same island-arc–marginal-basin system.

1. Mafic rocks

The tectonic setting of the mafic rocks of the Larsen Harbour Formation is suggested primarily from trace and minor element evidence and the conclusions are compared with mid-ocean ridge basalts. Average analyses of the mafic rocks are given in Table IV.

A preliminary study was made using major elements to identify the tectonic setting of the Larsen Harbour and Annenkov Island formations, as outlined by Pearce and others (1977). Analyses of both groups plotted apart, and the general oceanic nature of the Larsen Harbour Formation was established, although in the field of ocean-island rather than ocean-floor basalts. The Annenkov Island Formation andesites plotted as island-arc rocks (Pearce and others, 1977), but the associated basic sills were characterized (erroneously) as ocean-floor basalts. This investigation was not pursued further as it was felt that trace and minor element data would allow a more consistent separation to be made between the contrasting rock types.

The lavas, dykes, gabbros (Wheeler Glacier and Drygalski Fjord Complex) and diorites (Smaaland Cove intrusion) have Y/Nb ratios greater than 3 (most exceed 6), indicating their tholeiitic character (Pearce and Cann, 1973); analyses are plotted with respect to TiO_2 and Y/Nb after Floyd and Winchester (1975) in Fig. 37. The Drygalski Fjord Complex rocks have Y/Nb values approaching those of continental tholeiites. Ce/Y ratios for all rocks are low (cf. Table IV) and do not overlap those of calc-alkaline rocks. A mid-ocean ridge origin for the lavas and dykes is indicated by Ti–Zr–Y abundances in Fig. 38. Similarly, in Fig. 39 they plot as ocean-floor basalts, outlining a trend of Ti increasing with Zr content. The areas defined for oceanic basalts in Figs 38 and 39 overlap those of other igneous environments but a single field for mid-ocean ridge rocks is identified using Ti–Zr–Sr relationships, and this contains most of the lava and dyke analyses (Fig. 40). Some of the variation may be due to the mobility of Sr during

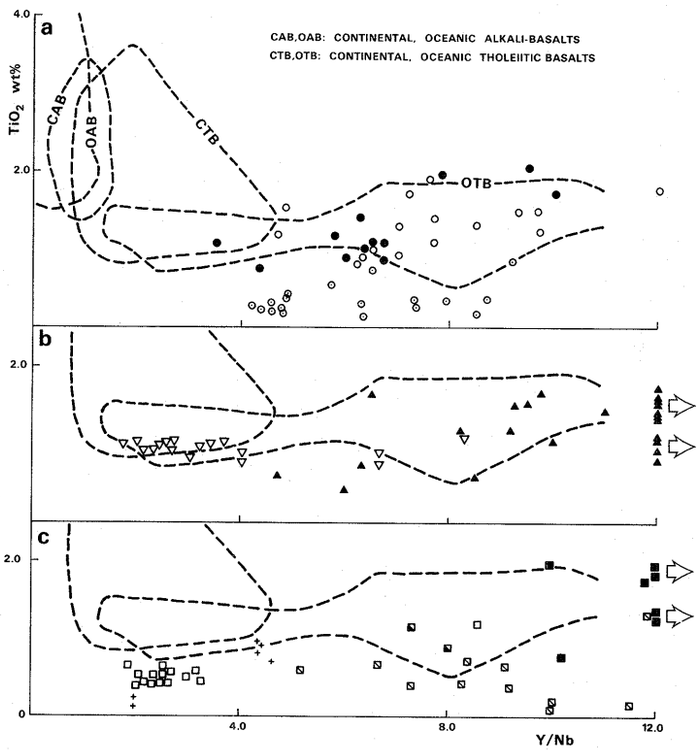

Fig. 37. TiO_2–Y/Nb relationships of oceanic and continental, alkali and tholeiitic basalts (Floyd and Winchester, 1975). a. Mafic and silicic lavas (LHF). b. Dykes (LHF) and sills (AIF). c. Plagiogranites and diorites (SCI), gabbros (WG and DFC) and andesites (AIF).

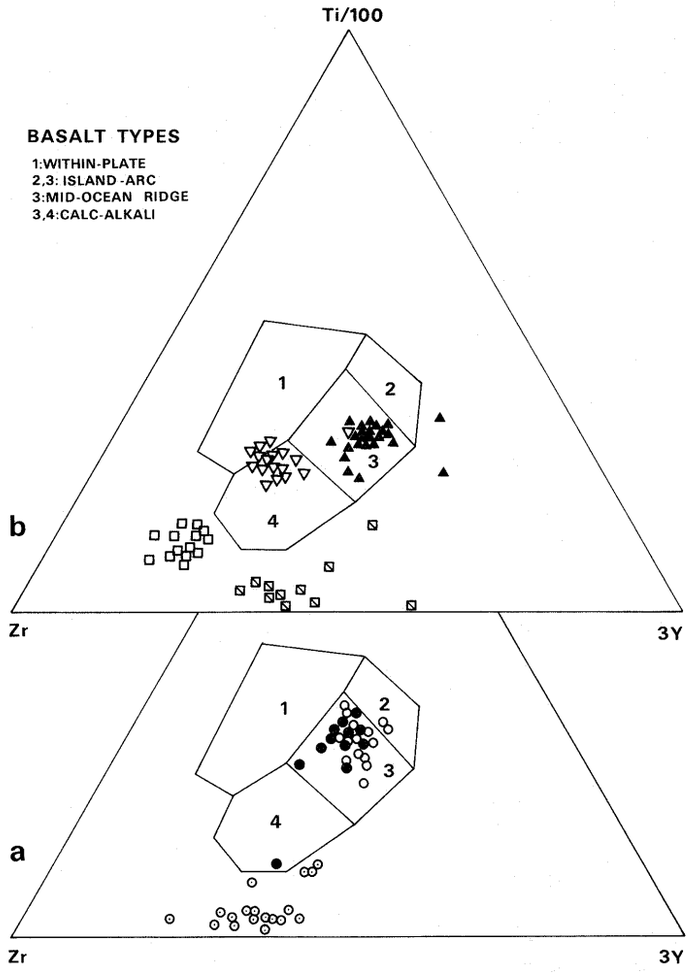

Fig. 38. a. Mafic and silicic lavas (LHF). b. Dykes (LHF), sills and andesites (AIF), and plagiogranites (SCI) plotted on a Ti/100–Zr–3Y diagram (Pearce and Cann, 1973). Silicic rocks are for comparison only.

hydrothermal alteration. Although the gabbro analyses may be unsuitable for use with Figs 38 and 40 because of their possible cumulate nature, the plutonic rocks show some correlation with the field of ocean-floor basalts in Fig. 39 and a tholeiitic trend of Ti increasing with Zr is suggested. The lavas and dykes have characteristics of oceanic tholeiites.

The oceanic nature of this formation is suggested again in Fig. 41, using TiO_2–P_2O_5–K_2O relationships (Pearce and others, 1975); in spite of possible enrichment of K_2O during metamorphism, the lavas and dykes plot within the designated oceanic field.

2. Comparison of mafic rocks to oceanic basalts

Mafic rock analyses of the Larsen Harbour Formation and associated gabbros and diorites as compared directly with the fields of oceanic basalts are compiled by Saunders and others (1979) (Fig. 42). Fe*/Mg is used as an indicator of fractionation, where Fe* equals total iron as Fe^{2+}.

Fe*/Mg ratios increase with differentiation from 0.84 to 1.74 and from 1.12 to 1.64 in the Drygalski Fjord Complex and Wheeler Glacier gabbros, respectively, and from 1.89 to 2.36 in the diorites of the Smaaland Cove intrusion. High ratios for the lavas (1.08–3.11) and dykes (0.89–3.09) are thought to result from the effects of alteration rather than differentiation. The basic dykes and gabbros (except the Wheeler Glacier gabbro) maintain a steep positive correlation between Zr and Fe*/Mg (Fig. 42) within the defined field. The lavas follow a similar trend but higher Fe*/Mg values at equivalent Zr contents cause most to fall outside the limits of ocean-floor basalts. The Zr-depleted Drygalski Fjord Complex gabbros may contain cumulate phases (personal communication from B. C. Storey). TiO_2 and Fe*/Mg values for the mafic rocks correlate positively with those of ocean-floor basalts (Fig. 43). The high TiO_2 content of the more differentiated Smaaland Cove intrusion diorites contrasts with the low levels in those of the Drygalski Fjord Complex. The Cr and Ni contents of all rock types show a negative relationship with Fe*/Mg, suggesting extensive fractionation, but they conform within varying limits to the given fields of ocean-floor basalts (Figs 44 and 45). The four Drygalski Fjord Complex gabbro samples have high Cr and Ni contents. Cr is depleted in most lavas, in altered dykes and in some gabbros. Although regarded as immobile (Pearce and Cann, 1973), Cr appears to have been lost during metamorphism of the lavas and dykes, fresher specimens retaining their original higher values. However, the Wheeler Glacier gabbro is essentially unmetamorphosed, retaining its primary mineralogy; the variable Cr and low Ni contents may be an original feature (Figs 44 and 45) as in two similar gabbros from the Drygalski Fjord Complex.

The dykes correlate well with the trend of mid-ocean ridge basalts (Fig. 46), showing an increase of Fe* with Fe*/Mg as for

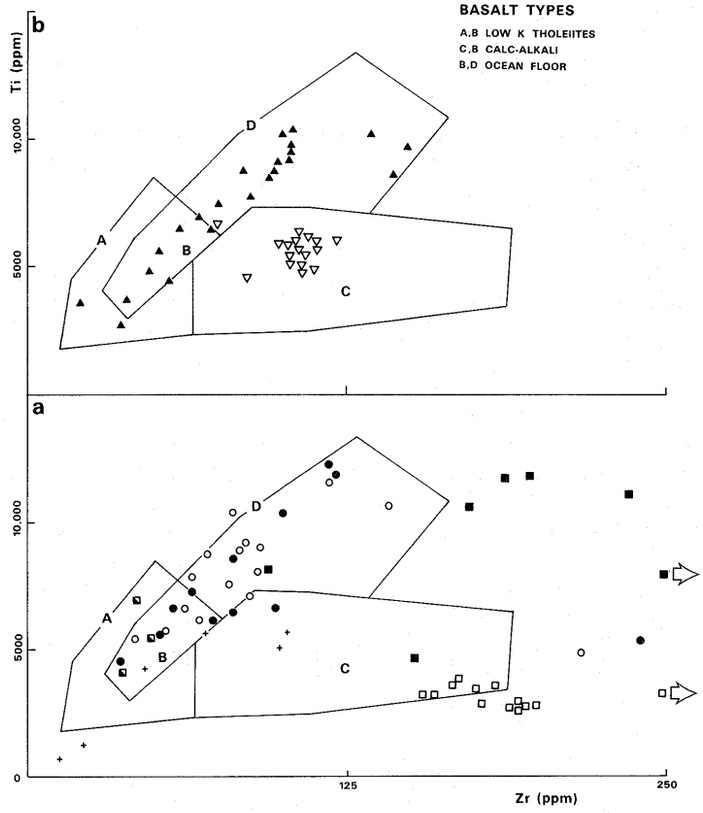

Fig. 39. a. Mafic lavas (LHF), diorites (SCI), gabbros (WG and DFC) and andesites (AIF). b. Dykes (LHF) and sills (AIF) plotted on a Ti–Zr diagram (Pearce and Cann, 1973).

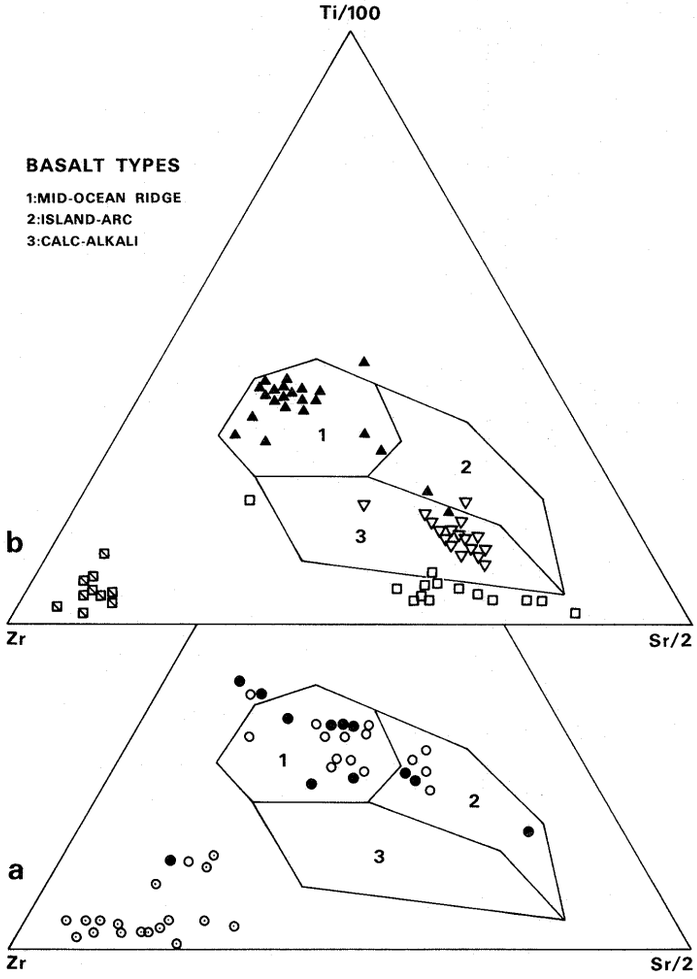

Fig. 40. a. Mafic and silicic lavas (LHF). b. Dykes (LHF), sills and andesites (AIF), and plagiogranites (SCI) plotted on a Ti/100–Zr–Sr/2 diagram (Pearce and Cann, 1973). Silicic rocks are for comparison only.

tholeiitic rocks (Miyashiro, 1973). The trend is followed more diffusely by the gabbroic rocks and lavas, the latter group showing variation in Fe* content in comparison with dykes and gabbros at equivalent Fe*/Mg levels, probably as a result of alteration. The dykes also follow a tholeiitic trend of near constant SiO_2 with increasing Fe*/Mg (Miyashiro, 1973) close to the mid-ocean ridge field (Fig. 47). The scatter of lava analyses due to an increase in SiO_2 approaches a calc-alkaline trend but field evidence suggests that SiO_2 has been introduced by secondary metasomatism in many of the lavas (cf. Troodos ophiolite; Church and Coish, 1976). This trend is also shown by the gabbroic rocks (Fig. 47), although SiO_2 enrichment in the diorites of the Smaaland Cove intrusion may be due to differentiation, as trace-element data show tholeiitic trends. The significance of SiO_2 enrichment in the Drygalski Fjord Complex gabbro is uncertain, although some analyses resemble continental tholeiites and may follow a calc-alkaline trend.

C. Silicic Rocks

The leucocratic rocks of the Smaaland Cove intrusion are thought to be oceanic plagiogranites and are chemically similar to the silicic lavas and dykes (dacites) described from the overlying Larsen Harbour Formation. Both rock types can be regarded as one geochemical group. Their close field relationship with the mafic oceanic tholeiites described above is significant and similar rocks constitute a volumetrically minor but important feature of other ophiolite sequences. The K_2O content of some of the silicic rocks exceeds that regarded as typical of plagiogranites by previous workers. Average analyses of both types are given in Table IV.

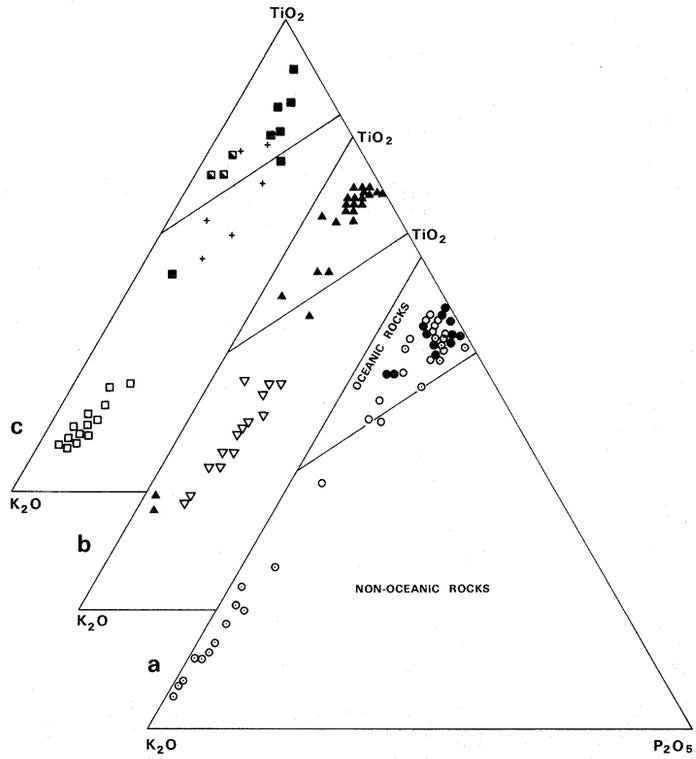

Fig. 41. TiO_2–K_2O–P_2O_5 relationships discriminating oceanic and non-oceanic rocks (Pearce and others, 1975). a. Mafic and silicic lavas (LHF). b. Dykes (LHF) and sills (AIF). c. Diorites (SCI), gabbros (WG and DFC) and andesites (AIF).

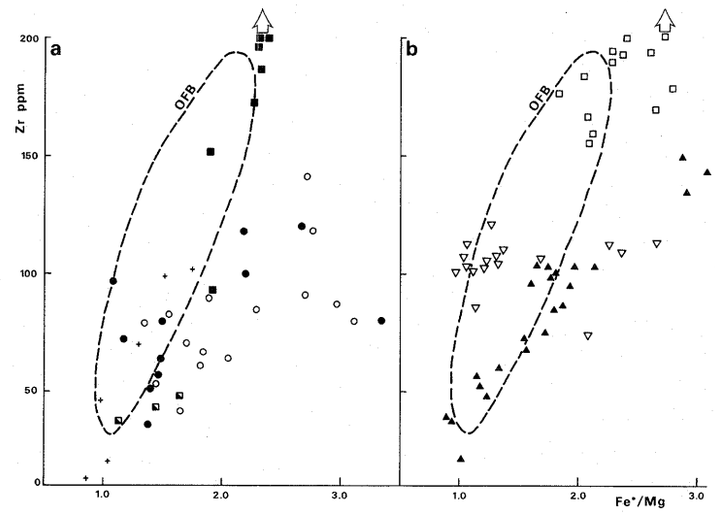

Fig. 42. Zr versus Fe*/Mg for: a. Mafic lavas (LHF), gabbros (WG and DFC) and diorites (SCI). b. Dykes (LHF), sills and andesites (AIF). OFB, ocean-floor basalt field (Saunders and others, 1979).

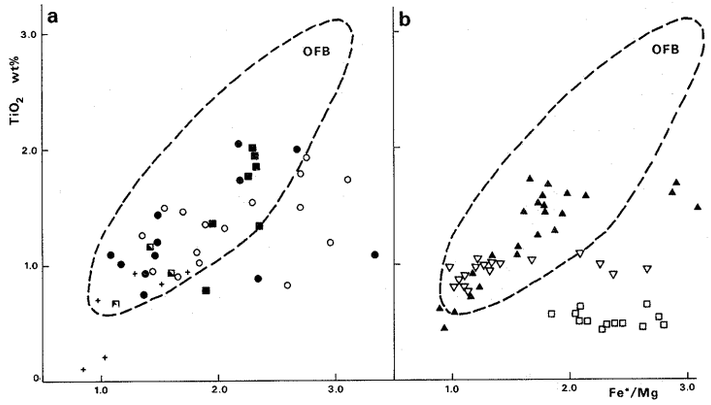

Fig. 43. TiO_2 versus Fe*/Mg for: a. Mafic lavas (LHF), gabbros (WG and DFC) and diorites (SCI). b. Dykes (LHF), sills and andesites (AIF). OFB, ocean-floor basalt field (Saunders and others, 1979).

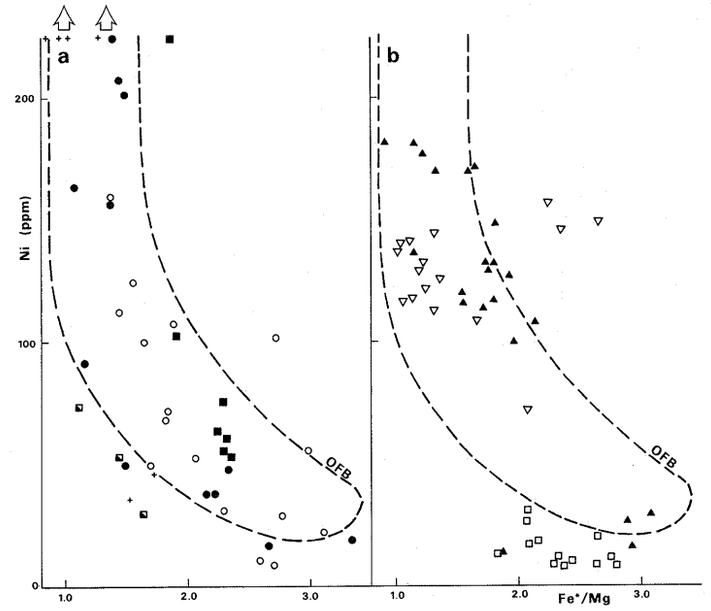

Fig. 44. Ni versus Fe*/Mg for: a. Mafic lavas (LHF), gabbros (WG and DFC) and diorites (SCI). b. Dykes (LHF), sills and andesites (AIF). OFB, ocean-floor basalt field (Saunders and others, 1979).

Coleman and Peterman (1975) first defined leucocratic rocks in ophiolite complexes as 'oceanic plagiogranites', being distinctive chemically from similar continental rocks by having higher SiO_2, moderate Al_2O_3, lower FeO and MgO, and extremely low K_2O contents. Plagiogranites were defined as having an alkali ratio ($K_20.100/(K_2O+Na_2O)$) of ~5% compared to ~49% for many continental rocks; they are regarded as differentiates of sub-alkaline basalt (Coleman and Peterman, 1975). Aldiss (1978) reviewed plagiogranites from five ophiolites and specified lack of potash feldspar, low Al_2O_3, high K/Rb ratio and a distinctive rare-earth element pattern as their characteristic features. Although 'typical' low-K_2O plagiogranites are common, Aldiss recorded similar K_2O-rich rocks from the Smartville ophiolite, California, which he also classified as plagiogranites. 'Typical' low-K_2O plagiogranites occur in the Sarmiento Complex (Saunders and others, 1979).

Both K_2O-rich and K_2O-poor silicic rocks have been recovered from present-day mid-ocean ridge systems (e.g. Engel and Fisher, 1975; Byerly and others, 1976) and are analogous to plagiogranites in ophiolite sequences as described by Aldiss (1978). The terminology thus awaits further clarification. It is noteworthy that the differentiation trend of the Thingmuli Province, Iceland, which culminates in K_2O-rich rhyolites and andesites (Carmichael, 1964), is used as a model of plagiogranite evolution (Coleman, 1977), although these rocks have alkali ratios outside the limits originally defined by Coleman and Peterman (1975).

The plagiogranites and dacites have higher Ce, Y and Nb contents but equivalent Y/Nb and Ce/Y ratios to the mafic rocks of the Larsen Harbour Formation (Fig. 37). The (CaO + MgO) screen excludes them from the discrimination diagrams of Pearce and Cann (1973) but analyses have been plotted (Figs 38 and 40) to show the similarity between them and their distinction from the andesites of the Annenkov Island Formation. All analyses fall outside the iso-alkaline limits of Pearce and others (1975) and cannot be used in their oceanic/non-oceanic plot.

The silicic rocks have higher Zr and lower TiO_2 contents than the mafic rocks and have high Fe*/Mg values, dacites ranging from 3.5 to 14.4 and plagiogranites from 4.8 to 20.2. The trend of increasing TiO_2 content with Fe*/Mg in the mafic rocks, reaching a maximum in analyses of the Smaaland Cove diorites (Fig. 39) with subsequent depletion at higher Fe*/Mg values in the plagiogranites and dacites, is characteristic of a tholeiitic differentiation sequence (Miyashiro and Shido, 1975). The high Zr content of the silicic rocks may thus reflect the high degree of crystallization required to produce them from a tholeiitic magma (Bruhn and others, 1978). The relationship between Ti and Zr with regard to the differentiation of the silicic

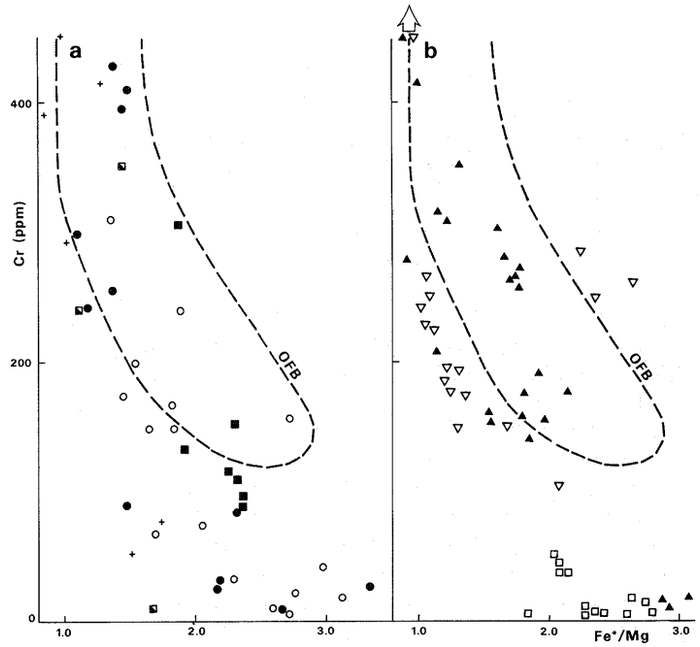

Fig. 45. Cr versus Fe*/Mg for: a. Mafic lavas (LHF), gabbros (WG and DFC) and diorites (SCI). b. Dykes (LHF), sills and andesites (AIF). OFB, ocean-floor basalt field (Saunders and others, 1979).

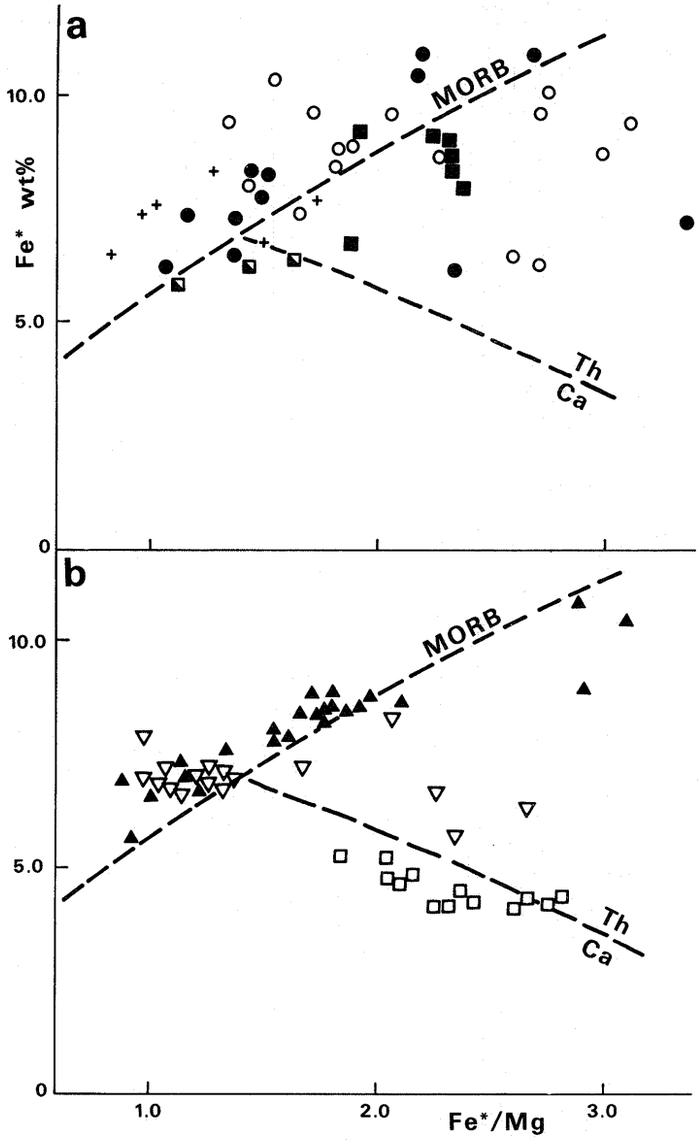

Fig. 46. Fe* versus Fe*/Mg for: a. Mafic lavas (LHF), gabbros (WG and DFC) and diorites (SCI). b. Dykes (LHF), sills and andesites (AIF). Fractionation trend of mid-ocean ridge basalts (MORB) from Saunders and others (1979), and calc-alkaline (Ca) and tholeiitic (Th) fields from Miyashiro (1973).

rocks is discussed later. The Cr content of the silicic rocks is usually below the limit of detection and Ni contents are also low, suggesting extensive fractionation. The high SiO_2 content probably reflects their formation by differentiation of a tholeiitic parent magma rather than a true calc-alkaline trend (cf. Troodos; Church and Coish, 1976).

The silicic rocks are enriched in Na_2O but K_2O is either enhanced or depleted relative to the mafic rocks, although the K_2O content remains below that of equivalent continental rocks. The K_2O-poor dacites and plagiogranites correspond to the original definition of 'oceanic plagiogranite' and have alkali ratios of 0.5–1.5% (six analyses) and 0.3–6.6% (five analyses), respectively. The K_2O-rich rocks of the Smaaland Cove intrusion have alkali ratios of 12.2–27.7% (six analyses); those of the dacites are more variable, having values of 13.0%, 16.7%, 26.2–42.3% (eight analyses) and 76%. The alkali ratios of the K_2O-rich silicic rocks are consistently less than those of continental rocks. Rb content exceeds that for the associated mafic rocks but K/Rb ratios are equivalent and not unlike those of continental rocks.

D. Annenkov Island Formation

The igneous intrusions of this formation include andesite stocks and minor sill-like basic bodies; the lithology of the associated Lower Tuff and Upper Breccia members suggests an island-arc environment (Suárez and Pettigrew, 1976). The andesites and basic sills are distinct from the mafic rocks of the Larsen Harbour Formation, having higher Al_2O_3 and K_2O, lower TiO_2 and total Fe, and from the silicic rocks in having higher Al_2O_3, MgO, CaO and K_2O. Trace and minor element contents are also different, the sills and andesites being enriched in Sr, Rb, Ba and depleted in Y. Average analyses are presented in Table IV.

Y/Nb ratios for the sills and andesites are transitional between tholeiitic and alkalic rocks (Pearce and Cann, 1973) but approximate to the continental tholeiite field in Fig. 37; Ce/Y values are higher than those for the ocean tholeiites. The sills plot consistently as calc-alkaline basalts, notably distinct from the Larsen Harbour Formation dykes in Figs 38–40. Andesite analyses are outside the screening limits for these diagrams but they are plotted for comparison and approach the calc-alkali basalt fields (Figs 38–40). The non-oceanic character of the sills is indicated in Fig. 41, the spread of analyses towards the K_2O apex possibly indicating some K_2O mobility. The sills correspond to continental calc-alkaline basalts and are

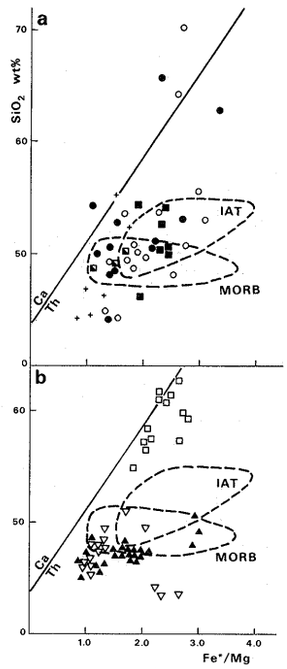

Fig. 47. SiO_2 versus Fe*/Mg for: a. Mafic lavas (LHF), gabbros (WG and DFC) and diorites (SCI). b. Dykes (LHF), sills and andesites (AIF). Island-arc tholeiite (IAT) and mid-ocean ridge basalt (MORB) fields from Saunders and others (1979) and calc-alkaline (Ca) and tholeiitic (Th) fields from Miyashiro (1973).

identified with the andesites on trace and minor element contents.

Fe*/Mg values for both rock types are restricted, varying from 1.8 to 2.8 in the andesites and from 1.0 to 2.7 in the associated basic sills. The former have higher Zr and lower TiO_2 contents than mid-ocean ridge basalts but neither parameter shows a positive correlation with increasing Fe*/Mg as for the tholeiitic rocks (Figs 42 and 43). Zr and TiO_2 contents of the sills overlap the fields of ocean-floor rocks and maintain the relationship shown by the andesites of near constant Zr and TiO_2 values with increasing Fe*/Mg (Figs 42 and 43). Ni and Cr abundances of the sills are generally lower than those of ocean-floor basalts at equivalent Fe*/Mg levels (Figs 44 and 45) and the andesites have both low Cr and Ni contents, typical of island-arc rocks (Garcia, 1978). The decrease in Fe* with increasing Fe*/Mg, especially in the andesites, corresponds to the field of calc-alkaline rocks defined by Miyashiro (1973) in Fig. 46. The calc-alkaline trend is also shown by an increase in SiO_2 content with increasing Fe*/Mg in Fig. 47.

The basic sills have lower SiO_2, Al_2O_3, Na_2O and higher TiO_2, total Fe, MgO and CaO contents than the andesites; P_2O_5 contents are similar in both. Rb, Sr, Zr and Ba abundances are enriched in the andesites but Y, Nb, La and Ce contents are equivalent to those of the sills. In comparison with the dykes of the Larsen Harbour Formation, the sills have equivalent SiO_2, MgO, Cr and Ni values but higher Al_2O_3, Na_2O, K_2O and P_2O_5 contents. Na_2O/K_2O is lower in the latter rocks. The andesites are less SiO_2- and Na_2O-rich than the plagiogranites or dacites but are enriched in all other major elements, notably K_2O. Their alkali ratios are generally higher than those of the K_2O-rich silicic rocks associated with the Larsen Harbour Formation, values of 25.5%, 28.4% and 35.2–49.6% (11 analyses) being obtained. Ba, Sr and Rb are enhanced and Zr, Y and Nb are depleted in the andesites with respect to the dacites and plagiogranites.

E. Differentiation Trends

Trace and minor element relationships in the mafic and silicic rocks of the Larsen Harbour Formation and the Smaaland Cove intrusion suggest their common tholeiitic origin. The trend established in an AFM diagram (where $A = Na_2O + K_2O$; F = total iron as FeO; M = MgO) correlates well with that of the Thingmuli Province, Iceland (Carmichael,1964), where it was deduced that silicic alkalic rocks are the end products of extensive differentiation of oceanic tholeiitic magma. It is tentatively suggested that at least part of the Drygalski Fjord Complex represents the basal cumulate rocks of the ophiolite, of which the Larsen Harbour Formation is the upper part, whereas the remainder may be related to continental tholeiites. The position of the Drygalski Fjord Complex gabbros in Fig. 48 shows their possible relation to both tholeiitic and calc-alkaline trends. The less altered dykes of the Larsen Harbour Formation define a clear tholeiitic trend of initial iron enrichment without increase in alkali content (Fig. 48). This trend is less clearly followed by the lavas and gabbros due to variations in alkali content probably caused by alteration. The diorites of the Smaaland Cove intrusion associated with the silicic plagiogranites represent the most differentiated mafic plutonic rocks (Fig. 48). The plagiogranites and dacites show a pattern of decreasing iron with increasing alkali content, analyses of the former plotting closely to the Thingmuli trend (Fig. 48).

A calc-alkaline trend (cf. Cascades Province; Carmichael, 1964) is followed by the andesites and sills of the Annenkov Island Formation (Fig. 48). The sills show some iron enrichment without significant increase in alkali content, approaching the trend of alkalic rocks (Irvine and Baragar, 1971).

The differentiation sequence of the Chilean ophiolites has been described by Bruhn and others (1978), using the relationship of Ti and Zr. Ti content increases initially with increasing Zr content to reach a maximum before decreasing to a minimum with continued increase in Zr (cf. formation of a plagiogranite in Sarmiento; Saunders and others, 1979). This differentiation trend is closely followed by the mafic and silicic rocks of the Larsen Harbour Formation and Smaaland Cove intrusion, and verifies the pattern indicated in an AFM diagram (Figs 48 and 49). The tholeiitic parentage of the dacites and plagiogranites is thus established and differentiated rocks from other ophiolites conform to the given trend. The Annenkov Island Formation rocks plot separately from the tholeiitic trend (Fig. 49) and maintain a negative correlation between Ti and Zr, which is typical of calc-alkaline rocks (Miyashiro, 1973). Fig. 49 also suggests a continental affinity for some of the Drygalski Fjord Complex rocks.

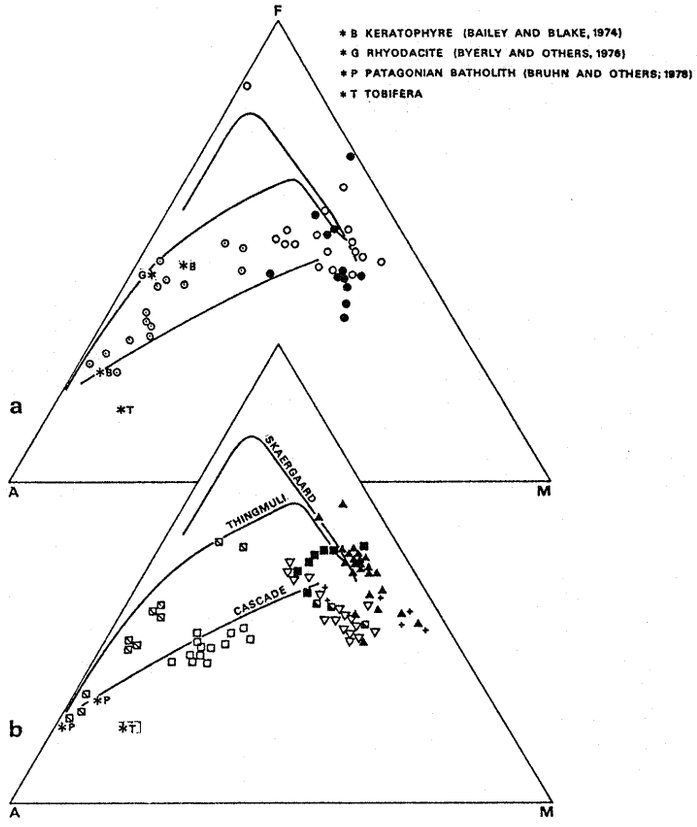

Fig. 48. AFM ($A=Na_2O+K_2O$; F=total iron as FeO; M=MgO) relationships of: a. Mafic and silicic lavas (LHF). b. Dykes (LHF), sills and andesites (AIF), gabbros (WG and DFC), and plagiogranites and diorites (SCI). Comparative trends are from Carmichael (1964).

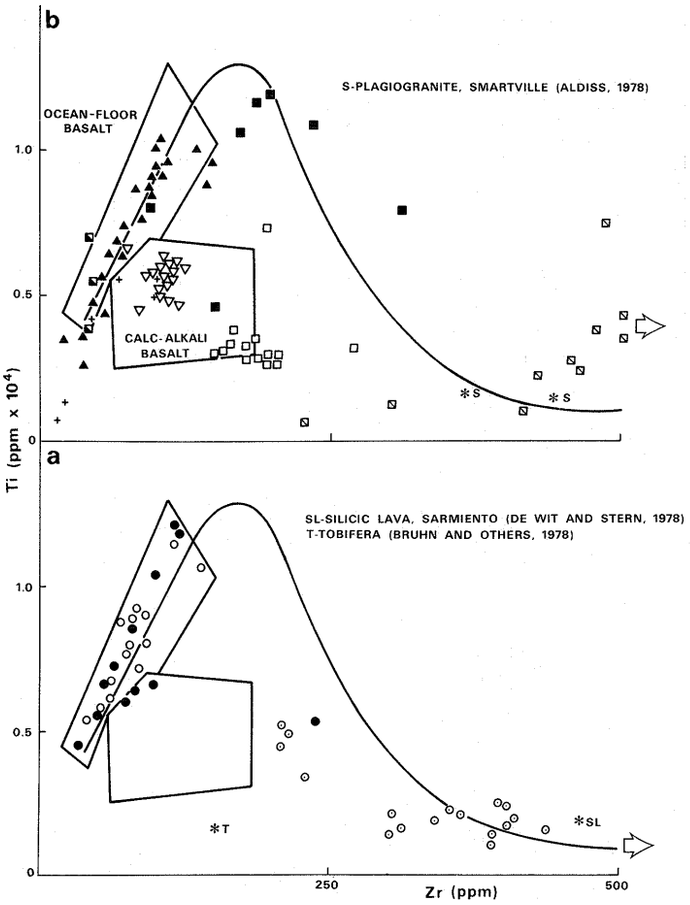

Fig. 49. Ti–Zr differentiation relationships of: a. Mafic and silicic lavas (LHF). b. Dykes (LHF), sills and andesites (AIF), gabbros (WG and DFC), and plagiogranites and diorites (SCI). Fields shown are from Pearce and Cann (1973) and the trend shown is for the Chilean ophiolites (Bruhn and others, 1978).

F. Discussion and Interpretation

1. Mafic rocks

The trace and minor element contents of the mafic rocks of the Larsen Harbour Formation identify them as oceanic tholeiites associated with the underlying Wheeler Glacier gabbro, Smaaland Cove intrusion diorites and parts of the Drygalski Fjord Complex. Cumulate rocks only occur in the latter unit and some of them show continental affinities.

The Larsen Harbour Formation is geochemically similar to the Sarmiento Complex, Chile, described by Saunders and others (1979); average analyses of its constituent rock types are given in Table V. Both ophiolites have higher Ba, Fe*/Mg and Ba/Sr ratios and lower K/Rb ratios than average ocean-floor basalts (Tables V and VI) but, whereas K and Rb are enriched in the Sarmiento rocks, they are generally depleted in the lavas and dykes of the Larsen Harbour Formation. Those sampled for the present investigation represent the lowest level of the extrusive unit, at greenschist and amphibolite facies, where hydrothermal activity is likely to have caused depletion of these elements (cf. altered rocks of the Sarmiento Complex; Saunders and others, 1979). The plutonic rocks contain varying amounts of K_2O and Rb, most containing higher K_2O than ocean-floor basalts, but Rb only is consistently enriched in the Drygalski Fjord Complex gabbros. The K/Rb ratios for all rocks remain below that for average ocean-floor basalts. The least-differentiated Wheeler Glacier and Drygalski Fjord Complex gabbros probably represent the more primitive units of the Larsen Harbour Formation ophiolite. The variable depletion of K_2O and Rb in the gabbroic rocks is consistent with their structural position below the main zone of hydrothermal alteration where the movement of elements by leaching is more sporadic and localized (Stern and others, 1976). It is suggested that the plutonic rocks associated with the Larsen Harbour Formation are essentially undepleted and hence equivalent to those of the Sarmiento Complex. The altered lavas and their associated dykes resemble normal depleted ocean-floor basalts, being low in K_2O and Rb, but they have been subjected to pervasive metamorphism. The geochemistry of the least-altered pillow lavas and dykes from the upper levels of the sequence is not available at present.

2. Silicic rocks

The plagiogranites (Smaaland Cove intrusion) and dacites (Larsen Harbour Formation) represent the end products of Thingmuli-type differentiation of a sub-alkaline tholeiitic magma. Both K_2O-rich and K_2O-poor examples occur, the former falling outside the original plagiogranite definition of Coleman and Peterman (1975). The silicic rocks have moderate Al_2O_3 and low K_2O (with respect to SiO_2) contents in comparison with continental rocks. Alkali ratios are consistently below those of continental rocks (Tables IV and V).

The dacites are analogous to keratophyres described from spilitic associations (e.g. Donnelly, 1966; Cann, 1969) and from ophiolite sequences (e.g. Bailey and Blake, 1974) (Tables IV and V; Fig. 48). Although Hughes (1973) attributed their formation to metasomatism, Coleman and Peterman (1975) maintained that there is sufficient evidence to support their formation by differentiation as is suggested here. Their association with ophiolite rocks (commonly spilitic) is well documented (e.g. Bamba, 1974), and Brown and others (1979) described them as a significant volcanic unit in the Fidalgo ophiolite, Washington, associated with plagiogranite. The K_2O-rich dacites correspond to the similar rock types from mid-ocean ridge systems which have survived secondary modification by alteration. The more typical low-K_2O differentiates also occur in Sarmiento (de Wit and Stern, 1978; Saunders and others, 1979) and the Troodos ophiolite (Coleman and Peterman, 1975). Potassium feldspar is an uncommon phase in the dacites but where retained it may explain the higher K_2O content of specific examples.

The plagiogranites compare with examples from Sarmiento (Saunders and others, 1979), Smartville (Aldiss, 1978) and present-day mid-ocean ridge systems such as Galapagos (Byerly and others, 1976) (Tables IV and V and Figs 48 and 49). The alkali ratios of the K_2O-poor types are within the limits of plagiogranites (Coleman and Peterman, 1975) but those of the K_2O-rich varieties are not, yet they do not reach the high values of continental rocks. The occurrence of both types in ophiolite sequences (cf. Smartville; Aldiss, 1978) and mid-ocean ridge systems suggests that the range of plagiogranites is more varied than first reported. Potassium feldspar occurs as perthitic intergrowths in rocks of the Smaaland Cove intrusion and its

Table V. Mean analyses of ophiolite, island-arc and mid-ocean ridge rocks.

	1	2	3	4	5	6	7	8	9	10	11	12
Oxides (%)												
SiO_2	49.21	48.97	50.94	48.60	74.59	74.59	71.52	69.27	59.98	57.4	48.80	72.5
TiO_2	1.39	1.66	1.37	1.43	0.30	0.19	0.28	0.55	0.61	0.65	0.18	0.21
Al_2O_3	15.81	14.62	15.31	15.61	12.60	12.15	14.12	12.10	17.42	17.7	11.94	14.0
Fe_2O_3	10.20	12.72	12.00	11.20	2.73	2.87	3.83	6.62	6.89	6.87	9.73	4.4
MnO	0.16	0.18	0.19	0.20	0.03	0.05	0.15	na	0.19	0.15	0.18	0.06
MgO	8.53	6.50	5.84	6.91	0.26	0.06	0.18	0.45	3.23	3.45	10.39	1.0
CaO	11.14	11.71	10.22	7.47	5.00	6.95	1.61	2.99	5.94	7.4	11.44	2.5
Na_2O	2.71	1.95	2.40	4.42	3.55	2.50	6.63	4.28	3.45	3.4	2.81	3.7
K_2O	0.26	0.40	0.23	0.33	0.15	0.01	1.33	1.37	1.66	1.25	1.52	0.33
P_2O_5	0.15	0.14	0.29	0.19	0.06	0.03	0.04	0.08	0.16	na	0.40	0.06
Trace elements (ppm)												
Cr	296	152	115	269	na	4	5	na	na	na	220	na
Ni	123	30	27	74	na	6	na	na	na	na	110	na
Rb	1.3	12	8	5	na	1	11	na	57	2	22	na
Sr	137	140	191	110	na	286	78	na	326	540	773	na
Y	32	21	32	26	na	107	66	na	na	18	14	na
Zr	122	53	122	121	470	465	367	na	92	95	54	na
Nb	3	1	3	6	na	12	9	na	13	na	na	na
Ba	9	96	92	171	na	12	333	na	484	270	620	na
La	na	4	9	6	na	27	na	na	na	9.1	14	na
Ce	na	10	22	17	na	69	na	na	na	17	29	na
Fe*/Mg	1.39	2.27	2.38	1.88	12.25	55.5	24.8	17.16	2.49	2.32	1.09	5.13
K/Rb	1 131	277	239	548	–	60	725	–	242	474	575	–
Rb/Sr	0.01	0.09	0.04	0.05	–	0.003	0.14	–	0.18	0.04	0.03	–
$\frac{K_2O.100}{(Na_2O + K_2O)}$	–	–	–	–	4.1	–	16.7	24.2	32.5	26.9	35.1	8.2

1, average mid-ocean ridge basalt (Saunders and others, 1979); 2, 3 and 4, averages of gabbros, dykes and lavas, respectively, Sarmiento Complex (Saunders and others, 1979); 5, average silicic lava, Sarmiento Complex (de Wit and Stern, 1978); 6, plagiogranite (PA28A), Sarmiento Complex (Saunders and others, 1979); 7, plagiogranite, Smartville ophiolite (Aldiss, 1978); 8, rhyodacite, Galapagos spreading centre (Byerly and others, 1976); 9, average Patagonian Batholith, Chile (Bruhn and others, 1978); 10 and 11, average andesite and shoshonite, respectively, Viti Levu (Gill, 1970); 12, quartz-keratophyre, Quinto Creek ophiolite (Bailey and Blake, 1974).
Fe_2O_3, total iron as Fe_2O; Fe*, total iron as Fe^{2+}; na, not analysed.

presence excludes it from Aldiss (1978) definition of plagiogranite, except for the orthoclase-porphyry types of Smartville. Ba and Sr are sympathetically depleted in the low-K_2O plagiogranites, suggesting their modification by leaching near the extrusive and plutonic unit interface in the ophiolite.

3. *Annenkov Island Formation*

The island-arc andesites and basic sills are continental tholeiites and follow a calc-alkaline differentiation trend; they correspond to similar rocks from the Viti Levu island-arc, Fiji (Gill, 1970), and the Patagonian Batholith, Chile (Bruhn and others, 1978) (Tables IV and V; Fig. 48). The andesites contain higher Na_2O, K_2O and P_2O_5 compared to the average batholith rocks, and other major oxides are equivalent. Sr, Ba and Zr are strongly enhanced in the andesites and in this respect they resemble rocks of the Tobífera Formation, South America (Bruhn and others, 1978).

The sills are K_2O-rich and approach the composition of shoshonitic rocks from the Viti Levu arc (Tables IV and V); these rocks do not appear to be represented in the island-arc sequences of South America. Both the andesites and sills are enriched in K, Rb, Sr and Ba in comparison with the average Patagonian Batholith rocks and they may represent the high-level calc-alkaline and shoshonitic rocks of an evolved island-arc on continental crust, as described from the Andean cordillera by Jakes and White (1971).

4. *Conclusion*

The Sarmiento Complex and Larsen Harbour Formation ophiolites contain silicic differentiates and their less-altered mafic rocks have undepleted characteristics. Available data suggest that the Larsen Harbour Formation has been formed by a similar process to that outlined for the Sarmiento Complex. This supports a transitional (continental–oceanic) tholeiitic geochemistry derived by partial melting of undepleted sub-continental mantle during the evolution of the marginal basin in a zone of limited extension (Saunders and others, 1979). The presence of K_2O-rich plagiogranites and dacites in the Larsen Harbour Formation and Smaaland Cove intrusion suggests that a broader classification of silicic rocks within ophiolites is necessary.

The marginal basin ophiolitic rocks of South Georgia are bordered to the west by the Annenkov Island Formation, which comprises a calc-alkaline assemblage of andesites and alkali-rich basic sills. These rocks constitute an island-arc environment, which probably formed on continental crust and split off from the main continental margin during the evolution of the marginal basin.

The Drygalski Fjord Complex contains rocks of both oceanic and continental characteristics, possibly associated with the Larsen Harbour Formation and with a possible remnant island-arc or continental margin, respectively, lying to the east of the ophiolite sequence.

V. MINERAL CHEMISTRY AND METAMORPHISM

The metamorphic and relict igneous mineral phases in rocks of the Larsen Harbour Formation and the Smaaland Cove intrusion have been analysed by microprobe (energy dispersive system) to determine the metamorphic zonation (if any) of the Larsen Harbour Formation, using analyses of the dominant metamorphic mineral phases (amphibole, albite, epidote and chlorite) and relict igneous mineral phases (plagioclase and clinopyroxene). Of equal importance was the need to verify the presence of prehnite and pumpellyite in the upper levels of the Larsen Harbour Formation and also the identification of both igneous and metamorphic amphibole in rocks of the Smaaland Cove intrusion.

Mineral analyses were carried out on a Cambridge Geoscan microprobe, using the energy dispersive system, at the University of Aberdeen. The microprobe analyses, as weight per cent oxides, were recalculated by computer as atomic proportions and relevant end-member compositions. Initially, all iron was calculated as FeO and then converted to total iron as Fe_2O_3 for certain minerals; the relative amounts of FeO and Fe_2O_3 in amphiboles were calculated by the method described by Leake (1978).

Structural formulae for all minerals are given on the basis of the number of oxygen atoms appropriate to anhydrous weight per cent totals.

A. Amphibole Analyses

Distinctive hornblende and actinolite have been recognized optically in the suite of rocks investigated. The importance of the FeO and Fe_2O_3 contents of both these phases has been discussed in the literature. Cooper and Lovering (1970) stated that in the deeply coloured hornblendes Fe_2O_3 may be significant and comprise up to 10% of the total iron present, but they published their analyses as FeO only. Fe_2O_3 is regarded as a minor constituent in actinolite in comparison to hornblende (Sampson and Fawcett, 1977), although Misch and Rice (1975) stated that Fe^{3+} can be exceeded by Fe^{2+} in metamorphic hornblendes. Analyses given here suggest that

Table VI. Typical amphibole analyses.

	1	*2*	*3*	*4*	*5*	*6*	*7*	*8*
SN	M.2078.5	M.3700.7	M.1837.2	M.2072.2	M.2075.9	M.1818	M.1828	M.3711.2
A(N)	1	1	1(4)	2(4)	1(2)	1(3)	1(3)	1
SiO_2	48.12	54.14	48.97	49.56	49.20	47.88	48.01	45.17
TiO_2	0.16	0.0	0.28	0.54	0.30	0.05	0.14	0.41
Al_2O_3	3.45	0.21	6.69	4.73	7.07	4.66	6.23	7.89
ΣFeO	22.42	19.02	19.23	20.87	18.27	21.17	19.40	11.69
MnO	0.67	0.56	0.30	0.35	0.22	0.29	0.35	0.22
MgO	7.98	10.93	10.29	10.17	11.25	11.28	12.05	16.32
CaO	11.83	11.40	12.35	12.12	12.65	10.02	9.42	13.87
Na_2O	0.45	0.0	0.52	0.57	0.0	0.0	0.13	0.0
K_2O	0.0	0.0	0.05	0.02	0.0	0.0	0.03	0.0
Total	95.08	96.26	98.78	98.93	98.96	95.35	95.76	95.57
Structural formulae on the basis of 23(O)								
Si	7.492	8.086	7.167	7.285	7.107	7.059	6.940	6.594
Al^{IV}	0.508	–	0.833	0.715	0.893	0.809	1.060	1.358
Fe^{3+}	–	–	–	–	–	0.132	–	0.048
Ti^{IV}	–	–	–	–	–	–	–	–
T	8.00	8.09	8.00	8.00	8.00	8.00	8.00	8.00
Al^{VI}	0.124	0.036	0.321	0.104	0.411	–	0.001	–
Ti^{VI}	0.018	0.0	0.031	0.060	0.032	0.005	0.015	0.045
Fe^{3+}	0.267	0.143	0.421	0.509	0.602	1.766	2.070	0.977
Mg	1.851	2.432	2.245	2.227	2.423	2.479	2.596	3.549
Fe^{2+}	2.652	2.232	1.945	2.057	1.532	0.713	0.276	0.402
Mn	0.088	0.071	0.037	0.043	–	0.036	0.042	0.027
C	5.00	4.91	5.00	5.00	5.00	5.00	5.00	5.00
Fe^{2+}	–	–	–	–	0.073	–	–	–
Mn	–	–	–	–	0.027	–	0.001	–
Mg	–	–	–	–	–	–	–	–
Ca	1.973	1.825	1.936	1.883	1.957	1.582	1.459	2.170
Na	0.027	0.0	0.064	0.110	–	0.0	0.036	0.0
B	2.00	1.83	2.00	1.99	2.06	1.58	1.50	2.17
Na	0.109	–	0.082	–	0.0	–	–	–
K	0.0	0.0	0.010	0.0	0.0	0.0	0.005	0.0
A	0.11	0.00	0.09	0.00	0.00	0.00	0.01	0.0

Fe^{3+} content calculated after Leake (1978). SN, specimen number; A(N): A, analysis number, N, number of analyses averaged.
1 and 2, pillow lavas; 3–5, massive lavas; 6–9, basic dykes; 10–13, granodiorites; 14 and 15, Smaaland Cove gabbro.

Fe^{2+} exceeds Fe^{3+} in actinolite and in most hornblende (Table VI).

Recent amphibole classification schemes require some knowledge of relative amounts of FeO and Fe_2O_3, and a numerical method (Leake, 1978) was used to calculate them. Analyses quoting FeO alone are common in the literature (Kawachi, 1975; Coombs and others, 1976; Nakajima and others, 1977; Sampson and Fawcett, 1977; Hutchison, 1978). A selection of typical analyses and structural formulae is given in Table VI and classified after Leake (1978) in Fig. 50.

1. Pillow and massive lava amphibole

Hornblende and actinolite can be distinguished on Ti content and occupancy of the A-site in the structure (Cooper and Lovering, 1970), and Al_2O_3 content (Liou and others, 1974). Amphibole in the mafic lavas is actinolite and hornblende (Fig. 50). In contrast to the amphiboles from the other rock types, they contain Al in both T and C sites, and Fe^{3+} is exceeded by the Fe^{2+} content (Table VI). Al_2O_3 ranges from 0.21 to 7.13 wt % for actinolite and hornblende, and TiO_2 content (0.00–0.54 wt %) is low for both types. A possible increase in metamorphic grade from Rogged Bay (1) to Smaaland Cove (2 and 3), indicated by the higher TiO_2 (Ti^{VI}) and Al_2O_3 (Al^{IV}) contents of the lava amphibole (Cooper and Lovering, 1970), is suggested in Fig. 51a and b. An apparent metamorphic gradation between west (2) and east (3) in Smaaland Cove is indicated in Fig. 51b but insufficient data are available for further interpretation. Al vs (Fe + Mn)/(Fe + Mn + Mg) for mafic lava amphibole plots outside the amphibole fields of the particular metamorphic facies of Sobolev and Kostyuk (1972) in Fig. 52.

The A-site occupancy of both hornblende and actinolite is low and more typical of the latter amphibole. This parameter has been used by Cooper and Lovering (1970) and Misch and Rice (1975) to distinguish both types; actinolite contains 0.0–0.23 atoms per formula unit and hornblende 0.28–0.45 atoms per formula unit.

2. Dyke amphibole

Many of the basic dykes post-date the hydrothermal metamorphism of the lava pile and are equivalent to 'dykes within pillow lavas' of the Sarmiento Complex (Elthon and

Table VI. Typical amphibole analyses (continued).

	9	*10*	*11*	*12*	*13*	*14*	*15*
SN	M.3753.8	M.1814.2	M.1814.2	M.1831.1	M.1831.1	M.1852.2	M.1852.2
A(N)	2(9)	1(2)	3(2)	2	3(2)	1	3
SiO_2	50.79	47.26	52.33	47.80	45.72	49.89	47.48
TiO_2	0.53	1.40	0.0	0.0	1.46	0.27	1.23
Al_2O_3	3.52	5.41	1.96	3.72	5.82	2.40	4.98
ΣFeO	16.30	20.47	19.26	27.89	25.23	20.02	21.68
MnO	0.31	0.30	0.32	0.62	0.54	0.12	0.36
MgO	14.10	10.99	12.14	5.91	7.60	11.30	9.28
CaO	10.42	10.48	10.81	10.18	9.87	11.11	11.00
Na_2O	0.51	1.34	0.0	0.0	1.73	0.68	0.98
K_2O	0.19	0.28	0.0	0.22	0.40	0.22	0.21
TOTAL	96.67	97.93	96.82	96.34	98.37	96.21	97.20
Structural formulae on the basis of 23(O)							
Si	7.317	6.946	7.633	7.325	6.866	7.474	7.133
Al^{IV}	0.597	0.937	0.338	0.672	1.030	0.425	0.867
Fe^{3+}	0.086	0.117	0.029	–	0.104	0.101	–
Ti^{IV}	–	–	–	–	–	–	–
T	8.00	8.00	8.00	8.00	8.00	8.00	8.00
Al^{VI}	–	–	–	–	–	–	0.015
Ti^{VI}	0.057	0.155	0.0	0.0	0.165	0.031	0.139
Fe^{3+}	1.176	1.107	0.987	1.294	1.046	0.658	0.708
Mg	3.027	2.408	2.640	1.349	1.701	2.522	2.077
Fe^{2+}	0.702	1.330	1.334	2.280	2.019	1.749	2.016
Mn	0.038	–	0.039	0.077	0.069	0.040	0.045
C	5.00	5.00	5.00	5.00	5.00	5.00	5.00
Fe^{2+}	–	0.062	–	–	–	–	–
Mn	–	0.037	0.001	0.003	–	0.001	–
Mg	–	–	–	–	–	–	–
Ca	1.609	1.651	1.690	1.671	1.588	1.783	1.771
Na	0.142	0.250	0.0	0.0	0.412	0.198	0.299
B	1.75	2.00	1.69	1.67	2.00	1.98	2.00
Na	–	0.132	–	–	0.093	–	0.056
K	0.034	0.053	0.0	0.043	0.077	0.043	0.040
A	0.03	0.19	0.0	0.04	0.17	0.04	0.10

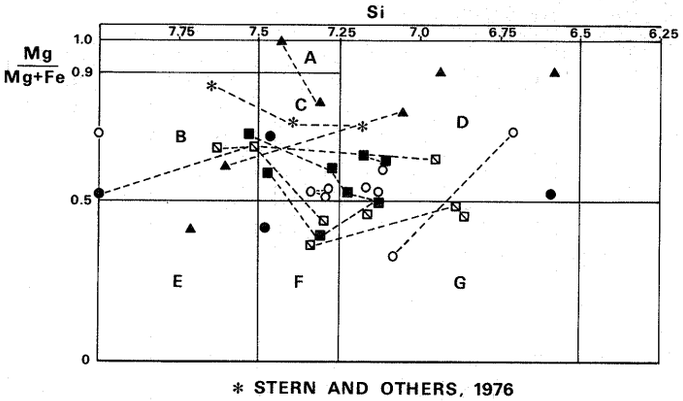

Fig. 50. Classification of amphiboles from the LHF and SCI using the method of Leake (1978). Analyses from the Chilean ophiolites (Stern and others, 1976) are plotted for comparison. Fields are: A, tremolitic hornblende; B, actinolite; C, actinolitic hornblende; D, magnesio-hornblende; E, ferro-actinolite; F, ferro-actinolitic hornblende; G, ferro-hornblende. In all the following figures the pecked lines join analyses from the same specimen.

Stern, 1978), but amphibole is developed in those from the lower structural levels. Some dykes of low amphibolite facies (this report) may represent the sheeted dyke layer of the Larsen Harbour Formation, which is comparable to that in the Chilean example.

Dyke amphibole is metamorphic and classified as actinolite, actinolitic hornblende and Mg hornblende (Fig. 50), showing wide Si variation. The Al_2O_3 content varies from 2.3 to 7.9 wt % and TiO_2 content from 0.00 to 0.53 wt %; the A-sites of the structure are usually empty. The relationship between Ti^{VI} and Al^{IV} contents for the dyke amphibole suggests that those analysed from east Smaaland Cove (3) approach actinolite in composition (low Al^{IV} and Ti^{VI}), representing a lower grade than those in the adjacent lavas (Fig. 51a). However, one analysis from Rogged Bay (1) contradicts this relationship, and dyke amphibole analyses from Nattriss Head (4) approach hornblende in composition (Fig. 51a). The differing metamorphic grades of the lavas and dykes of Smaaland Cove are again indicated in Fig. 51b using amphibole and whole-rock analyses. Fe^{3+} and Fe^{2+} contents vary unsystematically between actinolite and hornblende (Table VI). The amphibole present in rocks of the lower levels of the lava sequence is appropriate to greenschist or lower amphibolite facies.

3. Plagiogranite and gabbro amphibole

Both primary and secondary amphibole occur within the Smaaland Cove intrusion but these phases were not identified in the Wheeler Glacier gabbro. Two amphiboles, essentially actinolite and hornblende, have been determined optically by their contrasting colour and form in the intrusion, the actinolite visibly replacing the latter mineral. From microprobe analyses, it is apparent that some of the hornblende is chemically distinctive, on the basis of TiO_2 content, from that with similar optical properties. Typical analyses and structural formulae are given in Table VI and classified in Fig. 50.

Igneous and metamorphic amphibole have been distinguished using total Al content and f ($f = (Fe^{2+} + Fe^{3+} + Mn).100/(Fe^{2+} + Fe^{3+} + Mn + Mg)$) by Sobolev and Kostyuk (1972). The fields defined by these authors seem unduly restricted and the analysed amphibole does not lie within these fields (Fig. 52). Hutchison (1978) showed that igneous amphibole contains 0.23–0.34 Ti atoms whereas metamorphic amphibole contains 0.03–0.05 Ti atoms in their structural formulae. Two groups have been established in the present rocks using these criteria, containing 0.0–0.08 and 0.11–0.17 Ti atoms per formula unit and both outside the limits given by Hutchison, but this may reflect the Ti-poor nature of the assemblages.

By comparison with amphibole of other metamorphic and igneous regimes, the following three amphibole groups have been recognized on a chemical basis: actinolite, metamorphic hornblende and igneous hornblende, containing 2.0–2.5, 3.7–

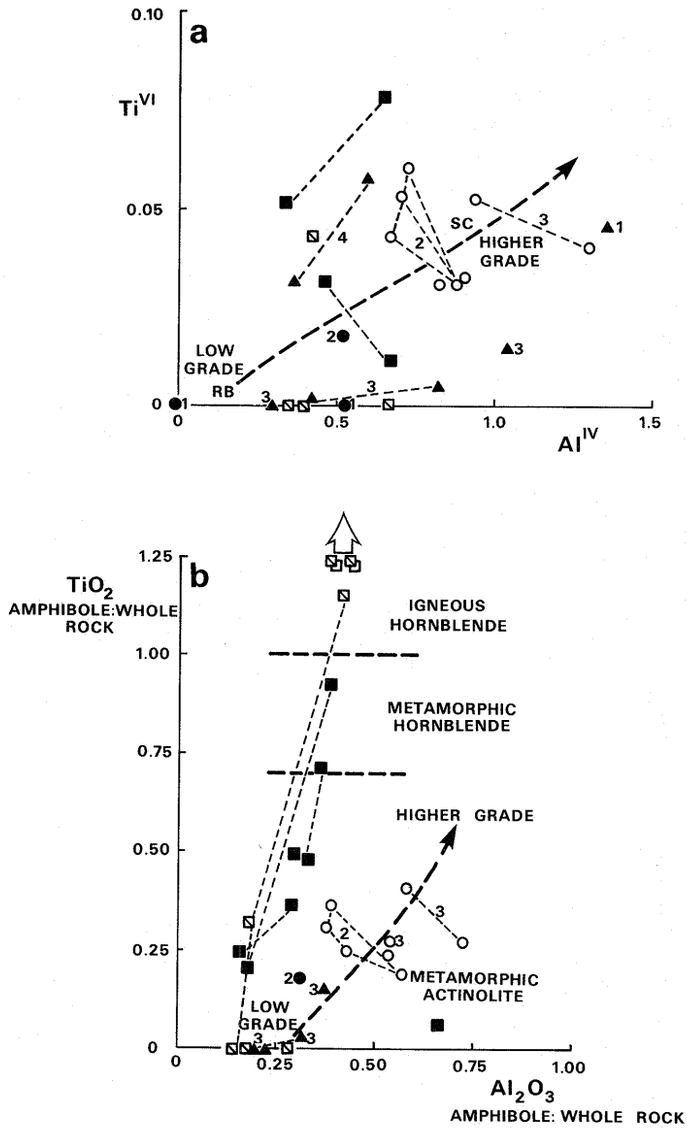

Fig. 51. a. Ti^{VI} vs Al^{IV} content in amphiboles, after Cooper and Lovering (1970), showing an increase in grade within lavas from Rogged Bay (RB) to Smaaland Cove (SC). 1, Rogged Bay; 2 and 3, west and east Smaaland Cove, respectively; 4, Nattriss Head. b. Variations in TiO_2 and Al_2O_3 content of amphibole and parent rock with metamorphic grade, after Cooper and Lovering (1970). The key is the same as in Fig. 51a.

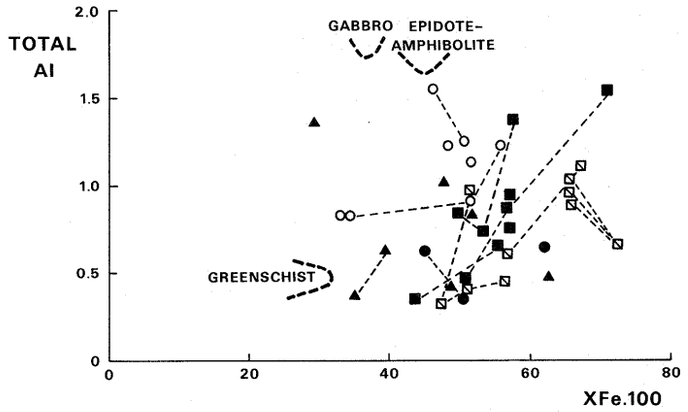

Fig. 52. Amphibole analyses from the LHF and SCI compared with those of greenschist facies, epidote-amphibolite facies and gabbroic rocks as defined by Sobolev and Kostyuk (1972).
XFe=$(Fe^{2+}+Mn)/(Fe^{2+}+Mn+Mg)$.

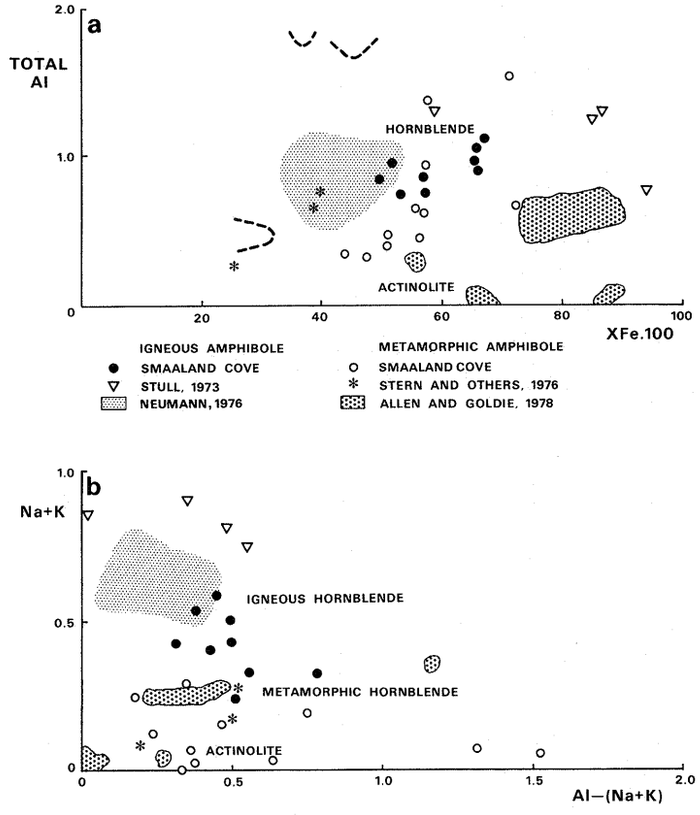

Fig. 53. a. Total Al vs XFE.100 for igneous (solid circles) and metamorphic (open circles) amphiboles of the SCI, compared with those of other workers; fields of Sobolev and Kostyuk (1972) as in Fig. 52. b. (Na + K) vs (Al − (Na + K)) for igneous and metamorphic amphiboles of the SCI, compared with those of other workers. The key is the same as in Fig. 53a.

4.9 and 3.9–5.8 wt % Al_2O_3, and 0.0–0.5, 0.7–1.1 and 1.0–1.5 wt % TiO_2, respectively. By plotting total Al against f, some correlation between the various amphibole and those of other authors can be established (Fig. 53a). Igneous amphibole reported here approaches the field of those of Neumann (1976), and the low-Al actinolites plot near those of Allen and Goldie (1978), having a true metamorphic origin. A clearer separation is obtained by plotting (Na + K) against Al − (Na + K) in Fig. 53b. The igneous hornblende has higher (Na + K) values and some correspond to that of Stull (1973) and Neumann (1976), while the low-(Na + K) actinolite plots near that of Allen and Goldie (1978). A third group, metamorphic hornblende, falls between the fields of those already described and is equivalent to similar phases of Stern and others (1976) and Allen and Goldie (1978) (Fig. 53b).

Allen and Goldie argued that co-existing hornblende and actinolite are separated by a miscibility gap, which is evident when (Na+K) and Al^{IV} are plotted against $Mg/(Mg + Fe^{2+})$. Such a gap exists (Fig. 54) between amphiboles (not necessarily in contact with each other) from the same specimen but it may not represent a true equilibrium assemblage. The separation of the three amphibole types in the rocks of the Smaaland Cove intrusion is outlined again, the metamorphic hornblendes reported here corresponding to those of Stern and others (1976). An overlap between the igneous and metamorphic types may indicate a gradational compositional change from one to the other.

B. Plagioclase Analyses

Changes in plagioclase composition (Table VII, Fig. 55) may reflect variation in metamorphic grade; greenschist facies contain albite ($An_{<7}$) with actinolite, and amphibolite facies contain oligoclase ($An_{>20}$) with hornblende, although a transitional assemblage containing actinolite and oligoclase

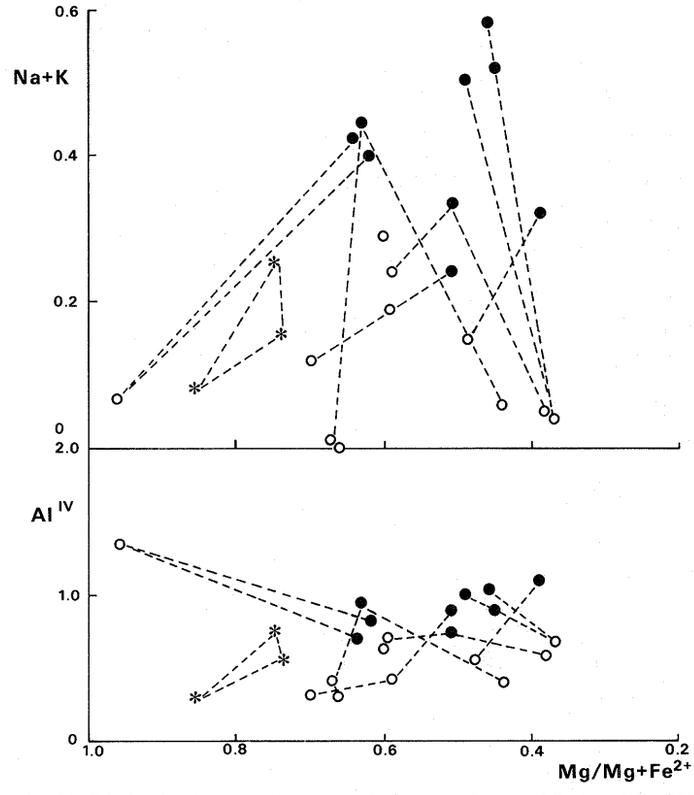

Fig. 54. Distinction between igneous and metamorphic amphiboles of the SCI using (Na+K) and Al^{IV} against $Mg/(Mg+Fe^{2+})$, after Allen and Goldie (1978). Amphibole analyses from the Chilean ophiolites are given for comparison. The key is the same as in Fig. 53a.

(An_{20-30}) can exist in a low-pressure environment (Liou and others, 1974). Relict labradorite and bytownite are common in the basic dykes and gabbros, andesine in the granodiorites (plagiogranite) and secondary albite-oligoclase is ubiquitous in the mafic lavas and sills.

Fe_2O_3 content of the analysed plagioclase is low (Table VII) and ranges from 0.0 to 0.5 wt %, higher than in other comparative analyses (Coombs and others, 1976). K_2O is not usually present in albite from the mafic lavas but up to 1.8% was recorded in oligoclase (M.3774.1).

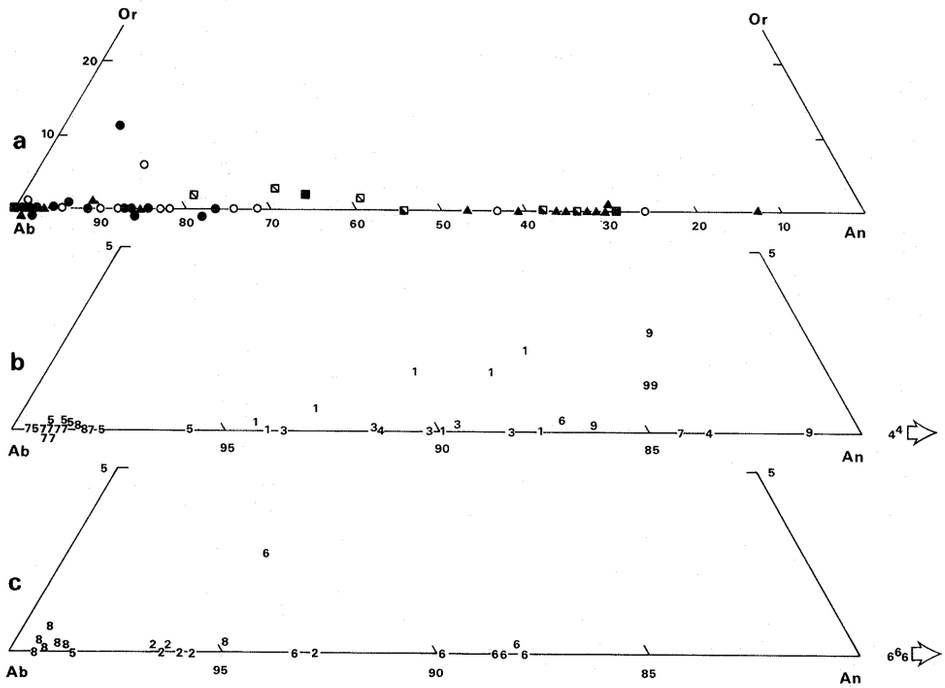

Fig. 55. a. Plagioclase analyses from all rock types. b. Plagioclase analyses from pillow lavas. The numbers refer to stratigraphical localities, increasing approximately with grade. 1, Leon Head; 2, Wheeler Glacier; 3, Diaz Cove; 4, Kupriyanov Islands; 5, Rogged Bay; 6, Smaaland Cove; 7, Doubtful Bay; 8, Larsen Harbour; 9, Nattriss Head. c. Plagioclase analyses from massive lavas. The key is the same as in Fig. 55b.

Table VII. Typical plagioclase analyses.

	1	*2*	*3*	*4*	*5*	*6*	*7*	*8*	*9*
SN	M.2758.1	M.3745.4	M.3755.4	M.3774.1	M.2075.9	M.2075.9	M.3747.6	M.1818	M.1822
A(N)	4(2)	5	3(2)	4(3)	2	6	3(2)	3	2(2)
SiO_2	69.92	67.09	65.50	63.98	62.02	51.63	67.97	53.79	68.92
Al_2O_3	18.99	20.50	21.60	22.26	22.63	28.53	19.31	28.71	19.02
Fe_2O_3	0.25	0.49	0.0	1.48	0.99	1.01	0.86	0.77	0.23
CaO	0.12	1.73	3.63	1.30	6.12	14.38	0.32	13.32	0.0
Na_2O	10.64	10.02	8.74	8.58	7.93	3.01	10.37	3.60	11.07
K_2O	0.0	0.0	0.0	1.76	0.0	1.13	0.0	0.0	0.0
TOTAL	99.92	99.83	99.47	99.36	99.69	99.69	98.83	100.19	99.24
Structural formulae on the basis of 32(O)									
Si	12.148	11.759	11.542	11.384	11.061	9.500	11.718	9.724	12.085
Al	3.890	4.235	4.488	4.669	4.758	6.189	4.228	6.120	3.932
Z	16.04	15.99	16.03	16.05	15.82	15.69	15.95	15.84	16.02
Fe^{3+}	0.033	0.065	0.0	0.198	0.132	0.139	0.165	0.105	0.031
Na	3.584	3.407	2.989	2.960	2.742	1.076	3.217	1.261	3.764
Ca	0.023	0.325	0.686	0.248	1.170	2.836	0.362	2.580	0.0
K	0.0	0.0	0.0	0.400	0.0	0.264	0.0	0.0	0.0
X	3.64	3.80	3.69	3.81	4.04	4.32	3.74	3.95	3.80
Ab%	99.4	91.3	81.3	82.0	70.1	25.8	89.9	32.8	100.0
An%	0.6	8.7	18.7	6.9	29.9	67.9	10.1	67.2	0.0
Or%	0.0	0.0	0.0	11.1	0.0	6.3	0.0	0.0	0.0

All iron is given as Fe_2O_3. SN, specimen number; A(N): A, analysis number, N, number of analyses averaged.
1–4, pillow lavas; 5–7, massive lavas; 8–11, basic dykes; 12, basic sill; 13, granite; 14, granodiorite; 15 and 16, quartz-gabbros; 17, Wheeler Glacier gabbro.

1. Pillow and massive lava plagioclases

Albite-oligoclase ($An_{<20}$), usually showing limited compositional variation, occurs in the mafic lavas; relict calcic plagioclase survives in some massive lavas and rocks of lower metamorphic grade. Compositional changes in individual crystals are usually non-gradational and albite may occur as thin rims on more An-rich relict phases. Pure albite ($An_{<3}$) occurs in both massive and pillow lavas at low levels in the sequence (areas 5, 7 and 8 in Fig. 55b and c) but oligoclase occurs in pillow lavas from the lower-grade rocks at high levels in the pile (areas 1, 3 and 4 in Fig. 55b). This suggests a relationship between composition and stratigraphical level or metamorphic grade for albite, as noted by Kuniyoshi and Liou (1976). Oligoclase in lavas from Nattriss Head (9) and Smaaland Cove (6) may be due to the instability of albite at a metamorphic grade above greenschist facies within a transitional facies assemblage.

2. Dyke plagioclases

Most of the dykes sampled were intruded after the main hydrothermal event and have retained almost completely their primary calcic feldspar in contrast to the surrounding albite-rich lavas. They are variably altered and albite is uncommon except in the more altered examples.

All of the least-altered dykes have retained labradorite and bytownite with calcic cores and sodic rims often showing complex zoning and non-gradational compositional changes (An_{73-61}, An_{85-71}). Albite is seldom present in rocks where igneous plagioclase persists. The altered dykes (M.1822 and 1844.1) have lost their original texture and plagioclase has been albitized completely. Albite does occur with labradorite in a partially altered dyke from Rogged Bay (M.3711.2) and as rims on oligoclase in a dyke from the Kupriyanov Islands (M.3745.2). The range of plagioclase compositions in the dykes compares with the relict feldspars in the mafic lavas.

3. Sill plagioclases

Three basic sills from different stratigraphical levels have a mineralogy similar to that of adjacent mafic lavas. Albite-oligoclase occurs in all three with relict labradorite in one sample from Nattriss Head (M.3753.3). The intensive albitization of the sills indicates closer correlation with the mafic lavas rather than with the essentially unaltered basic dykes.

4. Plagiogranite and gabbro plagioclases

Typical analyses are given in Table VII and plotted in Fig. 55a. Albite occurs as individual laths in an altered quartz-monzodiorite (M.1853.3) with relict andesine (An_{35}) and as thin rims on similar feldspar in granodiorite (M.1831.1). Andesine represents the relict felsic phase of the granodiorite but less sodic andesine (An_{48}) and bytownite (An_{71}) occur in the more mafic gabbros (M.1852.5). Although potassium feldspar occurs as perthitic fringes on plagioclase (Mair, 1983), none was analysed in this investigation. Many of the feldspars show complex, reversed or normal compositional zoning; core-to-rim variations are An_{26-3} (M.1813.2) and An_{39-18} (M.1831.1) in the acidic rocks and An_{65-33} (M.4072.8) in the gabbroic rocks. Compositional variation may not be regular and the more sodic phases are usually restricted to the rims of the calcic feldspar. The stability of calcic plagioclase in rocks of the Smaaland Cove intrusion suggests amphibolite-facies metamorphism; the occurrence of albite possibly represents subsequent retrogressive metamorphism at greenschist facies.

Table VII. Typical plagioclase analyses (continued).

	10	*11*	*12*	*13*	*14*	*15*	*16*	*17*
SN	M.3704.C	M.3794.7A	M.3774.G	M.1813.2	M.1814.2	M.1852.5	M.1853.3	M.4072.11
A(N)	1(2)	2(2)	1	1(8)	2(5)	2(2)	2(5)	3
SiO_2	53.85	51.59	67.81	65.11	57.45	57.01	67.64	54.54
Al_2O_3	28.73	29.76	20.58	21.90	25.81	26.74	19.45	28.71
Fe_2O_3	0.79	0.05	0.62	0.47	0.42	0.42	1.74	0.52
CaO	12.11	14.16	1.39	3.32	8.25	9.77	0.13	12.08
Na_2O	4.75	3.08	9.87	9.38	6.71	5.96	11.18	3.93
K_2O	0.0	0.0	1.48	0.35	0.20	0.09	0.0	0.0
TOTAL	100.23	99.09	100.75	100.53	98.84	99.99	100.24	99.78
Structural formulae on the basis of 32(O)								
Si	9.736	9.458	11.745	11.217	10.415	10.243	11.851	9.848
Al	6.125	6.433	4.203	4.757	5.517	5.665	4.017	6.112
Z	15.86	15.89	15.95	15.97	15.93	15.91	15.87	15.96
Fe^{3+}	0.107	0.069	0.081	0.034	0.057	0.056	0.229	0.071
Na	1.665	1.096	3.316	2.938	2.360	2.076	3.800	1.376
Ca	2.346	2.782	0.258	0.870	1.603	1.882	0.024	2.337
K	0.0	0.0	0.328	0.079	0.046	0.020	0.0	0.0
X	4.12	3.95	3.98	3.92	4.07	4.03	4.05	3.78
Ab%	41.5	28.3	85.0	75.6	58.9	52.2	99.4	37.0
An%	58.5	71.7	6.6	22.4	40.0	47.3	0.6	63.0
Or%	0.0	0.0	8.4	2.0	1.1	0.5	0.0	0.0

5. Discussion

Albite-oligoclase is characteristic of the mafic lavas and sills but it is a minor phase in the dykes, acid plagiogranites and associated gabbros. Relict andesine may be present in the lavas; primary labradorite and bytownite typifies the dykes and gabbros, and andesine is retained in the plagiogranite. Albite shows a limited chemical variation but zoning is common in the more calcic plagioclase. Albitization in the lavas represents diffusive replacement of more calcic feldspar during hydrothermal metamorphism and is characteristic of spilitic assemblages (Fiala, 1974).

The anorthite content of plagioclase is related to the Al_2O_3 content of amphibole (Liou and others, 1974). Amphibolite-facies rocks contain Al-rich hornblende and albite-oligoclase ($An_{<20}$), whereas greenschist facies rocks contain Al-poor actinolite and albite ($An_{<7}$). The amphibole–plagioclase relationship for all rock types is shown in Fig. 56 using XCa plagioclase (XCa = Ca/(Ca + Na + K)) and XSi, and XNa amphibole (XSi = Si/(Si + Al) and XNa = Na/(Na + K)) after Hutchison (1978). The mafic lavas support a greenschist to amphibolite-facies assemblage and the underlying plutonic rocks are predominantly of amphibolite facies (Fig. 56). The dykes contain either actinolite or hornblende, the former co-existing metastably with calcic plagioclase and the latter defining amphibolite facies. Amphibole and plagioclase assemblages of both greenschist and amphibolite facies occur in the plutonic rocks. A more detailed discussion and review of the metamorphic facies of the rocks investigated is given on p. 51–54. Ca and Na partitioning in amphibole and plagioclase is related to metamorphic grade (Hutchison, 1978) and the relative difference in grade between the mafic lavas and the plutonic rocks of the Larsen Harbour Formation is established (Fig. 57), although less clearly than in Fig. 56.

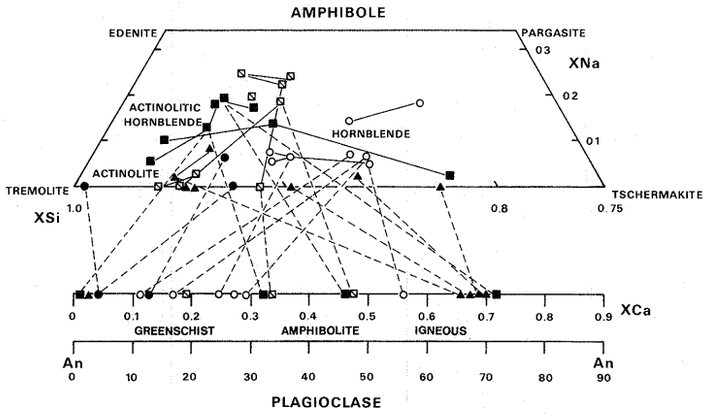

Fig. 56. Metamorphic facies relationships for amphibole and plagioclase in the same rock from the LHF and SCI; XNa = Na/(Na + Ca); XSi = Si/(Si + Al); XCa = Ca/(Ca + Na + K), after Hutchison (1978).

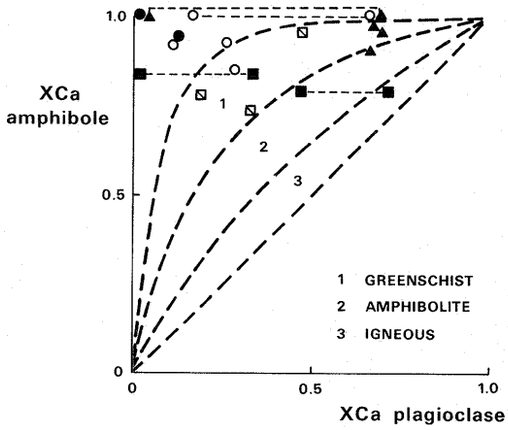

Fig. 57. Partitioning of alkali minerals in plagioclase and amphibole with respect to metamorphic facies (Hutchison, 1978).

Table VIII. Typical chlorite analyses.

	1	*2*	*3*	*4*	*5*	*6*	*7*	*8*
SN	M.3751.1	M.3700.7	M.3776.1	M.2072.2	M.3747.6	M.3711.13	M.3742	M.3753.8
A(N)	2	1	2	1	1(2)	1	1	1(2)
SiO_2	28.39	26.02	28.13	25.31	25.16	24.62	29.39	29.16
Al_2O_3	18.16	19.30	16.85	19.46	18.54	18.95	17.60	17.25
FeO	18.80	22.45	22.73	31.03	33.00	36.73	22.75	16.50
MnO	0.24	0.22	0.27	0.27	0.78	0.63	0.51	0.13
MgO	21.37	15.40	17.02	10.77	9.17	8.24	16.55	22.21
CaO	0.0	0.0	0.24	0.68	0.0	0.0	1.62	0.0
TOTAL	86.96	83.39	85.24	87.52	86.65	89.17	88.42	85.25
Structural formulae on the basis of 28(O)								
Si	5.815	5.687	6.015	5.536	5.632	5.459	6.061	6.009
Al	2.185	2.313	1.985	2.464	2.368	2.541	1.939	1.991
Z	8.00	8.00	8.00	8.00	8.00	8.00	8.00	8.00
Al	2.201	2.661	2.263	2.554	2.527	2.411	2.340	2.201
Fe^{2+}	3.222	4.104	4.066	5.676	6.180	6.811	3.924	2.845
Mn	0.041	0.041	0.049	0.050	0.149	0.119	0.088	0.022
Mg	6.524	5.015	5.354	3.512	3.061	2.722	5.086	6.822
Ca	0.0	0.0	0.033	0.159	0.0	0.0	0.357	0.0
W, X, Y	11.99	11.82	11.77	11.95	11.92	12.06	11.80	11.89

All iron is given as FeO. SN, specimen number; A(N): A, analysis number, N, number of analyses averaged.
1–3, pillow lavas; 4–7, massive lavas; 8–10, basic dykes; 11 and 12, basic sills; 13, granodiorite; 14 and 15, Smaaland Cove, Wheeler Glacier gabbros, respectively.

C. Chlorite Analyses

Chlorite is ubiquitous throughout the Larsen Harbour Formation and associated intrusions, and occurs in a variety of forms at all metamorphic grades, although it is less common at higher levels in the lava sequence. Typical analyses are given in Table VIII with structural formulae based on 28(O); all iron is given as FeO assuming Fe^{2+} is the most common ionic state of iron present (Kawachi, 1975). Chlorite analyses have been classified chemically as pycnochlorite and brunsvigite (Fig. 58) after Hey (1954). Comparative analyses from environments of a similar metamorphic grade are common in the literature (Hietanen, 1974; Kawachi, 1975; Coombs and others, 1976; Nakajima and others, 1977).

Al_2O_3 content varies from 25 to 36 wt % for all rock types (Fig. 59; Table VIII); Al^{IV} content averages 2.3 atoms per formula unit and Al^{VI} has a similar value (Table VIII), resembling chlorite analyses given by Hietanen (1974). There is considerable variation in the Mg/Fe ratio, indicated by the spread of analyses in Fig. 59; chlorite from plagiogranites and gabbros is more Fe-rich than those from the pillow-lava which are Mg-rich. Mg/Fe ratios for the different rock types are as follows: pillow lavas (1.0–2.0), massive lavas (0.4–1.3), acid plagiogranite (0.3–0.4), gabbro (0.5–0.8) and dykes (0.3–2.4).

The Mg/Fe ratio is regarded as being related to metamorphic grade (Hietanen, 1974); Liou and others (1974) stated that Mg in chlorite increases with grade, although this contradicts Iwasaki (1963), who reported that Fe^{2+} increases with grade. Kawachi (1975) considered bulk rock composition to be more important than metamorphic grade in determining chlorite chemistry. Preliminary work has been carried out for this report in order to relate grade to chlorite and/or whole-rock composition ion using Fe/(Fe + Mg) and Al/(Fe + Mg) (Kawachi, 1975) where Fe equals total iron. Lack of sufficient whole-rock data for one particular rock type, however, prevents significant conclusions being reached. Bulk rock composition does have some effect on chlorite composition and Mg content also appears to decrease with increasing grade between dykes and higher-grade lavas. This is supported by the slight increase with increasing grade of structural Fe within chlorite from the same rock group in the Larsen Harbour Formation (Fig. 60). The variation in Fe content of chlorite from dykes in Smaaland Cove (ES in Fig. 60) does not follow a regular pattern; both highest and lowest contents are found in separate heavily altered dykes (M.1822.1: 7.2; M.1844.1: 3.4 Fe atoms per formula unit). An increase of Fe content with grade agrees with Iwasaki (1963).

Equilibrium relationships between co-existing phases in low-grade metamorphic assemblages have been investigated by Kawachi (1975) and Coombs and others (1976). Kawachi

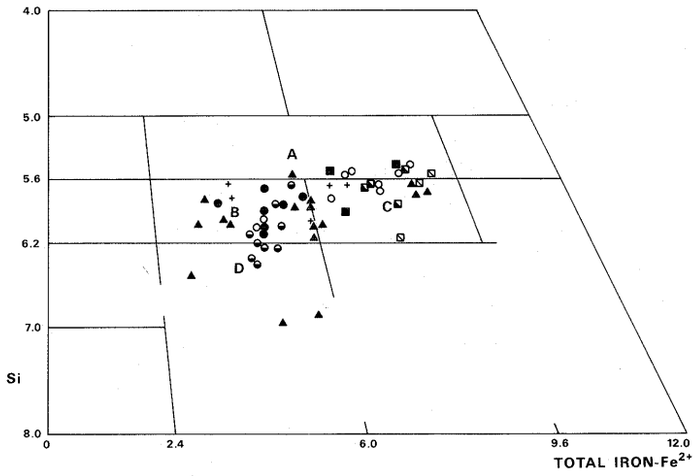

Fig. 58. Chemical classification of chlorite analyses from all rock types, after Hey (1954). Chlorite fields are: A, ripidolite; B, pycnochlorite; C, brunsvigite; D, diabantite.

Table VIII. Typical chlorite analyses (continued).

	9	*10*	*11*	*12*	*13*	*14*	*15*
SN	M.1822	M.3745.2	M.3753.3	M.3774.G	M.1813.2	M.1852.2	M.4072.11
A(N)	1	3	1	3	2	1	4
SiO_2	25.29	28.30	27.14	29.14	24.38	25.85	24.69
Al_2O_3	17.40	15.82	17.36	15.49	18.47	19.97	18.27
FeO	37.93	28.62	24.19	22.59	37.62	29.82	31.75
MnO	0.42	0.30	0.55	0.21	0.26	0.19	0.18
MgO	7.03	14.74	17.01	17.29	6.45	12.79	9.67
CaO	0.13	0.22	0.0	0.30	0.0	0.0	0.0
TOTAL	88.20	88.00	86.25	85.02	87.18	88.62	84.56
Structural formulae on the basis of 28(O)							
Si	5.708	6.049	5.798	6.237	5.562	5.518	5.628
Al	2.292	1.951	2.202	1.763	2.438	2.492	2.372
Z	8.00	8.00	8.00	8.00	8.00	8.00	8.00
Al	2.338	2.035	2.172	2.144	2.530	2.532	2.539
Fe^{2+}	7.161	5.117	4.323	4.042	7.178	5.323	6.054
Mn	0.080	0.054	0.100	0.037	0.050	0.034	0.035
Mg	2.365	4.696	5.417	5.514	2.194	4.067	3.285
Ca	0.030	0.051	0.0	0.068	0.0	0.0	0.0
W, X, Y	11.97	11.95	12.01	11.81	11.95	11.96	11.91

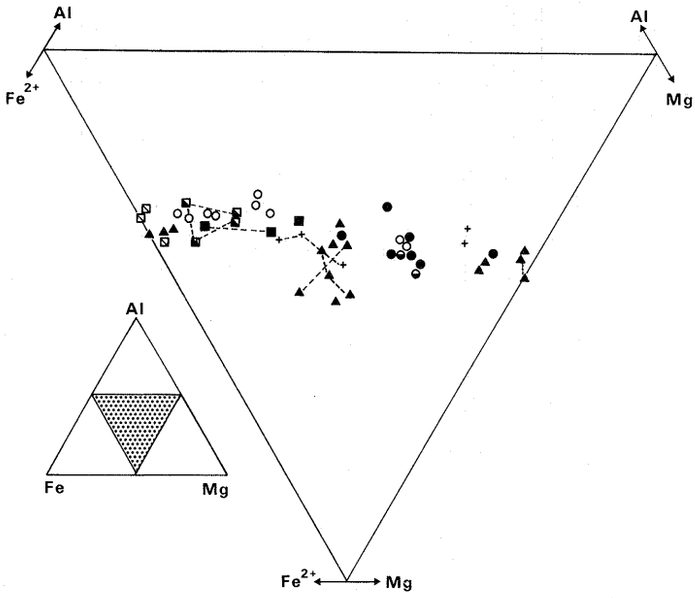

Fig. 59. Al–Fe^{2+}–Mg relationships for chlorite analyses from all rock types, after Kawachi (1975).

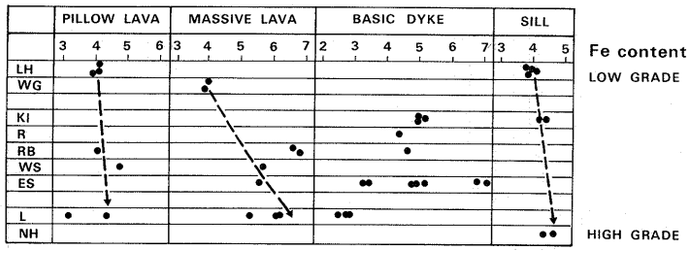

Fig. 60. Fe^{2+} content of chlorites from various rock types in relation to stratigraphical level. Localities are as in Fig. 7.

(1975) recorded a good correlation of Fe^{2+}:Mg substitution for actinolite–chlorite pairs but other co-existing phases lack uniform relationships. Both authors calculated a distribution coefficient of 1.7 for chlorite–actinolite equilibrium pairs in greenschist-facies rocks. Distribution relationships for actinolite–chlorite pairs from the same thin section are shown in Fig. 61. The scatter of points for individual rock types, and lack of consistent relationship to any coefficient slope, suggests that both phases are in disequilibrium. It is conceivable that equilibrium is limited only to those phases which are directly in contact and is not otherwise achieved at greater separation.

D. Epidote Analyses

As with chlorite, epidote is common throughout the Larsen Harbour Formation and Smaaland Cove intrusion. Typical analyses (all iron given as Fe_2O_3) and structural formulae, based on 12.5(O), are given in Table IX. Analyses of epidotes from regional pumpellyite–actinolite and greenschist-facies rocks provide the main sources of comparative data. Fe^{3+}/Al substitution is the main parameter affecting epidote composition (Brown, 1967). Pistacite content ($Fe^{3+}/(Fe^{3+} + Al)$) is given as a percentage (cf. Xp_{Fe}^{Ep} of Nakajima and others (1977) and analyses are plotted in Fig. 62.

Hietanen (1974) stated that Fe^{3+}/Al substitution is dependent on grade, Al-rich types indicating a higher grade. Epidote of the pumpellyite–actinolite facies (Kawachi, 1975) may contain up to 29% pistacite but it shows no systematic variation with grade or rock type. Coombs and others (1976) identified a compositional change from epidote to clinozoisite at higher temperature and variable pistacite compositions within single crystals (16–32%), indicating short-range disequilibrium.

Epidote from the Larsen Harbour Formation has a consistent structural formula: Si equal to 3.00, Ca equal to 2.00 atoms per formula unit, and varying overall from 17 to 34% pistacite (Table IX). Individual epidote crystals are generally homogeneous within one rock type and Fe/Al may reflect parent rock composition. Fe^{3+}/Al values for pillow and massive lavas vary from 0.25 to 0.52, dykes from 0.24 to 0.43 and plagiogranite from 0.20 to 0.53, the last group being richer in Al (Table IX). No MgO was recorded and MnO did not exceed 0.39 wt %. In the mafic lavas, epidote maintains a rough correlation of increasing Fe^{3+} content with grade (Fig. 62); those from higher-grade lavas in Smaaland Cove have an Fe^{3+}/Al ratio of 0.52 in contrast to those of lower grade in Rogged Bay ($Fe^{3+}/Al = 0.29$) and Leon Head ($Fe^{3+}/Al = 0.32$). Low-pistacitic epidote occurs in the plagiogranite, which is at equivalent or higher grade than the mafic lavas and therefore suggests that bulk rock composition is also important in determining epidote composition.

E. Clinopyroxene Analyses

Clinopyroxene is a common primary phase within the basic dykes and slightly altered Wheeler Glacier gabbro; it also occurs as igneous relicts in the low-grade prehnite–pumpellyite-facies lavas from Leon Head and Diaz Cove but it is replaced by greenschist-facies minerals lower in the sequence. Core-to-rim analyses have been averaged where no significant compositional difference is evident. Typical analyses (all iron as FeO), end-member compositions and structural formulae, based on 6(O), are given in Table X and are plotted on a

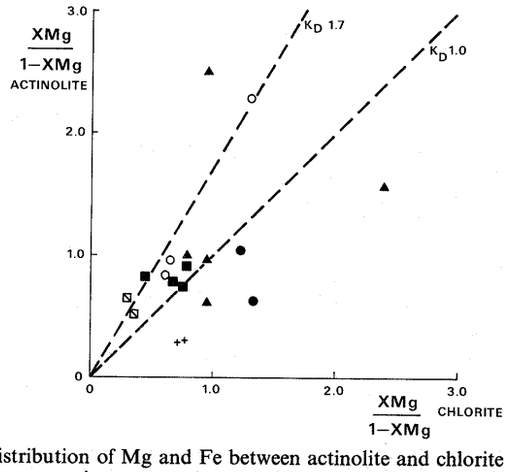

Fig. 61. Distribution of Mg and Fe between actinolite and chlorite from the same specimen to show possible equilibrium relationships; XMg = Mg/(Mg + Fe), after Kawachi (1975). The equilibrium coefficient of 1.7 is shown for reference.

Table IX. Typical epidote analyses.

	1	2	3	4	5	6	7	8	9	10	11	12
SN	M.2078.5	M.2758.2	M.3751.1	M.3700.7	M.3776.1	M.1837.2	M.3711.13	M.3747.6	M.1822	M.3711.2	M.1851.7	M.4072.11
A(N)	1	2	1	2	1	1	1	2	1	1(2)	1	1
SiO_2	37.45	37.91	38.31	38.73	38.30	39.09	38.21	38.62	38.23	39.42	37.61	38.03
TiO_2	0.33	0.09	0.14	0.0	0.0	0.26	0.0	0.0	0.0	0.0	0.0	0.0
Al_2O_3	21.27	21.79	22.01	24.48	23.79	25.02	23.23	22.50	22.68	24.44	25.05	25.51
Fe_2O_3	17.31	15.80	14.84	12.08	11.82	11.46	13.74	15.75	15.13	12.26	12.39	9.93
MnO	0.0	0.0	0.0	0.18	0.0	0.0	0.20	0.33	0.0	0.0	0.0	0.0
MgO	0.0	0.0	0.0	0.0	0.0	0.0	0.0	0.0	0.0	0.0	0.0	0.0
CaO	24.34	24.65	23.46	23.46	22.87	23.71	23.62	23.03	23.65	24.07	24.34	23.57
TOTAL	100.70	100.24	98.76	98.93	96.78	99.54	99.00	100.23	99.69	100.19	99.39	97.04
Structural formulae on the basis of 12.5(O)												
Si	2.951	2.985	3.037	3.031	3.059	3.032	3.013	3.022	3.006	3.048	2.946	3.016
Al	0.049	0.015	–	–	–	–	–	–	–	–	0.054	–
Z	3.00	3.00	3.04	3.03	3.06	3.03	3.01	3.02	3.01	3.05	3.00	3.02
Al	1.927	2.008	2.058	2.260	2.240	2.288	2.160	2.076	2.102	2.228	2.260	2.385
Ti	0.020	0.005	0.008	0.0	0.0	0.030	0.0	0.0	0.0	0.0	0.0	0.0
Fe^{3+}	1.026	0.936	0.886	0.712	0.711	0.669	0.816	0.927	0.895	0.713	0.730	0.593
Mn	0.0	0.0	0.0	0.024	0.0	0.0	0.014	0.022	0.0	0.0	0.0	0.0
Mg	0.0	0.0	0.0	0.0	0.0	0.0	0.0	0.0	0.0	0.0	0.0	0.0
X, Y	2.97	2.95	2.95	3.00	2.95	2.99	2.99	3.03	3.00	2.94	2.99	2.98
Ca	2.056	2.080	1.994	1.968	1.957	1.971	1.996	1.932	1.993	1.994	2.043	2.003
W	2.06	2.08	1.99	1.97	1.96	1.97	2.00	1.93	1.99	1.99	2.04	2.00
Pistacite %	34	32	30	24	24	23	27	31	30	24	25	20

All iron is given as Fe_2O_3; SN, specimen number; A(N): A, analysis number, N, number of analyses averaged.
1–5, pillow lavas; 6–8, massive lavas; 9 and 10, basic dykes; 11, granodiorite; 12, Wheeler Glacier gabbro.

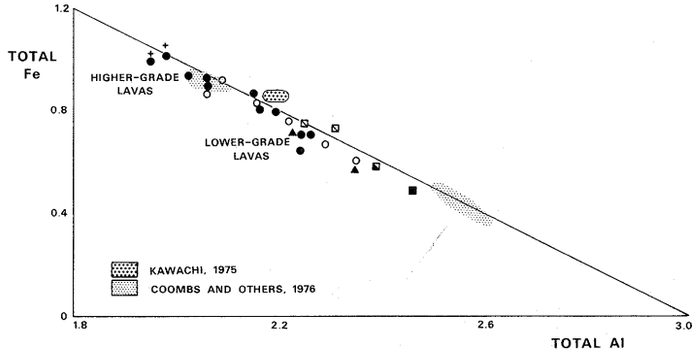

Fig. 62. All epidotes, plotted with respect to Fe^{3+} and Al content, after Hietanan (1974), and compared with analyses of other workers.

standard pyroxene trapezoid (Fig. 63a). All are augitic; those from the dyke rocks are usually compositionally zoned but those in the Wheeler Glacier gabbro and mafic lavas are more uniform (Fig. 63b).

Si and Al contents sum to 2.00 atoms in the Z-site; Al also occurs in the X-, Y-site which approaches 2.00 atoms per formula unit (Table X). Si:Al substitution varies, CaO content is uniform, not exceeding 21 wt %, and Mg:Fe is the most changeable parameter, although this is limited except in strongly zoned examples (Table X; Fig. 63b). TiO_2 seldom exceeds 1.0 wt %; Cr_2O_3 varies from 0.00 to 0.85 wt % and the maximum MnO recorded is 0.37 wt %.

Vallence (1974) used relict clinopyroxene from the Nundle spilite, New South Wales, to prove its genetic relationship to associated primary basalts. The Nundle pyroxene falls in the normal alkaline field (2) of Le Bas (1962) and indicates that the parent magma was less tholeiitic than that which produced the Larsen Harbour Formation (Fig. 64). Kawachi (1974) has analysed pyroxene from the Wakatipu Group, New Zealand, which plots in the non-alkaline field (1) of Le Bas and shows limited chemical variation. Similarly, clinopyroxene from the Borneo ophiolite (Hutchison, 1978) is augitic and of non-alkaline parentage (Fig. 64). All but three of the pyroxene analyses from the mafic rocks of the Larsen Harbour Formation fall in the non-alkaline field (1) of Le Bas (1962) (Fig. 64), in agreement with the tholeiitic character of the rocks as indicated by whole-rock geochemistry.

Clinopyroxene from the Larsen Harbour Formation was therefore derived from a non-alkaline magma but it shows limited compositional variation, except in the basic dykes, when compared to the trend of the pyroxene from the Skaergaard intrusion (Fig. 63). Limited fractionation suggests shallow-level differentiation of basic magma, which is not uncommon in the generation of an ophiolite sequence.

F. Pumpellyite Analyses

Pumpellyite was identified optically in a sample of epidosite from the Larsen Harbour Formation (Tanner, 1982) and was successfully analysed by microprobe in the adjacent Cumberland Bay Formation (personal communication from P. W. G. Tanner). Its presence had been suspected within the lower-grade upper-level lavas of the Larsen Harbour Formation and this is now verified. It is uncommon and

Table X. Typical clinopyroxene analyses.

	1	2	3	4	5	6	7	8	9	10
SN	M.2456.1	M.3776.1	M.1825.1	M.3704.C	M.3745.2	M.3753.8	M.3777.7B	M.3794.7A	M.4072.8	M.4072.11
A(N)	1	1(2)	1	1(2)	2(2)	2(2)	1	1	1(2)	2
SiO_2	52.33	48.74	53.68	51.00	50.30	50.86	51.58	52.28	52.54	51.36
TiO_2	0.58	1.40	0.35	0.94	0.86	0.64	0.53	1.11	0.50	0.70
Al_2O_3	3.68	5.11	2.22	1.65	3.31	2.63	2.86	3.18	2.14	1.97
Cr_2O_3	0.85	0.10	0.44	0.0	0.20	0.0	0.49	0.49	0.0	0.0
FeO	6.12	10.16	5.77	13.26	8.60	9.74	5.86	7.17	7.21	9.61
MnO	0.26	0.10	0.0	0.31	0.19	0.26	0.21	0.0	0.20	0.19
MgO	15.59	12.52	16.87	14.66	15.20	15.89	16.47	15.60	15.89	15.03
CaO	21.68	21.35	20.96	17.95	20.72	19.26	21.95	20.92	20.67	20.09
Na_2O	0.0	0.0	0.0	0.0	0.0	0.0	0.0	0.0	0.0	0.0
K_2O	0.0	0.0	0.0	0.0	0.0	0.0	0.0	0.0	0.0	0.0
TOTAL	101.09	99.71	100.29	99.77	99.38	99.28	99.95	100.75	99.15	98.95
Structural formulae on the basis of 6(O)										
Si	1.904	1.838	1.954	1.927	1.883	1.906	1.901	1.911	1.950	1.933
Al	0.096	0.162	0.046	0.073	0.117	0.094	0.099	0.089	0.050	0.067
Z	2.00	2.00	2.00	2.00	2.00	2.00	2.00	2.00	2.00	2.00
Al	0.062	0.065	0.049	–	0.029	0.022	0.025	0.048	0.044	0.020
Ti	0.016	0.040	0.010	0.027	0.024	0.018	0.015	0.030	0.014	0.020
Cr	0.025	0.003	0.013	0.0	0.006	0.0	0.014	0.014	0.0	0.0
Mg	0.846	0.704	0.916	0.825	0.848	0.888	0.905	0.850	0.879	0.843
Fe^{2+}	0.186	0.320	0.176	0.419	0.269	0.305	0.181	0.219	0.224	0.303
Mn	0.008	0.003	0.0	0.010	0.006	0.008	0.006	0.0	0.006	0.006
Ca	0.845	0.863	0.818	0.727	0.831	0.774	0.867	0.820	0.822	0.810
Na	0.0	0.0	0.0	0.0	0.0	0.0	0.0	0.0	0.0	0.0
K	0.0	0.0	0.0	0.0	0.0	0.0	0.0	0.0	0.0	0.0
X	1.99	2.02	1.98	2.01	2.01	2.02	2.01	1.98	1.99	2.00
Ca%	44.8	45.7	42.8	36.7	42.5	40.2	44.4	43.5	42.6	41.3
Mg%	44.9	37.2	48.0	41.7	43.4	46.9	46.2	45.0	45.5	43.0
Fe%	10.3	17.1	9.2	21.6	14.1	12.9	9.6	11.6	11.9	15.7

All iron is given as FeO. SN, specimen number; A(N): A, analysis number, N, number of analyses averaged.
1 and 2, pillow lavas; 3–8, basic dykes; 9 and 10, Wheeler Glacier gabbro.

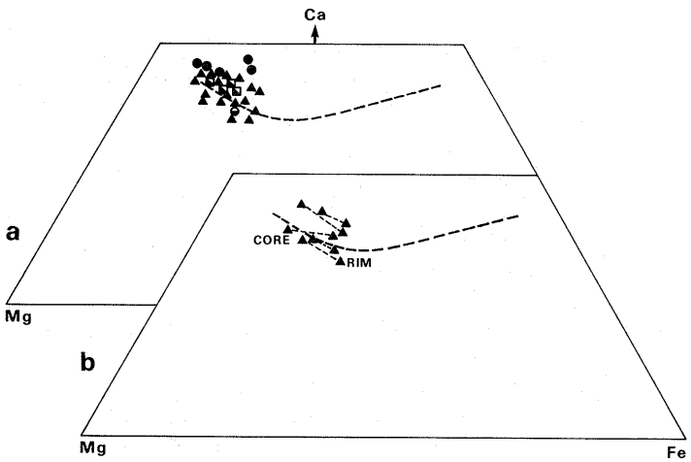

Fig. 63. a. Analyses of clinopyroxenes from the LHF and Wheeler Glacier gabbro. The Skaergaard crystallization trend is shown. b. Analyses of zoned clinopyroxenes from basic dykes.

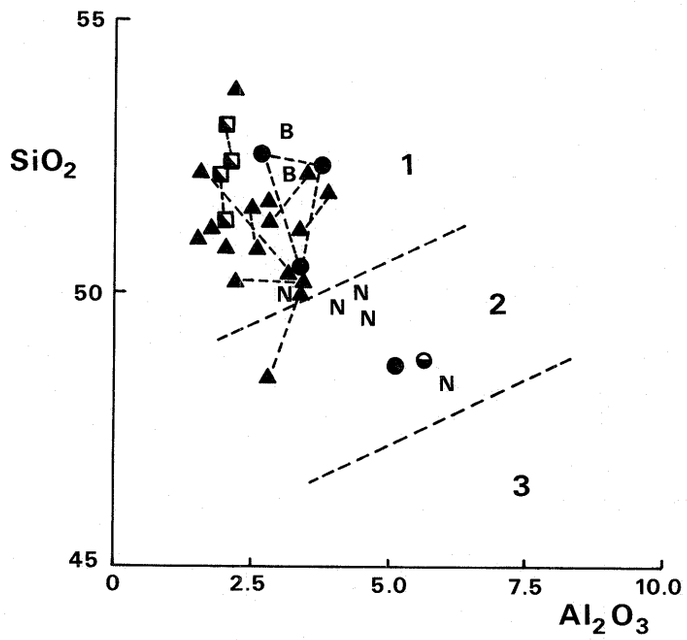

Fig. 64. SiO_2 vs Al_2O_3 relations for clinopyroxenes in the LHF, after Le Bas (1962). Fields are: 1, non-alkaline; 2, normal alkaline; 3, peralkaline. Analyses from the Nundle spilite (N) (Vallence, 1974) and the Borneo ophiolite (B) (Hutchison, 1978) are shown for comparison.

difficult to distinguish from associated epidote, chlorite and actinolite but eight crystals were analysed. Typical analyses (all iron as FeO) and structural formulae, based on 24.5(O) are given in Table XI. Analyses are plotted as atomic percentages of Al:Fe:Mg (Fig. 65) after Kawachi (1975). Pumpellyite cannot

Table XI. Typical pumpellyite analyses.

	1	2	3	4	5	6	7
SN	M.3742	M.3747.6	M.1822	M.1844.1	M.1844.1	M.4072.8	M.4072.11
A(N)	3	1	1	1	2	1(2)	1
SiO_2	36.48	38.21	36.29	40.35	43.43	38.42	38.95
Al_2O_3	21.98	22.56	22.25	24.63	24.14	26.75	22.09
FeO	8.99	13.20	8.77	8.04	0.75	2.52	7.34
MnO	0.0	0.20	0.0	0.22	0.0	0.0	0.0
MgO	1.70	0.0	1.33	1.26	0.0	2.88	1.46
CaO	22.79	23.00	22.74	24.31	27.22	23.33	21.02
TOTAL	91.94	97.17	91.38	98.81	95.54	93.90	90.86
Structural formulae on the basis of 24.5(O)							
Si	6.108	6.151	6.105	6.213	6.677	6.051	6.456
Z	6.11	6.15	6.11	6.21	6.68	6.05	6.46
Al	4.339	4.283	4.415	4.472	4.375	4.968	4.316
Fe^{2+}	1.258	1.777	1.234	1.036	0.097	0.332	1.018
Mn	0.0	0.027	0.0	0.029	0.0	0.0	0.0
Mg	0.425	0.0	0.333	0.289	0.0	0.675	0.362
X, Y	6.02	6.09	5.98	5.83	4.47	5.98	5.70
Ca	4.090	3.968	4.099	4.011	4.485	3.938	3.734
W	4.09	3.97	4.10	4.01	4.49	3.94	3.73

All iron is given as FeO. SN, specimen number; A(N): A, analysis number, N, number of analyses averaged.
1 and 2, massive lavas; 3–5, basic dykes; 6 and 7, Wheeler Glacier gabbro.

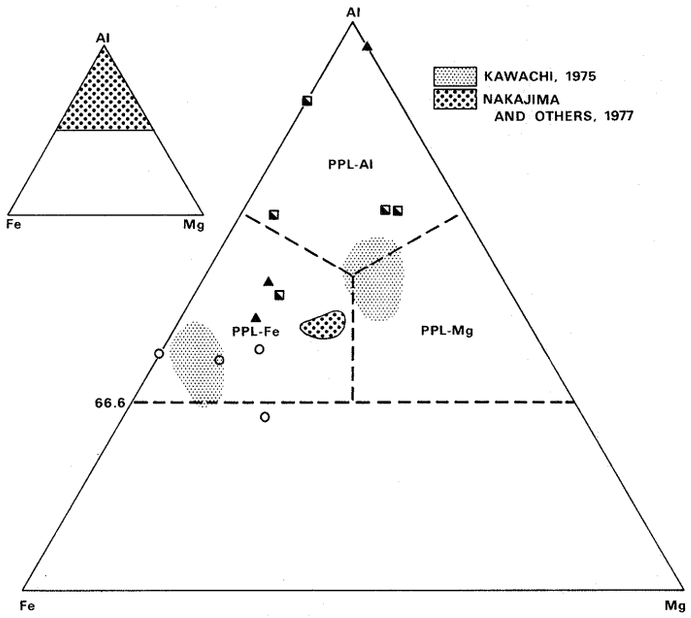

Fig. 65. Al–Fe–Mg triangular diagram for pumpellyite analyses as classified by Coombs and others (1976). PPL-Fe refers to pumpellyite –(Fe), etc. Comparative analyses of other workers are also shown.

be properly classified without a knowledge of FeO and Fe_2O_3 (Passaglia and Gottardi, 1973). However, Coombs and others (1976) used FeO alone as a basis for classification and this is followed in Fig. 65. Both pumpellyite-(Fe) and pumpellyite-(Al) occur in the Larsen Harbour Formation.

Pumpellyite from the Wakatipu Group comprises both Fe-rich strongly coloured low-grade types and Al-rich colourless higher-grade types, both of which plot separately on an Al:Fe:Mg diagram (Kawachi, 1975). Coombs and others (1976) also noted the positive correlation of Al content with increasing grade. Further analyses have been given by Nakajima and others (1977) and Bevins (1978). Pumpellyite of the Larsen Harbour Formation is classified and compared with that of other authors in Figs 65 and 66.

The pumpellyite of the Larsen Harbour Formation shows limited Mg variation, MgO varying from 0.0 to 2.9 wt %; MnO does not exceed 0.2 wt %; CaO is nearly constant at 21–24 wt % (Table XI). The number of Si atoms usually exceeds the 6 required for the Z-site; X-, Y-sites approach the ideal 6 atoms per formula unit and the W-site, containing Ca atoms, approaches 4 atoms per formula unit (Table XI). Al:Fe substitution is the main criterion for defining pumpellyite composition (Fig. 66) and analyses from the same crystal can show considerable variation (Table XI; M.4072.11).

Most pumpellyite from the Wheeler Glacier gabbro is Al-rich in contrast to that from the mafic lavas and altered basic dykes which is Fe-rich (Figs 65 and 66). Samples M.1844.1 and M.3747.6 were collected in an area previously thought to be greenschist facies and therefore the presence of pumpellyite is significant. Pumpellyite from the high-level low-grade lavas is more Fe-rich than that from the low-level higher-grade dykes (Fig. 65), agreeing with the conclusion of Kawachi (1975). The change from pumpellyite-(Fe) to pumpellyite-(Al) between lavas and gabbro in the Wheeler Glacier area may indicate a true metamorphic gradient rather than differences in bulk chemistry. Pumpellyite from the Cumberland Bay Formation is more Fe-rich than that in the Larsen Harbour Formation and this may be due either to grade or to whole-rock composition (Fig. 65).

The presence of pumpellyite in the higher levels of the lava sequence helps define a prehnite–pumpellyite assemblage, but at lower levels it cannot be established whether it co-exists or occurs metastably with amphibole to define a true pumpellyite–actinolite assemblage. It may indicate retrograde meta-

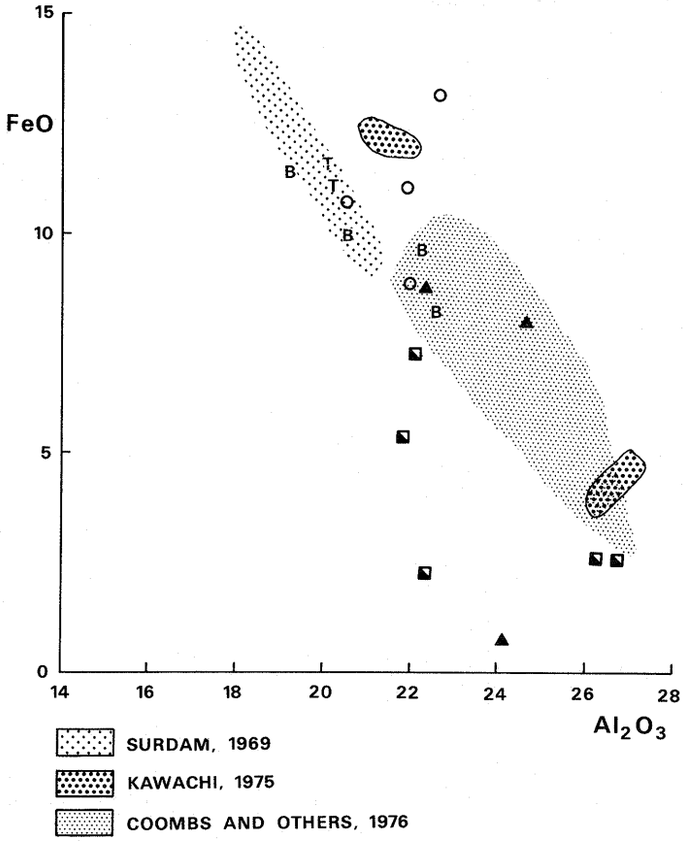

Fig. 66. Comparison of pumpellyites from the LHF with those from other metamorphic terrains using FeO vs Al_2O_3, after Bevins (1978). Pumpellyites from the CBF (T), South Georgia, and those of Bevins (B) are also shown.

morphism of greenschist facies to prehnite–pumpellyite facies, which is consistent with the process of ophiolite evolution. Local grade variations in rocks of prehnite–pumpellyite facies may cause Fe:Al substitution in pumpellyite from the Larsen Harbour Formation.

G. Prehnite Analyses

Prehnite has been identified optically in the lavas and interbedded tuffs of the Larsen Harbour Formation at Rogged Bay and Leon Head. Analyses (all iron as Fe_2O_3) and structural formulae, based on 22(O) for prehnite from the Wheeler Glacier gabbro (M.4072.11), a dyke and a sill from the Kupriyanov Islands (M.3745.2 and 3, respectively), are given in Table XII. The mineral is more widespread than the limited number of analyses suggest.

SiO_2 and CaO contents show little variation, whereas Al_2O_3 varies according to the amount of Fe_2O_3 present as this is the only appreciable substitution. Fe_2O_3 content varies from 1.96 to 3.62 wt % and the $Fe^{3+}/(Fe^{3+} + Al)$ ratio from 0.05 to 0.10 (Table XII). Prehnite from the Olympic Peninsula metabasalts contains up to 7% Fe_2O_3 and have $Fe^{3+}/(Fe^{3+} + Al)$ ratios of 0.01–0.20 (Glassley, 1975); average prehnite from the Karmutsen Volcanic Group contains 1.8% Fe_2O_3 and has an $Fe^{3+}/(Fe^{3+} + Al)$ ratio of 0.05 (Kuniyoshi and Liou, 1976).

The limited number of prehnite analyses for the Larsen Harbour Formation correlates with those of regional prehnite–pumpellyite-facies regimes in the Fe_2O_3 content and the $Fe^{3+}/(Fe^{3+} + Al)$ ratio. In association with pumpellyite, it defines a prehnite–pumpellyite assemblage in the upper levels of the lava sequence.

H. Summary

Microprobe analyses of the main phases of rocks of the Larsen Harbour Formation have been presented in order to correlate metamorphic grade and structural level within the ophiolite. Variation in bulk rock chemistry between individual rock types may limit direct correlation of phases present in each type. The pillow and massive lavas, and dykes which intrude them, can be considered as an isochemical group, the extrusive unit occurring structurally above the plutonic unit of gabbro and plagiogranite. A metamorphic zonation is developed in the extrusive unit.

Metamorphic actinolite, actinolitic hornblende and Mg-hornblende occur in the higher-grade rocks, partly defining greenschist and amphibolite facies. Relict igneous hornblende is retained in the coarse-grained plutonic rocks. Albite is characteristic of the mafic lavas but it is less common in the dykes and plutonic rocks where more calcic plagioclase is present. Epidote occurs in all rocks and its composition is related to host-rock composition and metamorphic grade; more pistacitic Fe-epidote occurs in the mafic lavas, where Fe content increases with grade, than in the gabbros and plagiogranites. Similarly, chlorite is present in all rocks and is more Fe-rich in the higher-grade mafic lavas. Pumpellyite occurs in the low-grade high-level extrusive rocks, in the Wheeler Glacier gabbro and within altered dykes at lower levels. Al- and Fe-pumpellyite possibly indicate local variations in grade, the former indicating a higher grade in the Wheeler

Table XII. Typical prehnite analyses.

	1	*2*	*3*
SN	M.3745.2	M.3745.3	M.4072.11
A(N)	1	1	1(6)
SiO_2	42.55	43.26	43.46
Al_2O_3	23.52	21.93	21.96
Fe_2O_3	2.50	3.62	2.70
MgO	0.37	0.50	0.0
CaO	26.48	25.37	26.45
TOTAL	95.42	94.68	94.57
Structural formulae on the basis of 22(O)			
Si	5.907	6.049	6.084
Al	0.093	–	–
Z	6.00	6.05	6.08
Al	3.757	3.615	3.619
Fe^{3+}	0.262	0.381	0.286
Mg	0.076	0.105	0.0
X, Y	4.10	4.10	3.91
Ca	3.940	3.802	3.972
W	3.94	3.80	3.97

All iron is given as Fe_2O_3. SN, specimen number; A(N): A, analysis number, N, number of analyses averaged.
1, basic dyke; 2, basic sill; 3, Wheeler Glacier gabbro.

Glacier gabbro than in adjacent lavas. Prehnite is found in late veins within the higher-grade extrusive rocks but it defines a prehnite–pumpellyite assemblage in the upper levels of the sequence. Relict clinopyroxene, analysed from lava, dyke rocks and gabbro, indicates the non-alkaline nature of the parent magma of the Larsen Harbour Formation.

I. Discussion

1. *Ophiolite metamorphism and metamorphic facies*

Metamorphic zonation within the Chilean ophiolites has been described by Stern and others (1976) and Elthon and Stern (1978), from within the Betts Cove ophiolite, Newfoundland, by Coish (1977), and in the Borneo ophiolite by Hutchison (1978). The varied metamorphic regimes of ophiolites in different tectonic environments have been described in detail by Coleman (1977). Spooner and Fyfe (1973) referred to the Ligurian ophiolite in order to establish their model of sub-sea-floor geothermal metamorphism for oceanic crust and ophiolitic rocks. The hypothesis of hydrothermal metamorphism within oceanic rocks has gained acceptance by most recent authors for the following reasons:

i. Actinolite is present at shallow depth in ophiolites and indicates a high geothermal gradient, typical of mid-ocean ridge systems, rather than burial metamorphic regimes.
ii. Metamorphic zonation, from zeolite to amphibolite facies with increasing depth, eventually grading into fresh gabbro, implies a limited depth of fluid movement which originated from above.
iii. Igneous textures are often preserved without recrystallization or the development of schistosity.
iv. Retrogressive assemblages are common and boundaries between adjacent facies are often complex and irregular.
v. Oxygen-isotope studies point to circulation of heated sea-water rather than meteoric water as a means of alteration.

The zone of fresh gabbro (ii) is not exposed in the Larsen Harbour Formation, although the low-level plutonic rocks show only sporadic alteration. The other points are directly applicable to the mafic sequence on South Georgia. A model of hydrothermal metamorphism, such as described by Stern and others (1976), is accepted as the mechanism of alteration of this formation.

The zonation developed by oceanic hydrothermal metamorphism in a basalt–diabase–gabbro mafic ophiolite sequence comprises zeolite–greenschist–amphibolite facies with increasing depth (Coleman, 1977). Local conditions involve steep thermal gradients, no deformation and minor metasomatism. Zeolite-facies rocks are not always developed and chlorite–albite–pumpellyite assemblages can be present (Coleman, 1977). The metamorphic sequence given by Coleman occurs in the Chilean ophiolites (Stern and others, 1976), although greenschist and amphibolite facies are 're-defined' by Elthon and Stern (1978). Coish (1977) described zonation in the Betts Cove ophiolite as 'the degree of greenschist facies metamorphism increases with stratigraphic depth in the ophiolite', culminating in an albite–actinolite–epidote–chlorite assemblage in the gabbro unit.

Metamorphic facies of regional prograde terrains, involving phases present in the Larsen Harbour Formation but of differing origin, have been used for comparative purposes throughout this discussion and typical assemblages of each are given in Table XIII together with those from ophiolite sequences. Regional sequences from mafic rocks, for instance, the Karmutsen Volcanic Group (Kuniyoshi and Liou, 1976) and the Wakatipu Group (Kawachi, 1975), correlate closely with similar assemblages in the Larsen Harbour Formation but differ genetically. Liou and others (1974) have defined greenschist and amphibolite facies in the basaltic system (Table XIII) and their system of classification has been followed. The criteria for the prehnite–pumpellyite facies as outlined by Kawachi (1975) are also used. The greenschist (chlorite–epidote–sodic plagioclase)- and actinolite-facies assemblages given by Elthon and Stern (1978) are noted for comparison; their transitional assemblage correlates with the greenschist facies of other authors (Table XIII).

2. *Metamorphism of the Larsen Harbour Formation*

The assemblages given have been identified by microprobe analyses and additional data derived by optical determination (Tables XIV and XV); the identification of consistent equilibrium assemblages requires further work and disequilibrium appears to be more common in retrograde environments. Field observations suggest that a sheeted dyke unit was present but this feature has not been identified and may have been obscured by the plagiogranite intrusion. The extrusive unit is therefore described as directly overlying the plutonic unit without an intervening sheeted dyke (diabase) layer. A zonation of prehnite–pumpellyite-, greenschist- and lower amphibolite-facies rocks from high to low level is developed in the extrusive unit; the underlying plutonic unit contains amphibolite-facies rocks with retrograde greenschist assemblages (Tables XIV and XV). The dykes within lavas contain varied assemblages and most post-date the main alteration of the lavas.

3. *Extrusive unit*

The pillow and massive lavas support an increase in grade with depth from prehnite–pumpellyite through greenschist to amphibolite facies from Leon Head to Nattriss Head (Table XIV). Relict clinopyroxene is retained in the low-grade rocks but it is replaced completely at greenschist facies or above. Calcite is common in the lower-grade rocks, and quartz and sphene occur throughout.

Assemblages within the lavas of the extrusive unit are:

albite/oligoclase + Fe-poor chlorite ± Fe-poor epidote ± prehnite ± pumpellyite,
albite ($An_{<10}$) ± oligoclase ($An_{<20}$) ± actinolite/actinolitic hornblende + Fe-rich epidote ± Fe-rich chlorite,
oligoclase ± albite ± labradorite + Mg-hornblende + Fe-epidote + Fe-chlorite.

Prehnite–pumpellyite-facies rocks occur from Leon Head to Ranvik and may also be present in Larsen Harbour (Table XV); greenschist and lower amphibolite facies constitute the lower part of the sequence from Rogged Bay to Nattriss Head. Higher Al content in hornblende with stable calcic plagioclase identifies the amphibolite-facies rocks, although albite and

Table XIII. Summary of low-grade regional and ophiolite metamorphic facies.

	Metamorphic facies			
Authors	*Prehnite–pumpellyite*	*Pumpellyite–actinolite*	*Greenschist*	*Amphibolite*
Liou and others, 1974	ppl + cal + chl epd + cal + chl		alb($An_{<7}$) + chl + epd + act(Al-poor)	olg-and($An_{>20}$) + hbl(Al-rich)
			Transition plg + act + chl	
Franks, 1974	alb + cal + qtz + prh + chl + epd ± ppl			
Glassley, 1975†	prh + ppl + cal + epd + chl prh + ppl + cal + epd cal + chl ± prh ± ppl ± epd			
Kawachi, 1975†	ppl + prh + chl ppl + epd + chl ppl + prh + calc	epd + act + ppl + chl epd + act + amp(alkali) + chl epd + act + chl epd + chl	epd + act + chl epd + chl	
Coombs and others, 1976		ppl + act + chl + qtz		
Kuniyoshi and Liou, 1976	alb + chl + ppl + sph + mag ± qtz ± prh ± epd			
Coish, 1977*			alb + chl + epd + act	
Nakajima and others, 1977		ppl + act + epd + chl	chl + epd + act	
Elthon and Stern, 1978*			plg($An_{<15}$) + chl + epd	*Lower act*, 2.5–5.0% Al_2O_3 in amp + plg($An_{>50}$) + sph + bio + cal *Upper act*, 5.0–8.0% Al_2O_3 in amp + plg($An_{>50}$) + ilm + Ti-mag
			Transition act + chl + epd + alb + sph + qtz	

act, actinolite; alb, albite; amp, amphibole; and, andesine; bio, biotite; byt, bytownite; cal, calcite; chl, chlorite; epd, epidote; hbl, hornblende; ilm, ilmenite; lab, labradorite; mag, magnetite; olg, oligoclase; plg, plagioclase; ppl, pumpellyite; prh, prehnite; qtz, quartz; sph, sphene.
* papers concerned with ophiolites; † assemblages include qtz + alb + sph.

hornblende occur together defining a transitional assemblage with greenschist facies. Chlorite is present at all levels and epidote is less common higher in the sequence. The possible occurrence of amphibole at Ranvik and Diaz Cove, and pumpellyite in Larsen Harbour, reflects the irregularity of the metamorphic zonation.

Most of the dykes sampled show little alteration but phases analysed represent grades equivalent to those of the surrounding lavas (Table XIV). Calcic plagioclase exists metastably with actinolite and metamorphic replacement is limited. Two altered dykes from Smaaland Cove contain low-grade assemblages in contrast to those of other dykes from the same area (Table XIV) and possibly represent intensive local hydrothermal activity (cf. 'domains' of Coleman (1977)).

4. Plutonic unit

The gabbros and plagiogranite of the plutonic unit represent the lowest levels of the Larsen Harbour Formation and contain both greenschist and amphibolite assemblages (Table XV), the former often seen to be replacing the latter. Igneous hornblende has been identified within the plutonic unit, where low-Ti metamorphic hornblende and actinolite are also present. Albite is uncommon but it constitutes greenschist facies with actinolite (Table XV). Chlorite is present in most rocks and low-Fe epidote also occurs. Calcic plagioclase is retained, indicative of its stability with hornblende at amphibolite-facies grade. Metamorphic assemblages developed are:

albite + actinolite + chlorite ± epidote,
andesine + actinolitic hornblende + chlorite + epidote,
labradorite + Mg-hornblende + chlorite.

The preservation of igneous amphibole may indicate that hydrothermal circulation was limited at this depth or was prevented by the coarse-grained nature of the plutonic unit. Similar assemblages are found in both gabbro and plagiogranite of the Smaaland Cove intrusion.

The Wheeler Glacier gabbro is distinct from the Smaaland Cove intrusion both in mineralogy and structural level. It contains a prehnite–pumpellyite assemblage (Table XV) similar to that within the lavas of that area. Its structural level and age of intrusion are uncertain and it may represent an off-axis intrusion into low-grade mafic lavas late in the evolution of the Larsen Harbour Formation. No albite was identified and the assemblage comprises:

labradorite ± pumpellyite ± prehnite ± epidote ± chlorite.

The pumpellyite is Al-rich rather than Fe-rich as in the adjacent ? lower-grade lavas.

5. Conclusion

A metamorphic zonation is developed in the extrusive and plutonic rocks of the Larsen Harbour Formation not unlike

Table XIV. Summary of microprobe analyses and metamorphic facies of Larsen Harbour Formation rocks

Location	R	Amphibole	1	Plagioclase	Epidote	Chlorite	Pumpellyite	Prehnite	Relict cpx	Facies A	Facies B
Leon Head	P			alb, olg($An_{6,18}$)	epd(0.3)	chl(1.3)	*	*	cpx	PF	
	M			alb*		*	*	*	*	PF	
	D			lab(An_{66})		*		*	*		
Wheeler Glacier	M			alb(An_{10})		chl(1.3)	ppl(0.2, 0.4)		*	PF	
Diaz Cove	P			alb, olg($An_{7,12}$)	*	*	*	prh	cpx	PF	
	M	*?		alb*	*	*	*	*		PF	
Kupriyanov Islands	P			alb, olg($An_{9,12}$)		*	*			?PF	
	D			olg(An_{16})		chl(1.0)		prh	cpx	?PF	
Ranvik	P	*?		alb*	*	*		*		?PF	
	D			byt(An_{72})		chl(1.0)			cpx		
Rogged Bay	P	act; act–hbl	(0.2, 3.5)	alb(An_4)	epd(0.3)	chl(1.2)				PF	LA
	M			alb(An_4)	epd(0.4)	chl(0.4)					
	D	Mg–hbl	(7.9)	alb, byt(An_{10}, An_{73})	epd(0.3)	chl(0.1)		*	cpx	GF/AF	LA/A
Smaaland Cove	P	Fe–act–hbl	(3.4)	olg(An_{13})	epd(0.5)	chl(1.0)				GF	LA
	M (i)	Mg–hbl	(7.1)	olg, lab($An_{17,30,60}$)		*				AF	UA
	M (ii)	act–hbl	(4.7)	olg($An_{26,31}$)	epd(0.3)	chl(0.6)				GF/AF	LA
	M (iii)	Mg–hbl	(6.7)	olg(An_{18})	epd(0.3, 0.4)	chl(0.7)				AF	UA
	M (iv)	Fe–hbl; Mg–hbl	(7.1, 8.8)	olg(An_{29})						AF	UA
	D (i)	act; Mg–hbl	(2.5, 4.7)	lab($An_{55,68}$)		chl(0.9)			cpx	GF/AF	LA
	D (ii)	Fe–act	(2.7)	lab, byt($An_{53,74}$)		chl(0.9)			cpx	GF/AF	LA
	D (iii)	Mg–hbl	(6.2)	lab, byt($An_{70,84}$)		*			cpx	AF	UA
	D (iv)			alb(Ab_{100})	epd(0.4)	chl(0.3)	ppl(0.3)			PF	
	D (v)			alb(An_2)	epd(0.2)	chl(1.9)	ppl(0.3)			PF	
Doubtful Bay	P	*		alb, olg($An_{2,16}$)	epd(0.4)					GF	?LA
Larsen Harbour	P	*		alb(An_2)	epd(0.4)	chl(1.2, 2.0)				GF	?LA
	M			alb, olg($An_{2,13}$)	epd(0.3, 0.5)	chl(0.5)	ppl			PF	
Nattriss Head	P	*		olg(An_{17})	*	*				GF	?LA
	D	act–hbl	(2.8)	lab(An_{66})	*	chl(2.3)			cpx	GF/AF	LA

Amphibole: 1, Al_2O_3 content as wt %. Values in brackets for epidote, chlorite and pumpellyite are Fe^{3+}/Al, Mg/Fe^{2+} and Mg/Fe^{2+}, respectively, using total iron.
Facies: A (after Liou and others, 1974); AF, GF and PF, amphibolite, greenschist and prehnite–pumpellyite facies, respectively. B (after Elthon and Stern, 1978); LA and UA, lower and upper actinolite facies, respectively. * minerals identified optically; R host rock; P, M and D pillow lava, massive lava and dyke.

Table XV. Summary of microprobe analyses and metamorphic facies of Smaaland Cove intrusion rocks.

Specimen	Amphibole: Igneous	1	2	Amphibole: Metamorphic	1	2	Plagioclase	Epidote	Chlorite	Pumpellyite	Prehnite	Facies A	Facies B
M.1813.2	Fe–hbl	6.3	0.36	Fe–act–hbl	3.6	0.06	olg(An_{19-24})		chl(0.3)			AF	LA
M.1831.1	Fe–hbl	5.6	0.15										
	Fe–hbl	5.8	0.17	Fe–act–hbl	3.7	0.0	alb,* and(An_{32-36})		chl(0.4)			AF	LA
	Fe–hbl	5.1	0.14										
M.1814.2	Mg–hbl	5.4	0.16	act	2.0	0.0	and(An_{41-49})	*	*			GF on AF	LA
				act	2.3	0.0							
				Fe–act–hbl	2.5	0.04							
M.1852.2	Mg–hbl	5.0	0.10	act–hbl	2.4	0.03	alb*, and(An_{36})	epd(0.2)	chl(0.8)			AF	LA
				Fe–act–hbl	8.6	0.01							UA
M.1852.5	Mg–hbl	4.8	0.15										
	Fe–act–hbl	4.2	0.11	Mg–hbl	8.0	0.02	and, byt($An_{48,71}$)	*				AF	UA
M.1853.3	Mg–hbl	4.3	0.27	act–hbl	3.6	0.16							
				act	2.0	0.05	alb, and($An_{1,35}$)	*	chl(0.5, 0.7)			GF on AF	LA
				act–hbl	3.7	0.08							
M.4072.8							lab(An_{56-67})			ppl(1.9)		PF	
M.4072.11							and, lab(An_{46-63})	epd(0.3)	chl(0.4, 0.6)		prh	PF	

Amphibole: 1 and 2, Al_2O_3 wt % and Ti atoms in structure, respectively. Values in brackets for epidote, chlorite and pumpellyite are Fe^{3+}/Al, Mg/Fe^{2+} and Mg/Fe^{2+}, respectively, using total iron.
Facies: A (after Liou and others, 1974); AF, GF and PF, amphibolite, greenschist and prehnite–pumpellyite facies, respectively. B (after Elthon and Stern, 1978); LA and UA, lower and upper actinolite facies, respectively. * minerals identified optically.

those of other ophiolite sequences but it contains a prehnite–pumpellyite assemblage at a high level rather than zeolite facies as reported elsewhere, notably in the Sarmiento ophiolite (Elthon and Stern, 1978). Prehnite–pumpellyite-facies rocks are found in the Ducloz Head Formation to the north of the Larsen Harbour Formation (Storey, 1983*b*) and zeolite-facies rocks occur in the Annenkov Island Formation which overlies the Larsen Harbour Formation to the west. These assemblages are not necessarily linked to that within the Larsen Harbour Formation.

The possibility that the metamorphic zonation of the Larsen Harbour Formation was not caused solely by hydrothermal metamorphism cannot be overlooked. The mafic sequence may have undergone burial metamorphism subsequent to initial hydrothermal alteration, as it is overlain to the west by the Annenkov Island Formation; high-level intrusions, such as the Wheeler Glacier gabbro, may have provided sufficient heat to cause local thermal alteration. The presence of prehnite–pumpellyite-facies rocks at high level in the mafic sequence could be explained by bulk-rock composition, tectonic environment and local pressure conditions of the Larsen Harbour Formation, which may have been different from those in other ophiolites.

VI. DISCUSSION AND INTERPRETATION

A. Summary of the Larsen Harbour Formation

The Larsen Harbour Formation, which is approximately 2 km thick, represents the upper part of an autochthonous ophiolite sequence. It is intruded by, and probably structurally underlain by, a composite gabbro and plagiogranite pluton (Smaaland Cove intrusion) and smaller gabbroic bodies at higher (?) levels. The formation has a rough pseudostratigraphy, containing primary breccias, silicic differentiates, multiple dykes and subordinate pillow lavas at low levels in contrast to voluminous pillow lavas, secondary breccias and thicker sedimentary units at the top of the sequence. Three separate dyke trends have been identified in specific areas and the number of dykes increases with depth in the ophiolite, although a sheeted dyke layer has not been identified. The lavas are tilted from 20° to 40° to the west throughout, becoming steeper to the north, and have also undergone quartz veining and complex faulting. The ophiolite contains zones of metamorphic assemblages which developed as a result of hydrothermal metamorphism. The Smaaland Cove intrusion maintains a sharp roof contact with the overlying lavas; by analogy with other ophiolites, its structural level should approach that of layer 3 in oceanic crust (Christensen, 1977) below the sheeted dyke layer.

The original augite–andesine/labradorite mineralogy of most lavas has been completely replaced by secondary phases due to pervasive metamorphism but it has survived at a lower metamorphic grade. The igneous mineralogy and texture of the associated basic dykes have been retained except where they are heavily altered at low levels in the sequence. The mineralogy of the altered dykes and the lavas classifies them as spilites. The dacites (cf. keratophyres) are quartz–andesine leucocratic rocks of varying fine-grained texture and containing extensive graphic intergrowths and secondary phases. Breccias comprise both primary and secondary types, the former having been produced contemporaneously with the extrusion of magma rather than as a result of post-consolidation mechanisms. Crystal and lithic tuffs occur throughout, having been derived from mafic lavas at low levels, and having an equivalent petrography to the island-arc tuffs nearer the top of the ophiolite. Igneous textures and mineralogy are retained in the plutonic rocks below the extrusive sequence and have been only sporadically altered by hydrothermal metamorphism.

The mafic lavas, dykes and gabbros approach oceanic tholeiites in chemical composition; the less-altered low-level plutonic rocks show more transitional undepleted characteristics in contrast to the lavas and dykes. The dacites and plagiogranites have distinctive compositions and are the products of differentiation of a tholeiitic magma.

B. Metamorphic Zonation

It has been concluded (p. 52–54) that a zonation of prehnite–pumpellyite, greenschist and amphibolite facies, increasing in grade with depth, is developed in the Larsen Harbour Formation. This assemblage contrasts with the zeolite-, greenschist- and amphibolite-facies sequences of other ophiolites (Spooner and Fyfe, 1973; Stern and others, 1976) and therefore warrants further discussion. Coleman (1977) reported such a sequence from the arc–trench side of an island arc but this position conflicts with the current plate-tectonic model for South Georgia.

The arguments in favour of hydrothermal metamorphism during the extrusion of this formation have already been given (p. 51) and they suggest that burial metamorphism was not the main mechanism of alteration. The presence of actinolite within approximately 2 km of the top of the sequence allows the necessary geothermal gradient for hydrothermal metamorphism to be estimated. The thickness of the formation has been estimated at between 1.4 km and 3.6 km (Table III). The disappearance of actinolite at 475°C and 2 kbar pressure defines the upper limit of the greenschist faces (Liou and others, 1974) and in the Larsen Harbour Formation this occurs near the base of the extrusive unit. The thicknesses given above suggest a geothermal gradient of between 130 and 330°C/km, which corresponds to the values of 150 to 250°C/km for other ophiolites (Stern and others, 1976; Coleman, 1977).

In the light of the current work, the following hypotheses are presented concerning the occurrence of the prehnite–pumpellyite facies in the Larsen Harbour Formation:

i. Prehnite and pumpellyite are not in equilibrium and the facies has been misidentified.
ii. The original hydrothermal zeolite facies of the upper part of the sequence has been upgraded by a local thermal event.
iii. The original hydrothermal zeolite facies has been upgraded by burial metamorphism associated with a presumed overlying equivalent of the Annenkov Island Formation.

i. The first hypothesis cannot be proved or disproved until further investigation of the equilibrium relationships has been carried out. Liou (1979) reported zeolite-facies rocks containing pumpellyite from the Taiwan ophiolite; prehnite also occurs but never in the same rock and represents a vein assemblage. If it is assumed that the prehnite–pumpellyite association is not in equilibrium in the Larsen Harbour Formation, the assemblage pumpellyite–chlorite–albite (Table VI) defines the zeolite facies as described above (Liou, 1979). However, no zeolite has been observed in any of the low-grade rocks and it is suggested that the prehnite–pumpellyite association is indicative of the prehnite–pumpellyite facies.

ii. The original zeolite-facies assemblages of the upper part of the Larsen Harbour Formation may have been upgraded to prehnite–pumpellyite facies by local thermal metamorphism caused by the intrusion of the Wheeler Glacier gabbro. The age and structural level of the gabbro is uncertain, although it has been correlated with the other gabbros which are thought to form the basal unit of the ophiolite. Both prehnite and pumpellyite occur in the gabbro, which has extensively altered margins, although its actual contact with the surrounding lavas is obscured.

Franks (1974) described the localized thermal metamorphism of the 2 km thick New Bay Formation, Newfoundland, which was caused by mafic intrusions soon after its deposition. The Wheeler Glacier gabbro may represent a late and high-level off-axis intrusion of oceanic magma into the upper lavas of the Larsen Harbour Formation, thereby causing thermal metamorphism at a specific level. Contact metamorphism associated with the intrusion of magma in 'leaky fracture zones' within oceanic crust has been recognized as part of the complex submarine hydrothermal system (Stern and others, 1976). As local geothermal gradients remain high in oceanic crust, even at a considerable distance from the spreading centre (up to 150°C/km at over 100 km; Coleman, 1977), the effects of contact metamorphism would be lessened because of the smaller temperature differential between the country rock and intruding gabbro. An overall rise in temperature throughout the country rock could be sufficient to upgrade their metamorphic assemblage to the prehnite–pumpellyite facies, occurring at pressures of 1–2.5 kbar and at 250–350°C (Kuniyoshi and Liou, 1976), since prehnite alone occurs at lower pressures and higher temperatures, 2.5 kbar, 320–360°C (Nitsch, 1971). The conditions within the New Bay Formation during metamorphism have been given as 1 kbar pressure (0.8–2.8 km overburden) and 300°C as a result of mafic intrusions (Franks, 1974). Similar low confining pressures would be found in the upper levels of the Larsen Harbour Formation, assuming that not all of the overlying Annenkov Island Formation had been emplaced at the time of gabbro intrusion and associated metamorphism. Although physical conditions are satisfied in the above scheme, it does not explain the presence of prehnite and pumpellyite in the gabbro itself.

iii. The Annenkov Island Formation (~3 km) may overlie at least part of the Larsen Harbour Formation and therefore the imprint of burial metamorphism on the original hydrothermally derived metamorphic zonation cannot be overlooked. Stern and others (1976) noted that this mechanism may be significant in ophiolites from areas where local sedimentation rates are high. Quartz–prehnite veins occur in the lavas of greenschist facies at the base of the sequence; a K–Ar age of 78 ± 3 Ma on hornblende has been obtained from the Smaaland Cove intrusion, which gives a Rb–Sr whole-rock isochron age of 127 ± 4 Ma (Tanner and Rex, 1979). These late veins and the possibility that 78 ± 3 Ma is a reset age may be the result of burial metamorphism by ~3 km overburden of the Annenkov Island Formation but there is no evidence of extensive modification of the assemblages produced by the initial hydrothermal event in the ophiolite. The precise stratigraphical correlation of individual parts of the Larsen Harbour Formation is uncertain, although overall the sequence youngs northward. It is suggested that part of this formation is overlain by the shelf-facies sediments, producing a prograde prehnite–pumpellyite assemblage, and elsewhere the primary hydrothermal zonation remains little affected. The burial model helps to explain the occurrence of prehnite and pumpellyite in the Wheeler Glacier gabbro and the reset age of the Smaaland Cove intrusion, although this could be the time of uplift of the ophiolite sequence. The zeolite facies of the Annenkov Island Formation and the prehnite–pumpellyite facies of the Larsen Harbour Formation may form a continuous regional prograde event.

The identification of metamorphic facies in the upper parts of the Larsen Harbour Formation requires further investigation. In the light of available data, the author suggests that the zeolite-facies rocks of the ophiolite sequence were subjected to local burial metamorphism to prehnite–pumpellyite facies following the deposition of the Annenkov Island Formation or its equivalent.

C. Local Relationships

The oceanic and ophiolitic nature of the Larsen Harbour Formation has been established in this report and hence verifies the original hypothesis (Bell and others, 1977; Storey and others, 1977) that it represented oceanic crust in a marginal basin–island-arc system in South Georgia.

Possible plate-tectonic models for South Georgia have been given by Tanner and others (1981, figs 24 and 25) and Storey (1983*a*; fig. 97). Their cross-sections illustrate the suggested relationships between the tectonic units of the marginal basin–island-arc system. The marginal basin floor in South Georgia probably consists of ocean crust (Larsen Harbour Formation) and fragments of continental crust (Drygalski Fjord Complex). The floor is overlain by shelf- and turbidite-facies sediments deposited in spatially distinct parts of the basin and separated by the Cooper Bay dislocation (fault zone) and the Drygalski Fjord Complex. The turbidite sequences consist of the Sandebugten and Cooper Bay formations, derived from quartz-rich continental crust (continental margin) (Dalziel and others, 1975; Stone, 1980), the Cumberland Bay Formation which is at least 8 km thick and contains abundant andesitic island-arc-derived debris (Trendall, 1959; Stone, 1980). The shelf-facies sequence is thinner and comprises at least 3 km of tuffs and andesite breccias (Annenkov Island Formation) deposited adjacent to the island arc which bordered the marginal basin to the west (Suárez and Pettigrew, 1976; Tanner and others, 1981). The Annenkov Island Formation may overlie part of the Larsen Harbour Formation and may interdigitate with the Cumberland Bay Formation within the turbidite basin. The Ducloz Head Formation (Storey, 1983*b*)

contains rocks comparable with the turbidite facies (coastal member) and the shelf facies (inland member) brought together by faulting near the Cooper Bay dislocation. The Cumberland Bay Formation shows increasing deformation towards the north-east, and is metamorphosed to at least prehnite–pumpellyite facies (Tanner, 1982). It is thrust over the underlying, more intensely deformed, greenschist-facies rocks of the Sandebugten and Cooper Bay formations (Trendall, 1959; Dalziel and others, 1975; Stone, 1982; Tanner, 1982). By contrast, the shelf-facies rocks are undeformed apart from tilting towards the west, and zeolite and prehnite–pumpellyite assemblages are developed in the Annenkov Island and the Ducloz Head formations, respectively (Suárez and Pettigrew, 1976; Storey, 1983*b*).

The Larsen Harbour Formation is probably conformably overlain to the west by the Annenkov Island Formation, as concluded separately by Tanner and others (1981), and is separated from the Cumberland Bay Formation and Drygalski Fjord Complex to the east by an inferred tectonic break. Pillow lavas and basic sills within the Ducloz Head Formation (Storey, 1983*b*) have been correlated with the mafic rocks in the ophiolite and may represent the early stages of basic magmatism in the marginal basin, although geochemical verification of this is still necessary. Suárez and Pettigrew (1976) suggested that sills and a single pillow-lava flow within the Annenkov Island Formation may be related to the Larsen Harbour Formation. Geochemically the sills have a calc-alkaline affinity (this report) and are distinct from the ophiolite rocks; the characteristics of the single lava outcrop cannot be established at present. Pre-tectonic, gabbroic and dioritic sills intrude the lower levels of the turbidite-facies rocks (Cumberland Bay, Sandebugten and Cooper Bay formations) and have been attributed to the final stages of basic activity of the basin floor after the onset of sedimentation (Stone, 1980, 1982; Mair, 1981). Although likely, this relationship cannot be further qualified without geochemical evidence. The Larsen Harbour Formation is flanked to the east by the Drygalski Fjord Complex, which is intruded by numerous basic dykes, some of which may correspond to those within the Larsen Harbour Formation (Storey, 1983*a*). The correlation of 'younger' gabbros in the Drygalski Fjord Complex with the mafic rocks of the Larsen Harbour Formation has been suggested elsewhere (Storey and others, 1977; Tanner and Rex, 1979).

The differentiated nature of the dacites within the ophiolite sequence discounts the suggestion by the author (Mair, 1983) that they were associated with the final stages of continental silicic volcanism during the opening of the marginal basin. Their geochemistry also distinguishes them from the felsites of the Ducloz Head Formation described by Storey (1983*b*). The preliminary investigation of the geochemistry of the tuffs from the Annenkov Island and Larsen Harbour formations has shown that the tuffs from the lower levels of the ophiolite have a similar chemistry to the surrounding basaltic lavas, from which they are formed, and are distinct from those of the island-arc assemblage. In view of the fact that tuffs from the higher levels of the ophiolite have a similar petrography to that of the island-arc rocks, it is suggested that the source of tuffaceous material changed with time and that the island arc became active near the final stages of lava extrusion in the basin. The conditions affecting the formation of tuffs from the mafic lavas may also have varied with time within the basin.

D. Timing of Events on South Georgia

The timing of events on South Georgia has been established using radiometric and palaeontological evidence (Tanner and Rex, 1979; Thomson and others, 1982); a summary of their work is given in Table XVI and outlined below. The granodiorite and gabbro plutons of the Drygalski Fjord Complex have minimum ages of 180–200 Ma and are possibly related to an early pre-marginal basin magmatic arc of the Gondwana continent. Younger gabbros and dykes which intrude the complex are of ? Andean age and correspond to a thermal event (140 Ma) thought to represent the intrusion of mafic magma during the opening of the marginal basin and extrusion of the Larsen Harbour Formation. The continuation of magmatic activity beyond the time of crystallization or hydrothermal metamorphism of the Smaaland Cove intrusion (127 ± 4 Ma), is indicated by cross-cutting basic dykes. Basic sills, thought to be related to the Larsen Harbour Formation, also intrude the lower units of the turbidite-facies sediments. The ages of the Sandebugten and Cooper Bay formations are unknown but sedimentation of the overlying Cumberland Bay Formation began during the late Jurassic–earliest Cretaceous (Thomson and others, 1982). The Annenkov Island Formation is slightly younger in age, although Thomson and others (1982) suggested that it may range back in age to the Neocomian, and the top of the sequence is dated at 100 Ma. The Upper Breccia Member of the Annenkov Island Formation (100–110 Ma) formed contemporaneously from andesite intrusions in the island arc which have been dated at 100–103 Ma (K–Ar); younger intrusions (81 Ma) occur within the island-arc sequence at deeper levels towards the east.

Reset ages of 78 ± 3 Ma (K–Ar) from hornblende in the Smaaland Cove intrusion and 77 Ma on whole-rock and mineral determinations on the Drygalski Fjord Complex (Tanner and Rex (1979)) are roughly co-eval with the estimated time of deformation (82–91 Ma; K–Ar) of the Cumberland Bay Formation (Thomson and others, 1982) and may indicate the time of uplift of the shelf facies and underlying rocks.

E. Relationship to South America

The relationship of the strato-tectonic units of South Georgia to those in South America is well established (Dalziel and Elliot, 1971; Katz, 1972, 1973; Dalziel and others, 1974, 1975; Suárez and Pettigrew, 1976; Storey and others, 1977; Tanner, 1982). The Larsen Harbour Formation can be correlated and compared directly with the Chilean ophiolites, which occur as discontinuous *en échelon* lenses for over 1 000 km, between the island-arc rocks of the Patagonian Batholith and the continental margin in South America (Katz, 1973; Dalziel and others, 1974). Two ophiolites, the Sarmiento and Tortuga complexes, have been investigated in detail (Stern and others, 1976; de Wit and Stern, 1978; Elthon and Stern, 1978; Saunders and others, 1979). Both are autochthonous and undeformed, and represent different stages in the evolution of the marginal basin system on the southern edge of Gondwana.

The more northerly Sarmiento Complex consists of ~ 1 km of chemically layered plutonic rocks, crystalline gabbros and plagiogranites, a 300 m thick sheeted dyke unit containing silicic dykes, overlain by ~ 2 km of primary tuffs, 'intrusive pillow lavas' and water-lain pillow lavas (de Wit and Stern,

Table XVI. Timing of events on South Georgia.

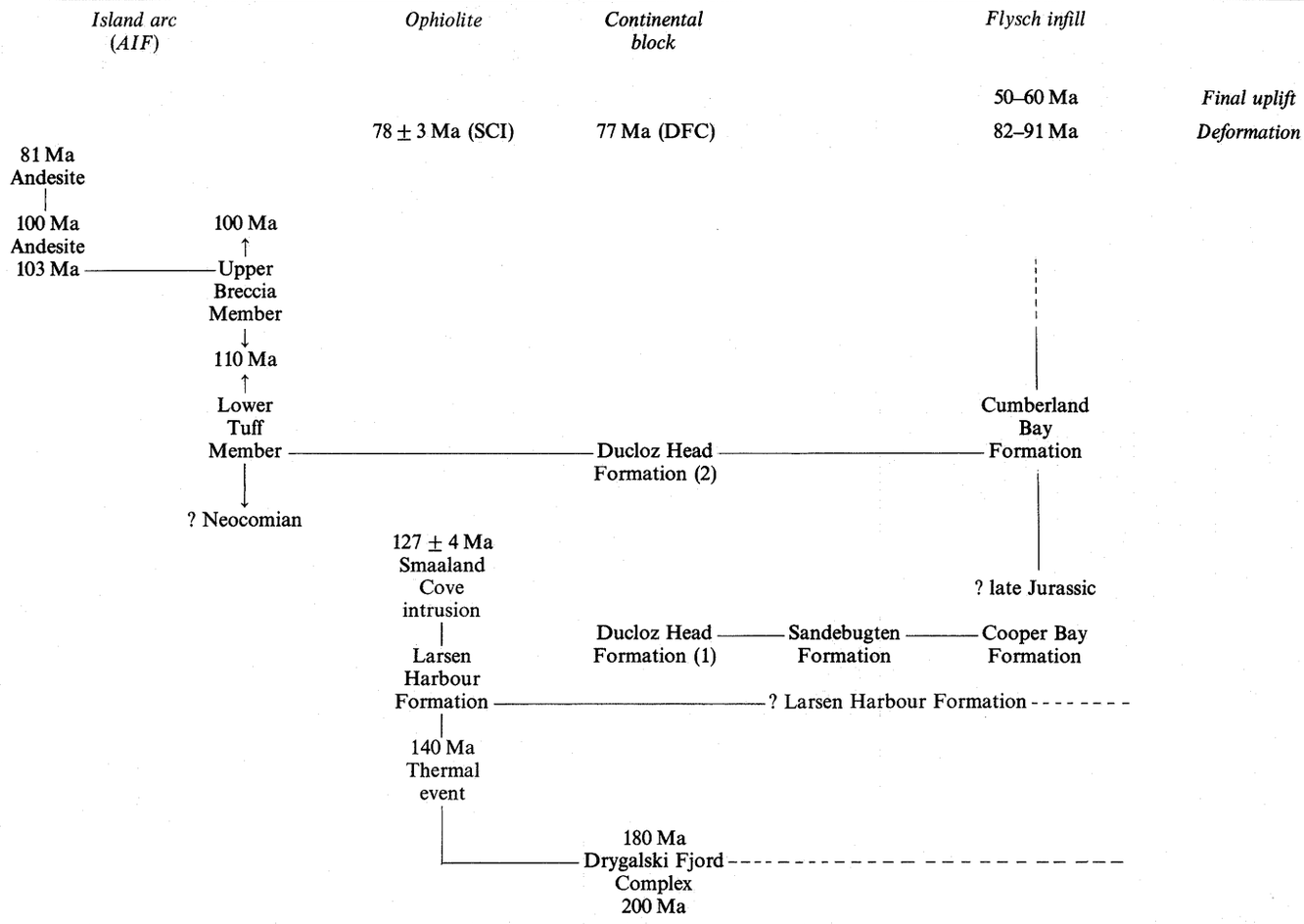

Dating from Tanner and Rex (1979), Thomson and others (1982). SCI, Smaaland Cove intrusion; DFC, Drygalski Fjord Complex; AIF, Annenkov Island Formation; Ducloz Head Formation (1) and (2), coastal and inland members, respectively.

1978). Silicic differentiates do not occur in the Tortuga Complex, which comprises ~1 km of mineralogically layered gabbro, ~1 km of diabase transitional to sheeted dykes, and a 1 km thick extrusive unit of abundant water-lain pillow lavas and secondary breccias (de Wit and Stern, 1978). The ophiolites show an increase in the amount of water-lain pillow lavas and a decrease in aquagene tuffs and 'intrusive pillows' from north to south, corresponding to the volume of extrusive rocks relative to extensional dykes and the range and volume of differentiated rocks within the ophiolites (de Wit and Stern, 1978). These authors concluded that the more northerly Sarmiento Complex may represent an early marginal basin approximately 25 km wide, whereas the Tortuga Complex corresponds to a more evolved marginal basin over 100 km in width. This is supported by the differing geochemical features of both complexes. The Sarmiento rocks are undepleted transitional (oceanic–continental) tholeiites derived from melted sub-continental mantle and representing the initial magmatism of back-arc activity in a narrow restricted basin (Saunders and others, 1979). By contrast, the Tortuga rocks have depleted characteristics typical of ocean-floor basalts and were derived from oceanic mantle following continued extension in the back-arc basin (Saunders and others, 1979).

The Larsen Harbour Formation correlates more closely with the Sarmiento Complex than with the Tortuga Complex as regards lithology (p. 7–23) and geochemistry (p. 29–37), although the upper levels of the formation contain abundant secondary breccias typical of the more mature Tortuga ophiolite. The absence of a sheeted dyke layer and the occurrence of prehnite–pumpellyite rocks in the South Georgia ophiolite indicate the variability of the features of ophiolites within the same marginal basin system. Tanner (1982) suggested that the marginal basin was approximately 200 km wide in the reconstructed position of South Georgia adjacent to the southern Andes and possibly narrowed to the east. From the above correlation with the Sarmiento Complex, it is inferred that the Larsen Harbour Formation represents a strip of oceanic crust approximately 25 km wide which formed at a discrete spreading centre, between an island arc (Annenkov Island Formation) and a remnant continental block (Drygalski Fjord Complex), and was subsequently overlain by shelf-facies sediments (Tanner and others, 1981). It developed in parallel to similar (? wider) strips of oceanic crust which are thought to form the floor of the remainder of the marginal basin to the east of the Drygalski Fjord Complex where they are overlain by thicker turbidite-facies sediments.

VII. ACKNOWLEDGEMENTS

I am grateful to Dr P. W. G. Tanner, my supervisor in the Survey, and to Drs C. M. Bell, D. I. M. Macdonald and B. C. Storey for their companionship in the field and helpful discussion. The field work would not have been completed without the logistic support provided by the officers and crews of HMS *Endurance*, RRS *John Biscoe* and RRS *Bransfield*, and the Survey's personnel (especially D. J. Orchard, D. Burkitt and T. D. Fogg) at Grytviken, South Georgia.

I wish to thank Professor E. A. Tait for use of facilities in the Department of Geology, University of Aberdeen, and other members of the staff for their specialist assistance, notably Drs M. A. Lappin and F. E. Tocher; Dr M. Munro deserves special thanks for his supervision and encouragement. Microprobe analysis was carried out by G. Taylor at the University of Aberdeen, and B. Fulton assisted with the compilation of the larger figures.

VIII. REFERENCES

ALDISS, D. T. 1978. *Granitic rocks of ophiolites*. Ph.D. thesis, The Open University, 134 pp. [Unpublished.]

ALLEN, J. M. *and* GOLDIE, R. 1978. Coexisting amphiboles from Noranda area, Quebec: extension of the actinolite–hornblende miscibility gap to iron-rich bulk composition. *American Mineralogist*, **63**, 205–9.

BAILEY, E. H. *and* BLAKE, M. C. 1974. Major chemical characteristics of Mesozoic coast ophiolite in California. *Journal of Research of the U.S. Geological Survey*, **2**, 637–56.

BAMBA, T. 1974. A series of magmatism related to the formation of spilite. (*In* AMSTUTZ, G. C., *ed. Spilites and spilitic rocks*. Berlin, Heidelberg, New York, Springer-Verlag, 83–112.)

BARTH, T. F. W. *and* HOLMSEN, P. 1939. Rocks from the Antarctandes and Southern Antilles. Being a description of rock samples collected by Olaf Holtedahl, 1927–28, and a discussion of their mode of origin. *Scientific Results of the Norwegian Antarctic Expeditions, 1927–29*, No. 18, 64 pp.

BELL, C. M., MAIR, B. F. *and* STOREY, B. C. 1977. The geology of part of an island arc-marginal basin system in southern South Georgia. *British Antarctic Survey Bulletin*, No. 46, 109–27.

BEVINS, R. E. 1978. Pumpellyite-bearing basic igneous rocks from the Lower Ordovician of north Pembrokeshire, Wales. *Mineralogical Magazine*, **42**, 81–83.

BONATTI, E. 1965. Palagonite, hyaloclastites and alteration of volcanic glass in the ocean. *Bullétin Volcanologique*, **28**, 257–69.

BONATTI, E. 1967. Mechanisms of deep sea volcanism in the South Pacific. (*In* ABELSON, P. H., *ed. Researches in geochemistry*, **2**. New York, Wiley and Sons, 453–91.)

BRADY, J. B. 1974. Coexisting actinolite and hornblende from west-central New Hampshire. *American Mineralogist*, **59**, 529–35.

BROWN, E. H. 1967. The greenschist facies in part of eastern Otago, New Zealand. *Contributions to Mineralogy and Petrology*, **14**, 259–92.

BROWN, E. H., BRADSHAW, J. Y. *and* MUSTOE, G. E. 1979. Plagiogranite and keratophyre in ophiolite on Fidalgo Island, Washington. *Geological Society of America Bulletin*, **90**, 493–507.

BRUHN, R. L., STERN, C. R. *and* DE WIT, M. J. 1978. Field and geochemical data bearing on the development of a Mesozoic volcanic-tectonic rift zone and back-arc basin in southernmost South America. *Earth and Planetary Science Letters*, **41**, 32–46.

BYERLY, G. R., MELSON, W. G. *and* VOGT, P. R. 1976. Rhyodacites, andesites, ferro-basalts and ocean tholeiites from the Galapagos spreading centre. *Earth and Planetary Science Letters*, **30**, 215–21.

CANN, J. R. 1969. Spilites from the Carlsberg Ridge, Indian Ocean. *Journal of Petrology*, **10**, 1–19.

CANN, J. R. 1970. Rb, Sr, Zr and Nb in some ocean floor basaltic rocks. *Earth and Planetary Science Letters*, **10**, 7–11.

CARLISLE, D. 1963. Pillow breccias and aquagene tuffs, Quadra Island, British Columbia. *Journal of Geology*, **71**, 48–71.

CARMICHAEL, I. S. E. 1964. The petrology of Thingmuli, a Tertiary volcano in eastern Iceland. *Journal of Petrology*, **5**, 435–60.

CHRISTENSEN, N. I. 1977. The geophysical significance of oceanic plagiogranite. *Earth and Planetary Science Letters*, **36**, 297–300.

CHURCH, W. R. *and* COISH, R. A. 1976. Oceanic versus island-arc origin of ophiolites. *Earth and Planetary Science Letters*, **31**, 8–14.

COISH, R. A. 1977. Ocean floor metamorphism in the Betts Cove ophiolite, Newfoundland. *Contributions to Mineralogy and Petrology*, **60**, 255–70.

COLEMAN, R. G. 1977. *Ophiolites*. Berlin, Heidelberg, New York, Springer-Verlag.

COLEMAN, R. G. *and* PETERMAN, Z. E. 1975. Oceanic plagiogranite. *Journal of Geophysical Research*, **80**, 109–89.

COOMBS, D. S., NAKAMURA, Y. *and* VUAGNAT, M. 1976. Pumpellyite–actinolite facies schists of the Taveyanne Formation near Loeche, Valais, Switzerland. *Journal of Petrology*, **17**, 440–71.

COOPER, A. F. *and* LOVERING, J. F. 1970. Greenschist amphiboles from the Haast River, New Zealand. *Contributions to Mineralogy and Petrology*, **27**, 11–24.

DALZIEL, I. W. D. *and* ELLIOT, D. H. 1971. Evolution of the Scotia arc. *Nature, London*, **233**, 246–52.

DALZIEL, I. W. D., DE WIT, M. J. *and* PALMER, K. F. 1974. Fossil marginal basin in the southern Andes. *Nature, London*, **250**, 291–4.

DALZIEL, I. W. D., DOTT, R. H., WINN, R. D. *and* BRUHN, R. L. 1975. Tectonic relations of South Georgia island to the southernmost Andes. *Geological Society of America Bulletin*, **86**, 1034–40.

DE WIT, M. J. *and* STERN, C. 1978. Pillow talk. *Journal of Volcanology and Geothermal Research*, **4**, 55–80.

DONNELLY, T. W. 1966. Geology of St. Thomas and St. John, United States Virgin Islands. *Memoirs. Geological Society of America*, **98**, 85–176.

DOUGLAS, G. V. 1930. Topography and geology of South Georgia. (*In Report on the geological collections made during the voyage of the "Quest" on the Shackleton–Rowett Expedition to the South Atlantic and Weddell Sea in 1921–22*. London, Trustees of the British Museum, 4–24.)

ELTHON, D. *and* STERN, C. 1978. Metamorphic petrology of the Sarmiento ophiolite complex, Chile. *Geology*, **6**, 464–8.

ENGEL, C. E. *and* FISHER, R. L. 1975. Granitic to ultramafic rock complexes of the Indian Ocean ridge system, western Indian Ocean. *Geological Society of America Bulletin*, **86**, 1553–78.

FERGUSON, D., TYRRELL, G. W. *and* GREGORY, J. W. 1914. The geology of South Georgia. *Geological Magazine*, Decade 6, **1**, 53–64.

FIALA, F. 1974. Some notes on the problem of spilites. (*In* AMSTUTZ, G. C., *ed. Spilites and spilitic rocks*. New York, Heidelberg, Berlin, Springer-Verlag, 9–22.)

FLOYD, P. A. *and* WINCHESTER, J. A. 1975. Magma type and tectonic setting discrimination using immobile elements. *Earth and Planetary Science Letters*, **27**, 211–18.

FORNARI, D. J., MALAHOFF, A. *and* HEEZEN, B. C. 1978. Volcanic structure of the crest of the Puna Ridge, Hawaii: geophysical implications of submarine volcanic terrain. *Geological Society of America Bulletin*, **89**, 606–16.

FRANKS, S. G. 1974. Prehnite–pumpellyite facies metamorphism of the New Bay Formation, Exploits Zone, Newfoundland. *Canadian Mineralogist*, **12**, 456–62.

GARCIA, M. O. 1978. Criteria for the identification of ancient volcanic arcs. *Earth Sciences Review*, **14**, 147–65.

GILL, J. B. 1970. Geochemistry of Viti Levu, Fiji, and its evolution as an island-arc. *Contributions to Mineralogy and Petrology*, **27**, 179–203.

GLASSLEY, W. E. 1975. Low variance phase relationships in a prehnite-pumpellyite facies terrain. *Lithos*, **8**, 69–76.

HARTE, B. *and* GRAHAM, C. M. 1975. The graphical analysis of greenschist to amphibolite facies mineral assemblages in metabasites. *Journal of Petrology*, **16**, 347–70.

HEIM, F. 1912. Geologische Beobachtungen über Süd-Georgien. *Zeitschrift der Gesellschaft für Erdkunde zu Berlin*, 451–6.

HEY, M. H. 1954. A new review of the chlorites. *Mineralogical Magazine*, **30**, 277–92.

HIETANEN, A. 1974. Amphibole pairs, epidote minerals, chlorite and plagioclase in metamorphic rocks, northern Sierra Nevada, California. *American Mineralogist*, **59,** 22–40.

HOLTEDAHL, O. 1929. On the geology and physiography of some Antarctic and sub-Antarctic islands. *Scientific Results of the Norwegian Antarctic Expeditions, 1927–29*, No. 3, 172 pp.

HONNOREZ, J. 1963. Sur l'origine hyaloclastites. *Bullétin Volcanologique*, **25,** 253–8.

HUGHES, C. J. 1973. Spilites, keratophyres, and the igneous spectrum. *Geological Magazine*, **109,** 513–27.

HUTCHISON, C. S. 1978. Ophiolite metamorphism in northeast Borneo. *Lithos*, **11,** 195–208.

IRVINE, T. N. *and* BARAGAR, W. R. A. 1971. A guide to the chemical classification of the common volcanic rocks. *Canadian Journal of Earth Sciences*, **8,** 523–48.

IWASAKI, M. 1963. Metamorphic rocks of the Kotu-Bizan area, eastern Shikoku. *Journal of the Faculty Sciences, University of Tokyo*, Sect. II, **15,** 1–90.

JAKES, P. *and* WHITE, A. J. R. 1971. Composition of island-arcs and continental growth. *Earth and Planetary Science Letters*, **12,** 224–30.

JOHNSTON, W. C. Q. 1969. Pillow lava and pahoe-hoe: a discussion. *Journal of Geology*, **77,** 730–2.

JONES, J. G. 1969. Pillow lavas and pahoe-hoe. *Journal of Geology*, **76,** 485–8.

JUTEAU, T. *and* ROCCI, G. 1974. Vers une meilleure connaissance du problème des spilites a partir de données nouvelles sur le cortege spilite-keratypyrique hercynotype. (*In* AMSTUTZ, G. C., *ed. Spilites and spilitic rocks*. Berlin, Heidelberg, New York, Springer-Verlag, 253–330.)

KATZ, H. R. 1972. Plate tectonics and orogenic belts in the southeast Pacific. *Nature, London*, **237,** 31–2.

KATZ, H. R. 1973. Contrasts in tectonic evolution of orogenic belts in the southeast Pacific. *Journal of the Royal Society of New Zealand*, **3,** 333–62.

KAWACHI, Y. 1974. Geology and petrochemistry of weakly metamorphosed rocks in the Upper Wakatipu District, southern New Zealand. *New Zealand Journal of Geology and Geophysics*, **17,** 169–208.

KAWACHI, Y. 1975. Pumpellyite–actinolite and contiguous facies metamorphism in part of Upper Wakatipu district, South Island, New Zealand. *New Zealand Journal of Geology and Geophysics*, **18,** 401–41.

KIDD, R. G. W. 1977. A model for the process of formation of the upper oceanic crust. *Geophysical Journal of the Royal Astronomical Society*, **50,** 149–83.

KUNIYOSHI, S. *and* LIOU, J. G. 1976. Burial metamorphism of the Karmutsen volcanic rocks, northeastern Vancouver Island, British Columbia. *American Journal of Science*, **276,** 1096–119.

LE BAS, M. J. 1962. The role of aluminium in igneous clinopyroxenes with relation to their parentage. *American Journal of Science*, **260,** 267–88.

LEAKE, B. E. 1978. Nomenclature of amphiboles. *Minerlogical Magazine*, **42,** 533–63.

LEAKE, B. E., HENDRY, G. L., KEMP, A., PLANT, A. G., HARVEY, P. K., WILSON, J. R., COATS, J. S., AUCOTT, J. W., LUNEZ, T. *and* HOWARTH, R. J. 1969. The chemical analysis of rock powders by automatic X-ray fluorescence. *Chemical Geology*, **5,** 7–86.

LIOU, J. G. 1979. Zeolite facies metamorphism of basaltic rocks from the East Taiwan ophiolite. *American Mineralogist*, **64,** 1–14.

LIOU, J. G., KUNIYOSHI, S. *and* ITO, K. 1974. Experimental studies of the phase relations between greenschist and amphibolite in a basaltic system. *American Journal of Science*, **274**, 613–32.

MAIR, B. F. 1981. Geological observations in the Moraine Fjord area, South Georgia. *British Antarctic Survey Bulletin*, No. 53, 11–19.

MAIR, B. F. 1983. The Larsen Harbour Formation and associated intrusive rocks of southern South Georgia. *British Antarctic Survey Bulletin*, No. 52, 87–107.

MCBIRNEY, A. R. 1963. Factors governing the nature of submarine volcanism. *Bullétin Volcanologique*, **26,** 455–69.

MENARD, H. 1964. *Marine geology of the Pacific*. New York, McGraw-Hill.

MISCH, P. *and* RICE, J. M. 1975. Miscibility of tremolite and hornblende in progressive Skagit Metamorphic Suite, North Cascades, Washington. *Journal of Petrology*, **16,** 1–21.

MIYASHIRO, A. 1973. The Troodos ophiolitic complex was probably formed in an island arc. *Earth and Planetary Science Letters*, **19,** 218–24.

MIYASHIRO, A. 1975. Classification, characteristics, and origin of ophiolites. *Journal of Geology*, **83,** 249–81.

MIYASHIRO, A. *and* SHIDO, F. 1975. Tholeiitic and calc-alkaline series in relation to the behaviours of titanium, vanadium, chromium and nickel. *American Journal of Science*, **275**, 265–77.

MOORE, J. G. 1965. Petrology of deep sea basalt near Hawaii. *American Journal of Science*, **263,** 40–52.

MOORHOUSE, W. W. 1959. *The study of rocks in thin section*. New York, Harper and Row.

NAKAJIMA, T., BANNO, S. *and* SUZUKI, T. 1977. Reactions leading to the disappearance of pumpellyite in low-grade metamorphic rocks of the Sanbagawa metamorphic belt in central Shikoku, Japan. *Journal of Petrology*, **18,** 263–84.

NEUMANN, E. R. 1976. Compositional relations among pyroxenes, amphiboles and other mafic phases in the Oslo region plutonic rocks. *Lithos*, **9,** 75–110.

NITSCH, K. H. 1971. Stabilitätsbeziehungen von prehnit- und pumpellyit-haltigen Paragenesen. *Contributions to Mineralogy and Petrology*, **30,** 240–60.

PAPIKE, J. J., CAMERON, K. L. *and* BALDWIN, K. J. 1974. Amphiboles and pyroxenes: characterization of other than quadrilateral components and estimates of ferric iron from microprobe data. *Geological Society of America. Annual Meeting, Miami*, 1053–4.

PASSAGLIA, E. *and* GOTTARDI, G. 1973. Crystal chemistry and nomenclature of pumpellyites and julgoldites. *Canadian Mineralogist*, **12,** 219–23.

PEARCE, J. A. *and* CANN, J. R. 1971. Ophiolite origin investigated by discriminant analysis using Ti, Zr and Y. *Earth and Planetary Science Letters*, **12,** 339–49.

PEARCE, J. A. *and* CANN, J. R. 1973. Tectonic setting of basic volcanic rocks determined using trace element analyses. *Earth and Planetary Science Letters*, **19,** 290–300.

PEARCE, T. H., GORMANN, B. E. *and* BIRKETT, T. C. 1975. The TiO_2–K_2O–P_2O_5 diagram: a method of discriminating between oceanic and non-oceanic basalts. *Earth and Planetary Science Letters*, **24,** 419–26.

PEARCE, T. H., GORMANN, B. E. *and* BIRKETT, T. C. 1977. The relationship between major element chemistry and tectonic environment of basic and intermediate volcanic rocks. *Earth and Planetary Science Letters*, **36,** 121–32.

PICHLER, H. 1965. Acid hyaloclastites. *Bullétin Volcanologique*, **28,** 293–311.

ROBERTS, B. B. 1958. Chronological list of Antarctic expeditions. *Polar Record*, **9,** 97–134.

SAMPSON, G. A. *and* FAWCETT, J. J. 1977. Coexisting amphiboles from the Hastings region of southeastern Ontario. *Canadian Mineralogist*, **15,** 283–96.

SAUNDERS, A. D., TARNEY, J., STERN, C. R. *and* DALZIEL, I. W. D. 1979. Geochemistry of Mesozoic marginal basin floor igneous rocks from southern Chile. *Geological Society of America Bulletin*, **90,** 237–58.

SILVESTRI, S. C. 1963. Proposal for a genetic classification of hyaloclastites. *Bullétin Volcanologique*, **25,** 315–21.

SNYDER, G. L. *and* FRASER, G. D. 1963. Pillowed lavas, 1. Intrusive lava pods and pillowed lavas, Unalaska Island, Alaska. *U.S. Geological Survey. Professional Papers*, **454-B,** 23 pp.

SOBOLEV, V. S. *and* KOSTYUK, E. A. 1972. The amphibole group. (*In* SOBOLEV, V. S., *ed.*, translated by D. A. BROWN. *The facies of metamorphism*. Canberra, Australian National University, 331–52.)

SPOONER, E. T. C. *and* FYFE, W. S. 1973. Sub-sea-floor metamorphism, heat and mass transfer. *Contributions to Mineralogy and Petrology*, **42,** 287–304.

STERN, C. S., DE WIT, M. J. *and* LAWRENCE, J. R. 1976. Igneous and metamorphic processes associated with the formation of Chilean ophiolites and their implication for ocean floor metamorphism, seismic layering and magnetism. *Journal of Geophysical Research*, **81,** 4370–9.

STONE, P. 1980. The geology of South Georgia: IV. Barff Peninsula and Royal Bay areas. *British Antarctic Survey Scientific Reports*, No. 96, 45 pp.

STONE, P. 1982. Geological observations in the Cooper Bay–Wirik Bay area, South Georgia. *British Antarctic Survey Bulletin*, No. 51, 43–53.

STOREY, B. C. 1983*a*. The geology of South Georgia: V. Drygalski Fjord Complex. *British Antarctic Survey Scientific Reports*, No. 107, 88 pp.

STOREY, B. C. 1983*b*. The geology of the Ducloz Head area of South Georgia. *British Antarctic Survey Bulletin*, No. 52, 33–46.

STOREY, B. C., MAIR, B. F. *and* BELL, C. M. 1977. The occurrence of Mesozoic oceanic floor and ancient continental crust on South Georgia. *Geological Magazine*, **114**, 203–8.

STOUT, J. H. 1972. Phase petrology and mineral chemistry of coexisting amphiboles from Telemark, Norway. *Journal of Petrology*, **13,** 99–146.

STRECKEISEN, A. L. 1973. Plutonic rocks: classification and nomenclature recommended by the I.U.G.S. Subcommission on the Systematics of Igneous Rocks. *Geotimes*, No. 18, 26–30.

STULL, R. J. 1973. Calcic and alkalic amphiboles from the Adden Horn Batholith, North Cascades, Washington. *American Mineralogist*, **58,** 873–8.

SUÁREZ, M. *and* PETTIGREW, T. H. 1976. An Upper Mesozoic island-arc–back-arc system in the southern Andes and South Georgia. *Geological Magazine*, **113**, 305–28.

SURDAM, R. C. 1969. Electron microprobe study of prehnite and pumpellyite from the Karmutsen Group, Vancouver Island, British Columbia. *American Mineralogist*, **54,** 256–66.

TANNER, P. W. G. 1982. Geologic evolution of South Georgia. (*In* CRADDOCK, C., ed. *Antarctic geoscience*. Madison, University of Wisconsin Press, 167–76.)

TANNER, P. W. G. *and* REX, D. C. 1979. Timing of events in an early Cretaceous island arc–marginal basin system on South Georgia. *Geological Magazine*, **116,** 167–79.

TANNER, P. W. G., STOREY, B. C. *and* MACDONALD, D. I. M. 1981. Geology of an Upper Jurassic–Lower Cretaceous island-arc assemblage in Hauge Reef, the Pickersgill Islands and adjoining areas of South Georgia. *British Antarctic Survey Bulletin*, No. 53, 77–117.

THOMSON, M. R. A., TANNER, P. W. G. *and* REX, D. C. 1982. Fossil and radiometric evidence for ages of deposition and metamorphism of sedimentary sequences on South Georgia. (*In* CRADDOCK, C., *ed. Antarctic geoscience*. Madison, University of Wisconsin Press, 177–84.)

THURACH, H. 1890. Geognostische Beschreibung der Insel Süd-Georgian. Die Internationale Polarforschung 1882–83. (*In Die Deutschen Expeditionen und ihre Ergebnisse. 2: Beschriebende Naturwissenschaften in einzelnen Abhandlung*. Hamburg, 107–64.)

TRENDALL, A. F. 1953. The geology of South Georgia: I. *Falkland Islands Dependencies Survey Scientific Reports*, No. 7, 22 pp.

TRENDALL, A. F. 1959. The geology of South Georgia. II. *Falkland Islands Dependencies Survey Scientific Reports*, No. 19, 48 pp.

TYRRELL, G. W. 1915. The petrology of South Georgia. *Transactions of the Royal Society of Edinburgh*, **50,** 823–36.

TYRRELL, G. W. 1916. Further notes on the petrography of South Georgia. *Geological Magazione*, **3,** 435–41.

TYRRELL, G. W. 1918. Additional notes on the petrography of South Georgia. *Geological Magazine*, **6,** 483–9.

TYRRELL, G. W. 1930. The petrography and geology of South Georgia. (*In Report on the geological collections made during the voyage of the "Quest" on the Shackleton–Rowett Expedition to the South Atlantic and Weddell Sea in 1921–22*. London, Trustees of the British Museum, 28–54.)

VALLENCE, T. G. 1974. Pyroxenes and the basalt-spilite relation. (*In* AMSTUTZ, G. C., *ed. Spilites and spilitic rocks*. Berlin, Heidelberg, New York, Springer-Verlag, 59–70.)

VUAGNAT, M. 1975. Pillow lava flows: isolated sacks or connected tubes? *Bullétin Volcanologique*, **39,** 581–89.

WALKER, G. P. L. 1960. Zeolite zones and dyke distribution in relation to the structure of the basalts of East Greenland. *Journal of Geology*, **68,** 515–28.

WORDIE, J. M. 1921. Shackleton Antarctic Expedition 1914–17: geological observations in the Weddell Sea area. *Transactions of the Royal Society of Edinburgh*, **53,** 17–27.